공학박사학위논문

Biosynthesis of 12−hydroxy lauric acid in *Escherichia coli* using alkane monooxygenase and its application

알칸 모노옥시게나아제를 사용한
대장균에서의 12−수산화 라우르산의
생산 연구 및 응용

2021 년 8 월

서울대학교 대학원
공과대학 협동과정 바이오엔지니어링
유 희 왕

Biosynthesis of 12-hydroxy lauric acid in *Escherichia coli* using alkane monooxygenase and its application

A Thesis
Submitted to the Faculty of Seoul National University
by
Hee-Wang Yoo

In Partial Fulfillment of the Requirements
For the Degree of Doctor of Philosophy

Advisor: Professor Byung-Gee Kim, Ph. D.

In Partial Fulfillment of the Requirements
For the Degree of doctor of Philosophy

August 2021

Interdisciplinary Program for bioengineering
Seoul National University

Biosynthesis of 12-hydroxy lauric acid in *Escherichia coli* using alkane monooxygenase and its application

알칸 모노옥시게나아제를 사용한 대장균에서의 12-수산화 라우르산의 생산 연구 및 응용

지도교수 김 병 기

이 논문을 공학박사 학위논문으로 제출함
2021 년 8 월

서울대학교 대학원
공과대학 협동과정 바이오엔지니어링
유 희 왕

유희왕의 공학박사 학위논문을 인준함
2021 년 8 월

위 원 장 _____

부위원장 _____

위   원 _____

위   원 _____

위   원 _____

Abstract

Biosynthesis of 12-hydroxy lauric acid in *Escherichia coli* using alkane monooxygenase and its application

Hee-Wang Yoo

Interdisciplinary Program for bioengineering

Seoul National University

The production of biochemicals from vegetable oil derivatives has attracted great interest as an alternative mean to develop a sustainable and environmentally-friendly production process known as biorefinery. ω-Hydroxy fatty acids (ω-HFA) are materials frequently used as precursors for various biopolymer monomers. In an effort to make eco-friendly biopolymer monomers, researches are being conducted worldwide to produce such monomers through enzymatic reactions.

Here, production of 12-hydroxy dodecanoic acid (12-HDA) from dodecanoic acid methyl ester (DAME) with AlkBGT system in

Escherichia coli and biosynthesis of various biopolymer monomers (ω–amino fatty acid, α,ω–alkanediol, α,ω–alkanediamine) with multi–enzymatic cascade reactions were described. In a two–phase reaction system, 44.8 ± 7.5 mM of 12–hydroxy dodecanoic acid (12–HDA) and 31.8 ± 1.7 mM of dodecanedioic acid (DDDA) were produced after transporter engineering, promoter engineering and introduction of novel alkane monooxygenase. For the construction of multi–enzymatic cascade reaction system, three cell–based modules, including a hydroxylation module (cell–H^m), an amination module (cell–A^m), and a reduction module (cell–R^m), were designed. 46.3 mM of 12–amino dodecanoic acid, 27 mM of 1,12–dodecanediol, and 21.5 mM of 1,12–diaminododecane were synthesized from 100 mM of DAME and 12–ADA could be isolated using tert–butyloxy carbonyl (Boc)–protection with isolation yield of 66.5%.

To improve the hydroxylation activity of PpAlkB, an alkane monooxygenase from *Pseudomonas pelgia*, a random mutant library was constructed using error–prone PCR and screened for beneficial mutants with a high–throughput assay developed in this study. Expression of the antibiotic resistance gene was coupled with the

activity of PpAlkB, of which allowed screening of the mutants in high-throughput manner and in vivo. After two sequential screening with dodecane and DAME as substrates, with a triple mutant, H292L/F253I/S313P, was identified. It produced 12.95 mM (11 mM of 12-HDA and 1.96 mM of DDDA) from 100 mM of DAME, which was 64% increase from 7.88mM by the wild-type.

In conclusion, production of 12-HDA with AlkBGT system and biopolymer monomers with multi-enzymatic cascade reaction system were performed using *E. coli* cell-based modules. In addition, PpAlkB was engineered for enhanced activity toward DAME through the in vivo screening assay. This study presents a new avenue for biosynthesis of fatty acid derivatives in *E. coli* by utilizing alkB engineering and modularized cell reactions.

Keyword : Non-heme alkane monooxygenase, AlkBGT, 12-hydroy laurate, In vivo screening system.

Student Number : 2015-21215

Table of contents

List of tables

List of Figures

Chapter 1. Introduction

1.1. Biosynthesis of ω-Hydroxy fatty acid for biopolymer monomer

1.1.1 Importance of ω-hydroxy fatty acids as a biopolymer monomer

Until now, numerous petrochemicals are being produced from fossil fuels. However, fossil fuels are the main cause of environmental pollution and facing depletion (Perera 2017, Schoffelen and van Hest 2012). The recent energy shortage and the elevation of CO_2 levels that leads to the global warming effect have attracted interest in developing renewable resources, especially from biomass, to produce eco-friendly energy and bioplastics (Sung et al. 2015). The production of eco-friendly alternatives of the petrochemical materials from vegetable oil derivatives intrigued the development of sustainable and environmentally friendly production processes known as biorefinery (Zorn et al. 2016, Ahsan et al. 2018). Such interest is reflected through the growing global market size of biorefinery. According to the recent report by Market Research Future in 2019, the global market size of bio-based chemicals is estimated to grow with a CAGR of 10.47% to

reach USD 97.2 billion by 2023 (Ko et al. 2020).

Hydroxy fatty acids (HFAs) are important compounds that have hydroxyl groups in the carbon chain of fatty acids (Cao et al. 2016). Especially, ω-Hydroxy fatty acids (ω-HFAs), which have a hydroxy group at the ω position of the fatty acid, are widely used as precursors for various chemical additives in cosmetics, lubricants, antimicrobials or surfactants (Huf et al. 2011, Metzger and Bornscheuer 2006). Also, ω-HFAs are used as the intermediates for the synthesis of value-added products such as ceramides or polyamides (Cao et al. 2016, Van Bogaert et al. 2009).

1.1.2 Chemical and biological production of ω-hydroxy fatty acids

ω-HFAs are important chemicals as biopolymer monomers. However, large scale production of ω-HFAs are hindered due to the high production cost. Thus, many studies have been conducted to increase the yield of ω-HFAs and reduce the cost of production in both chemical and biological system.

Several methods had been developed to synthesize ω-HFAs chemically by utilizing ring opening of corresponding lactones (Stephan and Mohar 2006) and oxidation of fatty acids with

3

chemical catalysts (Hwang et al. 2017). However, most of the chemical synthesis process are employing harsh reaction conditions such as high temperature and pressure and are limited in controlling selectivity of hydroxylation reaction on the desired carbon atom (Liu et al. 2011). As a result, studies on biological synthesis of ω-HFAs have been conducted as an alternative to the chemical production(Table 1.1). Especially, microbial and plant ω-HFAs have often been used as precursors of biopolymers (Mutlu and Meier 2010). Among various hydroxylases, cytochrome P450s and alkane monooxygenase are of particular interest due to their ability to introduce ω-hydroxylation with high regioselectivity (Jung et al. 2016, Schrewe et al. 2014). In addition, ω-HFAs could also be produced from unsaturated fatty acids using cascade enzyme reactions with hydratase, alcohol dehydrogenase, and Baeyer–Villiger monooxygenase (Ji-Won Song 2020).

Table 1.1 Representative results of biotransformation of ω-HFA in microbes

Strain	Enzyme	Substrate	Product	Titer (g/L)	Time (h)	Refs
C. tropicalis	CYP52A17	Methyl myristate	14-hydroxy methyl myristate	174	148	(Lu et al. 2010)
E. coli	CYP153A$_{L.m}$	Laurate	12-hydroxy laurate	3.28	24	(Joo et al. 2019)
E. coli	CYP153A35	Palmitic acid	16-hydroxy palmitic acid	4.6	30	(Jung et al. 2016)
E. coli	Hydratase Alcohol dehydrogenase	Oleic acid	9-hydroxy nonanoic acaid	1.28	8	(Seo et al. 2019)

	BVMO					
E. coli	Hydratase	Oleic acid	10-hydroxy decanoic acid	49	4	(Joo et al. 2012)
E. coli	AlkB	Decanoic acid	10-hydroxy decanoic acid	0.3	24	(He et al. 2019)
E. coli	AlkB	Methyl laurate	12-hydroxy methyl laurate	76	18	(Kadisch, Julsing, et al. 2017)
E. coli	PpAlkB	Methyl laurate	12-hydroxy laurate	15.5	24	This study

1.2. Non-heme di iron alkane monooxygenase system (AlkBGT)

Oxygenases are most versatile with respect to the hydroxylation of carbon chain of fatty acids. Among the oxygenases, iron-containing oxygenases are the most abundant enzymes which can catalyze C-H oxyfunctionalization (Schrewe et al. 2011). For instance, P450s, a member of heme-containing monooxygenases, can catalyze the hydroxylation reaction on a broad range of substrates (O'Reilly et al. 2011). AlkBGT system from *Pseudomonas putida* Gpo1 alkane degradation pathway (Figure 1.1) is composed of non-heme alkane monooxygenase (AlkB), Rubredoxin (AlkG), Rubredoxin reductase (AlkT). This system is known to catalyze oxidation of fatty acids or alkanes at the terminal position (Kok, Oldenhuis, van der Linden, Meulenberg, et al. 1989). Unlike P450 which catalyzes hydroxylation of fatty acids by heme, AlkB oxidizes fatty acids by di-iron active site (Bertrand et al. 2005).

Figure 1. 1 Alkane degradation operon of *Pseudomonas putida* Gpo1

1.2.1 Structure of AlkB and the reaction mechanism of AlkBGT system

Many types of bacterial non-heme alkane monooxygenases such as AlkB play an important role in the microbial degradation of oils and other compounds (de Sousa et al. 2017). AlkB from *Pseudomonas putida* Gpo1 is a well-known enzyme for oxidation of fatty acids or alkanes (Bertrand et al. 2005). However, further study on AlkB is limited due to its unknown crystal structure (Alonso et al. 2014). Since there is no protein structures available for AlkB, its position and orientation of the active site and substrate binding pocket are not identified. A topological study on AlkB based on the analysis of the hydrophobicity and gene fusions with β-galactosidase and alkaline phosphatase suggested that it has six transmembrane helices with N-terminal and C-terminal loops which are exposed to the cytoplasm (Figure 1.2) (Van Beilen, Penninga, and Witholt 1992). AlkB contains two iron molecules, and eight conserved histidine residues (H138, H142, H168, H172, H173, H312, H315 and H316) of which are known to be essential for holding the di-iron molecules. A mutational study illustrated that AlkB was inactive when alanine screening of the eight conserved

9

histidine residues was performed (Shanklin and Whittle 2003).

More structural studies revealed that AlkB functions as an oligomer

rather than a monomer (Alonso and Roujeinikova 2012). These

studies suggested that AlkB's active site resides in the cytoplasm

and AlkB has a substrate tunnel that opens from the cytoplasm to

the inner periplasmic space (Naing et al. 2013).

Most of the proteins classified as the *alkB* genes are

consisted of only the alkane hydroxylase domain and they require

rubredoxin and rubredoxin reductase genes as electron partners to

be completely functional. However, there are reports of AlkB with

multi-domains such as alkane monooxygenase-rubredoxin fusion,

and ferredoxin-ferredoxin reductase-alkane monooxygenase

fusion proteins (Figure 1.3)(Nie et al. 2014).

The AlkBGT system from *Pseudomonas putida* Gpo1 is comprised

of three domains (AlkB : non-heme di-iron monooxygenase, AlkG :

rubredoxin reductase, AlkT : rubredoxin) (Kok, Oldenhuis, Van Der

Linden, Raatjes, et al. 1989).

AlkB utilizes O_2 to oxidize alkanes to generate alcohols while

the unused oxygen atom is reduced to H_2O by the following

reaction: n-alkane + 2 reduced rubredoxin + O_2 + $2H^+$ = 1-

alkanol + 2 oxidized rubredoxin + H_2O (de Sousa et al. 2017). AlkT transfers electrons from NADH to AlkG, which in turn transfers the electrons to the AlkB (Figure 1.4) (Rojo 2005).

In addition, AlkB is also known to catalyze the hydroxylation of branched aliphatic, alicyclic, and alkylaromatic compounds, oxidation of terminal alcohols to the corresponding aldehydes, demethylation of branched methyl ethers, sulfoxidation of thioethers, and epoxidation of terminal olefins and allyl alcohol derivatives (Van Beilen et al. 2005).
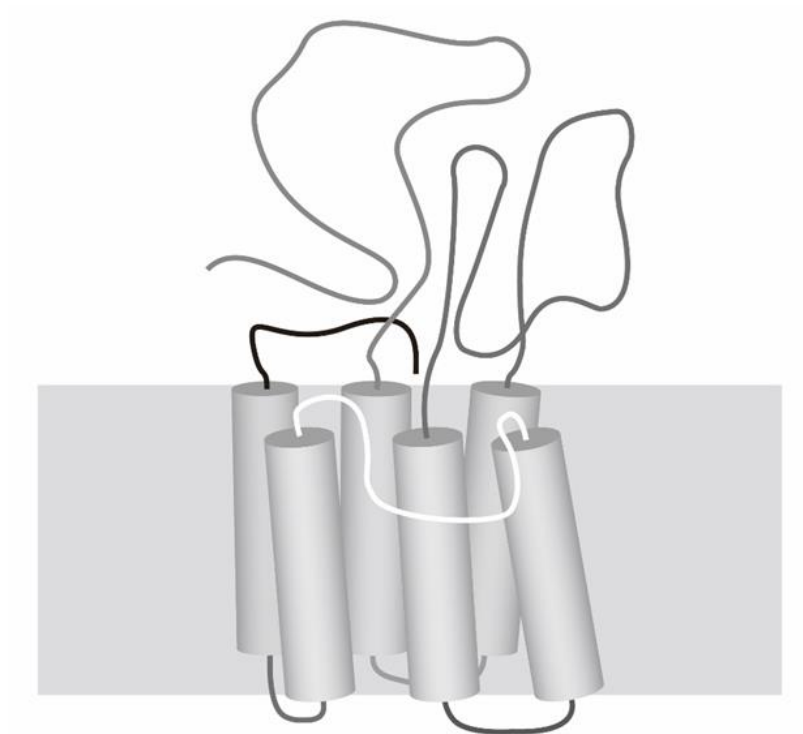
Figure 1. 2 Topological model of AlkB
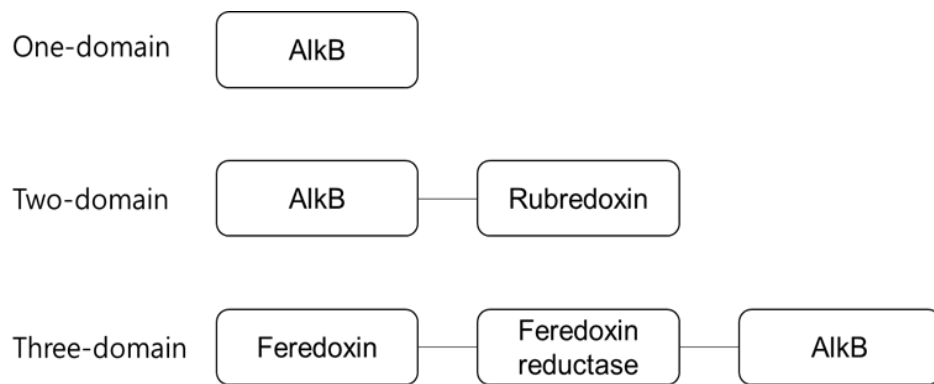
Figure 1. 3 Schematic view of conserved domain architecture of AlkB
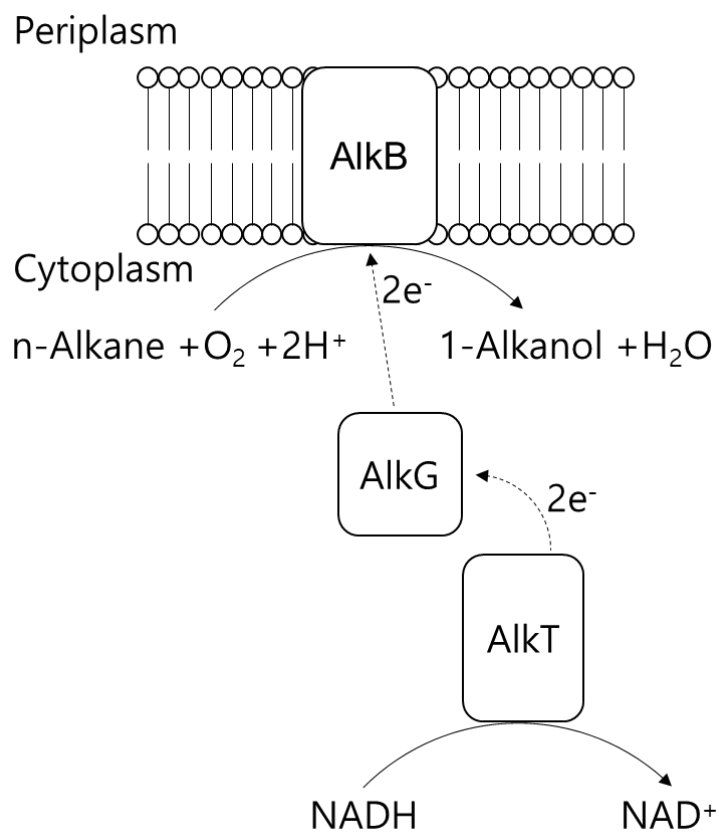
Figure 1. 4 Schematic diagram of AlkBGT system

1.2.2 Biosynthesis of ω—Hydroxy fatty acid with non—heme alkane monooxygenase

The selective oxidative activity of alkane monooxygenases under mild conditions opens the door for production of many polymer monomers used in the chemical, pharmaceutical and fragrance industries in an environmentally friendly approach (van Beilen et al. 2003).

AlkBs and P450s are often involved in the alkane degradation pathway of microorganisms (Nie et al. 2014). P450s use heme as the prosthetic group. However, P450s have a rather complex reaction mechanism involving heme, which limits industrial applications. Especially, when the heme does not function properly within the P450, P450 is expressed in an inactive form which is known as 'P420' form (Sun et al. 2013). In contrast to P450, AlkB is a heme—free monooxygenase, so there is less chance of getting the inactive form (van Nuland, Eggink, and Weusthuis 2016). As a result, many groups aimed to produce ω—Hydroxy fatty acids through non—heme alkane monooxygenases (Table 1.2). Julsing *et al.* produced 2.5g/L of 9—hydroxy pelargonate from methyl pelargonate by biphasic reaction and Clomburg *et al.* produced ω—

hydroxy fatty acid with carbon length of 6, 8, 10 from glucose by reverse beta oxidation and AlkBGT system. Also, He *et al.* synthesized 10-decanoic acid from decanoic acid with AlkBGT system and FadL as the transporter. Kadisch *et al.* produced 76.3 g/L of 12-hydroxy methyl laurate from methyl laurate with biphasic reaction.

Table 1.2 Summary of production of ω−hydroxy fatty acid using AlkBs

Origin	Substrate	Product	Titer (g/L)	Time	Ref
Pseudomonas Putida Gpo1	Methyl pelargonate	9−hydroxy methyl pelargonate	2.5	6	(Julsing et al. 2012)
Pseudomonas Putida Gpo1	Glucose	8−hydroxy octanoic acid	0.4	96	(Clomburg et al. 2015)
Pseudomonas Putida Gpo1	Decanoic acid	10−hydroxy decanoic acid	0.3	24	(He et al. 2019)
Pseudomonas Putida Gpo1	Methyl laurate	12−hydroxy methyl laurate	76.3	16	(Kadisch, Willrodt, et al. 2017)
Pseudomonas Putida pelagia	Methyl laurate	12−hydroxy laurate	15.5	24	This Study

1.2.3 Previously reported mutant study of AlkB

Since there are no available protein structures for AlkB, the location and orientation of the active site and substrate binding pocket are not identified. Due to the lack of information on protein structure, there is no report on AlkB mutant studies of rational design.

There are two mutational studies reported for the AlkB (Van Beilen et al. 2005, Koch et al. 2009). Each paper is the study that increases the activity of AlkB for butane and hexadecane. After preparing the AlkB mutant libraries using the error-prone PCR, the library was screened through the difference in cell growth rate of Pseudomonas containing the AlkB library with the target alkane as sole carbon source.

Van Beilen et al. reported that the side chain of Trp55 limits the entrance of long chain fatty acids and W55S or W55C mutant allows oxidation of tetradecane and hexadecane respectively, which means Trp55 blocks the bottom of the substrate binding pocket (Van Beilen et al. 2005). The W55S and W55C mutants of AlkB only induced increased activity toward tetradecane and hexadecane without changing the activity on the existing substrates. Also, Koch

et al. reported that AlkB with V129M, L132V and I233V mutations exhibited higher rates of 1-butanol production from butane (Koch et al. 2009).

1.3 The scope of thesis

The aim of this thesis is mainly to improve the production of biopolymer monomers such as ω-hydroxy fatty acid (ω-HFA), ω-amino fatty acid(ω-AFA) from fatty acid methyl ester (FAME) in *E. coli*. This thesis discusses the ways to increase concentration of the biopolymer monomers with biotransformation. In chapter 2, biotransformation of dodecanoic acid methyl ester (DAME) to 12-hydroxy dodecanoic acid (12-HDA) is described. In chapter 3, biosynthesis of ω-AFA, α,ω-alkanediol, α,ω-alkanediamine with multi-enzymatic cascade reaction is described. In chapter 4, in vivo screening in search for variants with enhanced activity toward DAME is described.

In chapter 2, production of 12-HDA in *E. coli* was designed with AlkBGT system. For the biosynthesis of 12-HDA in *E. coli*, a signal peptide of AlkL was replaced with the signal peptide from FadL to improve soluble expression and thereby facilitate the transport of DAME into *E. coli*. Promoter optimization for the efficient heterologous expression of the transporter $AlkL_f$ and AlkBGT system was also conducted. Moreover, bioinformatic studies led to the identification of novel monooxygenase from

Pseudomonas pelagia (PpAlkB), which exhibited 20% higher activity towards DAME compared to that of the AlkB from *Pseudomonas putida* Gpo1.

In chapter 3, biopolymer monomers such as ω-AFA, α,ω-alkanediol, α,ω-alkanediamine were biosynthesized with multi-enzymatic cascade reactions. The multi-enzymatic cascade reaction system was designed to produce the biopolymer monomers using cell-based modules that are capable of carrying out one-pot reactions for the monomer. The three cell-based modules include a hydroxylation module (cell-H^m) for conversion of fatty acid methyl ester to ω-HFA, an amination module (cell-A^m) for conversion of alcohols to amine compounds, and a reduction module (cell-R^m) for conversion of the carboxyl group of fatty acids to alcohol. ω-AFA, α,ω-alkanediol, and α,ω-alkanediamine with various carbon chain length (C8, C10, C12) could be synthesized via the developed enzyme cascade reaction system. Finally, 12-amino dodecanoic acid was isolated by tert-butyloxy carbonyl (Boc)-protection.

In chapter 4, engineering of PpAlkB was performed to search for variants with enhanced performance of ω-hydroxylation activity toward DAME via in vivo screening system. The mutant

library was produced using error-prone PCR. The in vivo screening system was designed to be a high-throughput screening system that couples the growth of *E. coli* to the ω-hydroxylation activity of AlkB. In the absence of fatty acids, FadR from *Thermus thermophilus* (TtFadR) inhibits the expression of antibiotic resistance gene (TetA) by binding to P_{ARTt}, a promoter which expresses the TetA. When lauroyl-CoA binds to TtFadR, the TtFadR is released from the P_{ARTt}, leading to the TetA expression and increasing survival of *E. coli* in the presence of tetracycline. Therefore, this screening system can be applied to activity screening of AlkB that can produce dodecanoic acid from dodecane.

Chapter 2. Production of 12-hydroxy dodecanoic acid using a signal peptide sequence-optimized transporter AlkL and a novel monooxygenase

A full reprint of the paper published in *Bioresource Technology* (2019) 291 : 121812

2.1 Introduction

The utilization of renewable raw materials has drawn great attention as an alternative to develop sustainable and green biochemical. As a renewable raw material, fatty acids are very important, and various oleo chemicals derived from fatty acids are not only very useful fine chemicals but also used as biodiesel because fatty acid derivatives are highly reduced and contain high-energy aliphatic compounds that are immiscible with water (Ahsan et al. 2018, Sherkhanov et al. 2016). Especially, ω-Hydroxy fatty acids (ω-HFAs) which has both a carboxylic group in the fatty acid itself and a hydroxy group at the ω position of the fatty acid are widely used as precursors for the synthesis of various chemical additives such as ceramide and polyamides (Huf et al. 2011, Metzger and Bornscheuer 2006). ω-HFAs are almost exclusively produced from petrochemical sources by chemical processes (Yokota and Watanabe 1993, Mountanea et al. 2019). However, the applications of chemical synthesis are limited by the use of labor-intensive multistep processes, sometimes requiring harsh reaction conditions and using toxic reaction intermediates (Patil et al. 2018).

Owing to their numerous advantages, various biocatalytic methods have emerged as proficient alternatives to chemical syntheses (Kawaguchi, Ogino, and Kondo 2017, Seo et al. 2018). Fatty acid methyl esters (FAMEs) are the most popular feedstock in recent years because it can be converted to free fatty acid if only methyl group is removed. FAMEs are produced by transesterification of waste frying oil or vegetable oils (Cao et al. 2007, Leung, Wu, and Leung 2010). The properties of various FAMEs are determined by the chemical structure of the fatty acid chain length and the functional groups which were attached to the carbon chain (Wadumesthrige, Salley, and Ng 2009). For example, the oxidation of FAME increases kinematic viscosity and alcohol group can easily be changed to other functional groups by chemical or enzymatic methods (Haak et al. 1997, Yamane et al. 2007). Therefore, many groups are conducting studies for regio-specific hydroxylation in FAME. In chemical study, various methods such as using solid metal catalysts and non-heme iron complexes have been devised for attaching hydroxyl groups to the sp^3 C-H bond (Burch and Hayes 1995, Gozzo 2001). However, since the chemical method is difficult to carry out site-specific hydroxylation, an enzyme-based

method has recently been in the spotlight.

There is a ubiquitous presence of hydroxylases in nature. Among these enzymes, P450s and alkane monooxygenase (AlkB) are of special interest owing to their ability to regioselectively hydroxylate the terminal carbon of fatty acids (Jung et al. 2016, Schrewe et al. 2011). For instance, CYP52A13 and CYP52A17 from engineered *Candida tropicalis* converted 200 g/L tetradecanoate to 174 g/L hydroxy tetradecanoic acid and 6.1 g/L 1,14–tetradecanedioic acid, respectively (Lu et al. 2010). Fungal CYPs, FoCYP539A7 and FoCYP655C2 are also known to catalyze regio– and stereoselective hydroxylation of fatty acids (Durairaj et al. 2015).

Although the production of hydroxy fatty acids has mainly been attempted using yeast as a host, the growth rate of yeast is slower and genetic tools are less developed than in *E. coli*. (Steen et al. 2010). Therefore, many research groups have used *E. coli* as a host for the synthesis of hydroxy fatty acids. Various CYP153As have been identified in several microbial strains and successfully expressed in *E. coli* for the synthesis of ω–HFAs (Malca et al. 2012, Jung et al. 2018, Ahsan et al. 2018). Similarly, alkane

monooxygenase AlkB, showing ω-functionalization toward FAMEs, has been also successfully expressed in *E. coli* (Schrewe et al. 2011) and 229 g/L of total products which were composed of HDAME, 12-oxo dodecanoic acid methyl ester and DDAME in organic phase were obtained from DAME substrate using biphasic reaction system (Kadisch, Julsing, et al. 2017).

Substrate uptake by host cell gives a great effect on the product titer and overall productivity of the reaction. Various strategies such as use of co-solvents (Ahsan et al. 2018, Kim et al. 2019) and surfactants (Patil et al. 2017) have been reported to improve the substrate uptake and membrane permeability. Overexpression of facilitator and transport system is another promising strategy to improve the substrate uptake. For instance, 2.4 g/L of 16-hydroxy palmitic acid was produced by overexpression of FadL, which is known as fatty acid transporter (Bae et al. 2014). In addition, introduction of AlkL, the outer membrane protein from *Pseudomonas putida* Gpo1, known as alkane transporter, has been reported to improve oxygenation activities towards DAME (Julsing et al. 2012, Scheps et al. 2013).

In this study, to increase the expression level of functional

form transporter AlkL, signal peptide of AlkL was replaced with signal peptides for *E. coli*-derived transporters FadL and OmpW (Call et al. 2016). Additionally, the promoter was optimized for efficient expression of four proteins (AlkB, AlkG, AlkT, AlkL) for higher product yield. Furthermore, novel non-heme alkane monooxygenases were expressed in *E. coli* and their ω-hydroxylation activities towards DAME were compared with that of the reported enzyme AlkB from *Pseudomonas putida* Gpo1.

2.2 Materials and methods

2.2.1 Bacterial strains and materials

All strains and plasmids used in this study are listed in Table 2.1. *E. coli* DH5α was used for genomic manipulation, and BW25113(DE3) was used for protein expression and cell reaction. Chloroform was obtained from Junsei (Tokyo, Japan). N,O-bis-(trimethylsilyl) trifluoroacetamide was purchased from Sigma-Aldrich Chemical Co.(St. Louis, MO, USA) Bacteriological agar, Luria Bertani (LB) broth, and terrific broth (TB) media were purchased from BD Difco (Franklin Lakes, NJ, USA). DAME was purchased from Tokyo Chemical Industry (Tokyo, Japan). HDAME was obtained from NeoPharm (Daejeon, South Korea).

2.2.2 DNA Manipulation Techniques

OCT plasmids harboring AlkB, AlkG, AlkT and AlkL were obtained from Prof Jin-byung Park, Ewha Womans University, Seoul, Korea. Each gene was amplified by PCR. The amplified genes were cloned in pCDF duet vector or pET duet vector and plasmids were transformed to *E. coli* DH5α cells.

Signal peptide in *E. coli* genome and AlkL without signal peptide in OCT plasmid were amplified using PCR. These amplified fractions were fused using assembly PCR. A novel transporter was constructed by assembly PCR (Stemmer et al. 1995) and cloned into a CDF duet vector using *Eco*RI and *Sal*I restriction enzymes. Construction of plasmids for promoter optimization was performed using T4 polynucleotide kinase & ligase (England and Uhlenbeck 1978). Genes encoding AlkB,G,T and L were cloned by Circular Polymerase Extension Cloning (Quan and Tian 2011) and plasmids were verified using DNA sequencing.

2.2.3 Identification of novel monooxygenase using bioinformatics tools

The amino acid sequence of AlkB from *Pseudomonas putida*

GPO1 was retrieved from UniProtKB (Primary accession number: Q9WWW6). The FASTA sequence was retrieved and subjected to NCBI BLASTp search (http://blast.ncbi.nlm.nih.gov) in order to find possible monooxygenase candidates.

Multiple sequence alignments were performed with ClustalW for the novel candidates with that of the reported ω-selective or specific non-heme alkane monooxygenases using the program MEGA7 (Kumar, Stecher, and Tamura 2016). Five putative enzymes were selected and the codon optimized genes encoding the corresponding proteins were synthesized by Bionics (Seoul, South Korea).

2.2.4 Cultivation and protein expression

For expression of the monooxygenase system AlkBGT and the transporter AlkL, plasmids harboring the corresponding genes were transformed to *E. coli* BW25113 (DE3) *ΔfadD* and the transformants were grown overnight in Luria-Bertani medium containing 100 μg/mL of ampicillin or 50 μg/mL streptomycin at 37 °C. This seed culture was used to inoculate 50 mL of Terrific-Broth and the cells were cultivated at 37 °C until the cell

concentration reached an optical density with 1 cm of path length, at 600 nm (OD_{600}) of 0.6. UV absorbance at 600 nm was measured with Multiskan spectrum (Thermo scientific, USA).

Following their induction by 0.01 mM IPTG, the cells were cultivated for 16 h at 30 ˚C. The cells were harvested by centrifugation (3000 rpm, 4 ˚C) and washed with potassium phosphate buffer (pH 7.5, 100 mM).

2.2.5 Biotransformations with cell extracts

To proceed the reaction with cell extracts, we induced BW25113(DE3) *ΔfadD* cells harboring pCDF duet with AlkL & AlkB and pET duet with AlkG & AlkT as mentioned above. After the cells were harvested to concentrate cells, the cells were diluted to OD_{600}=30 with 100 mM pH 7.5 potassium phosphate buffer, the cells were lysed by sonication.

Cell lysates were centrifuged at 13000 rpm, 4 ˚C for 30 min. The resultant cell free extract was used to catalyze the reaction in a final volume of 3 mL containing 5 mM DAME and 1% (w/v) glucose. The reaction mixtures were incubated at 30˚C and 200 rpm for 24 h to mix reaction mixture and oxygen aeration. All

experiments were validated with triplicate.

2.2.6 Screening of DAME uptake ability of cells through chimeric transporter

To illustrate the role of transporter in substrate uptake, cells expressing AlkL were harvested by centrifugation (3000 rpm, 4 °C) and washed with potassium phosphate buffer (pH 7.5, 100mM) to concentrate cell mass. The cells were diluted to OD_{600} = 30 to match the reaction volume and DAME (4 mM) and glucose (1% w/v) were added to the cell suspension in a final volume of 10 mL and the resulting cell suspension was agitated at 30 °C, 200 rpm for mixing reaction mixture and providing oxygen. Cells were centrifuged after 6 h, washed twice with pH 7.5 100mM potassium phosphate buffer and the amount of DAME uptaken by the cells was extracted with chloroform and determined using gas chromatography to compare the DAME concentration between total broth and inside the cell. All experiments were validated with triplicate.

2.2.7 Whole-Cell Biotransformations

For the screening of potential monooxygenase and optimization

of promoter for efficient hydroxylation of DAME, whole−cell biotransformations were performed by using 5 or 40 mM DAME substrate, 1% (w/v) glucose and density of the cell suspension was adjusted to OD_{600} of 30 using pH 7.5 100mM phosphate buffer by dilution of concentrated cells. The final volume of the reaction mixture was 10 mL in 100 mL flask. For 40 mM reaction, pH was measured every 6 h and adjusted to 7.5 using 5 M NaOH. The reaction mixtures were incubated for 24 h at 30 ° C and 200 rpm for mixing reaction mixture and oxygen aeration. Biphasic reactions were carried out similarly to that of resting cell reactions. At this experiment, the cell concentration was adjusted to OD_{600}=30, and the corresponding OD was adjusted to the aqueous layer only. The substrate DAME served as an organic phase in biphasic reactions. The total volume of the aqueous phase and DAME was fixed to 10mL, and only the ratio between DAME and aqueous phase was changed. All experiments were validated with triplicate.

2.2.8 Anaylsis by gas chromatography

Quantitative analysis was performed by gas chromatography (HP 6890 Series, Agilent Technologies, Santa Clara, CA, USA) with

flame ionization detector (GC/FID). 5 μL of the sample was injected by split less mode (a split less time of 0.8 min) and analyzed using a nonpolar capillary column (5% phenyl methyl siloxane capillary 30 m×320 μm i.d. 0.25 μm film thickness, HP−5 MS).

The oven temperature started at 100 °C for 1 min, and then increased by 15 °C/min to 250 °C, holding time at this temperature was 10 min. The temperature of the inlet was kept at 250 °C, and the temperature of the detector was 280 °C. The flow rate of the carrier gas was 1.0 mL/min, while flow rates of hydrogen, air, and helium in the FID were 45, 400, and 20 mL/min, respectively. Each peak in GC chromatogram was identified by comparison with that of an authentic sample. Errors in the analyses were corrected by using dodecane as an internal standard.

Table 2.1 Plasmids and strains used in this study

Plasmids	Description
pETduet-1	Double T7 promoters, ColE1 ori, Amp[r]
pCDFduet-1	Double T7 promoters, CloDF13 ori, Sm[r]
pGT	Derivative of pETDuet-1 with *alkG* and *alkT*
pBL	Derivative of pCDFDuet-1 with *alkL* and *alkB*
pBF	Derivative of pCDFDuet-1 with *fadL* and *alkB*
pL	Derivative of pCDFDuet-1 with *alkL*
pLO	Derivative of pCDFDuet-1 with a*lkL$_o$*
pLF	Derivative of pCDFDuet-1 with *alkL$_f$*
pF	Derivative of pCDFDuet-1 with *fadL*
pSS	Derivative of pCDFDuet-1 with T7 promoter for *alkL$_f$* and T7 promoter for *alkBGT*
pSM	Derivative of pCDFDuet-1 with T7 promoter for *alkL$_f$* and FC097 promoter for *alkBGT*
pSW	Derivative of pCDFDuet-1 with T7 promoter for *alkL$_f$* and FC109 promoter for *alkBGT*
pMS	Derivative of pCDFDuet-1 with FC097 promoter for *alkL$_f$* and T7 promoter for *alkBGT*
pMM	Derivative of pCDFDuet-1 with FC097 promoter for *alkL$_f$* and FC097 promoter for *alkBGT*
pMW	Derivative of pCDFDuet-1 with FC097 promoter for *alkL$_f$* and FC109 promoter for *alkBGT*
pWS	Derivative of pCDFDuet-1 with FC109 promoter for *alkL$_f$* andT7 promoter for *alkBGT*
pWM	Derivative of pCDFDuet-1 with FC109 promoter for *alkL$_f$* and FC097 promoter for *alkBGT*
pWW	Derivative of pCDFDuet-1 with FC109 promoter for *alkLf* and FC109 promoter for *alkBGT*
pMSP	Derivative of pCDFDuet-1 with FC097 promoter for *alkL$_f$* and T7 promoter for monooxygenase of *Pseudomonas pelagia* and *alkGT*
pToF	Derivative of pCDFDuet-1 with *fadL* and monooxygenase of *Thalassolituus oleivorans*
pCiF	Derivative of pCDFDuet-1 with *fadL* and monooxygenase

	of *Citreicella* sp. 357
pCuF	Derivative of pCDFDuet-1 with *fadL* and monooxygenase of *Curvibacter* sp. PAE-UM
pLaF	Derivative of pCDFDuet-1 with *fadL* and monooxygenase of *Leptospira alstonii*
pPpF	Derivative of pCDFDuet-1 with *fadL* and monooxygenase of *Pseudomonas pelagia*

E.coli Strains	Description
DH5α	*supE44 ΔlacU169 (Φ80 lacZΔM15) hsdR17, recA1, endA1, gyrA96, thi-1, relA1*
BW25113(DE3)	F-, DE(*araD-araB*)567, acZ4787(del)::*rrnB-3*, LAM-, *rph-1*, DE(*rhaD*-rhaB)568, *hsdR514*
AlkL	BW25113(DE3) *ΔfadD* + pL
AlkL$_o$	BW25113(DE3) *ΔfadD* + pLO
AlkL$_f$	BW25113(DE3) *ΔfadD* + pLF
FadL	BW25113(DE3) *ΔfadD* + pF
SS	BW25113(DE3) *ΔfadD* + pSS
SM	BW25113(DE3) *ΔfadD* + pSM
SW	BW25113(DE3) *ΔfadD* + pSW
MS	BW25113(DE3) *ΔfadD* + pMS
MM	BW25113(DE3) *ΔfadD* + pMM
MW	BW25113(DE3) *ΔfadD* + pMW
WS	BW25113(DE3) *ΔfadD* + pWS
WM	BW25113(DE3) *ΔfadD* + pWM
WW	BW25113(DE3) *ΔfadD* + pWW
MSP	BW25113(DE3) *ΔfadD* + pMSP
CuAlkB	BW25113(DE3) *ΔfadD* + pCuF + pGT
LaAlkB	BW25113(DE3) *ΔfadD* + pLaF + pGT
PpAlkB	BW25113(DE3) *ΔfadD* + pPpF + pGT
CiAlkB	BW25113(DE3) *ΔfadD* + pCiF + pGT

| ToAlkB | BW25113(DE3) *ΔfadD* + pToF + pGT |
| AlkB | BW25113(DE3) *ΔfadD* + pBF + pGT |

2.3 Results and discussion

2.3.1 Construction of novel chimeric transporters

We commenced this study with the cloning of AlkG and AlkT in pET duet vector and AlkB and AlkL into pCDF duet vector. Following the successful cloning of these genes in corresponding plasmids, this monooxygenase system was evaluated for the hydroxylation activity towards DAME substrate. A reaction was carried out using 5 mM DAME substrate. This experiment was carried out in the same manner as the 5 mM reaction described in section 2.7. Surprisingly, hydroxylation of DAME was not observed. We surmised that poor expression of one or more genes could be the plausible reason for the unsuccessful conversion of DAME to 12−hydroxy dodecanoic acid (12−HDA). In order to confirm whether the uptake of the substrate into inside cell was the problem, the reaction was proceeded with the cell free extract. Surprisingly, 1.1 ± 0.4 mM of 12−HDA was obtained in this case (Figure 2.1), implying that no product formation in the reaction was related with inclusion body formation of the transporter protein. To test this hypothesis, we checked the expression of proteins by using SDS

PAGE (Figure 2.2). The results showed that AlkB was expressed well as soluble form, but AlkL was expressed as inclusion bodies. Although AlkL is known to be expressed in functional form in *E. coli* (Julsing et al. 2012), it expressed as inclusion bodies in the present study (Figure 2.2). So, we turned our attention to obtain functional form of AlkL.

The protein destined for outer membrane is transferred to its destination by the signal peptides (Denks et al. 2014). The signal peptide plays an important role in the expression and translocation of outer membrane proteins (Coleman, Inukai, and Inouye 1985). Translocon protein recognizes the signal peptide of the outer membrane protein and migrates the protein to its destination (Voorhees and Hegde 2016). Therefore, if translocon and the signal peptide do not work, the protein will not be transported to the outer membrane.

Among amino acid sequences of AlkL 'MSFSNYKVIAMPVLVANFVLGAATAWA' is known as signal peptide. As signal peptide of AlkL is derived from the *Pseudomonas putida* Gpo1 host cell cannot recognize the information, so AlkL might be expressed as inclusion bodies. For example, it has

previously been reported that the expression and translocation of *E. coli* envelope proteins such as OmpA, maltose binding protein, ribose binding protein, alkaline phosphatase synthesized in *Bacillus subtilis* was poor, however, significantly enhanced following the replacement of the alkaline protease signal peptide derived from *Bacillus amyloliquefaciens*, which is recognizable in *Bacillus subtilis* (Collier 1994). Therefore, we carried out a study to replace the signal peptide of AlkL to the signal peptide of outer membrane protein of *E. coli* for the heterologous expression of AlkL in *E. coli*. We replaced the signal peptide of AlkL with other signal peptides, i.e. OmpW and FadL, which were typical fatty acid transporters of *E. coli*. (Call et al. 2016) The information for both the signal peptides was retrieved from UniProtKB (Table 2.2).

Replacement of the original signal peptide of AlkL with the new signal peptides derived from *E. coli* improved the expression level of functional form of AlkL (Figure 2.3). After obtaining these soluble proteins, we conducted a whole-cell biotransformation experiment to see if DAME could enter *E. coli* through engineered AlkL. To observe DAME uptake of *E. coli* through engineered AlkL, 4 mM DAME was added to the cells expressing each transporter.

After 6 hours of reaction, DAME in total broth and inside *E. coli* were extracted with chloroform and analyzed by GC respectively. To measure the concentration of DAME inside the *E. coli*, cells were centrifuged and washed twice with potassium phosphate buffer (pH 7.5, 100mM). After resuspension the cells with the same amount of buffer as the amount of broth, DAME was extracted with chloroform.

AlkL with the signal peptide of FadL (AlkL$_f$) successfully uptook 2.6 $\pm$ 0.4 mM DAME, which was 8-fold higher than that achieved by AlkL with the signal peptide of OmpW (AlkL$_o$; 0.7 $\pm$ 0.5 mM) (Figure 2.4). The amount of expression of level of functional AlkL$_f$ and AlkL$_o$ was similar in SDS PAGE (Figure 2.3). According to previous report, the expression level and stability of protein in *E. coli* have been increased due to the replacement of the signal peptide (Singh et al. 2013). Although we changed the signal peptide to increase the expression level of functional AlkL, we assume that the transporter activity changes due to the signal peptide replacement.

In this study, replacement of the signal peptide of AlkL with *E. coli* derived signal peptides FadL improved the expression and

translocation of the transporter protein in the present study. Therefore, further studies were performed using AlkL$_f$.
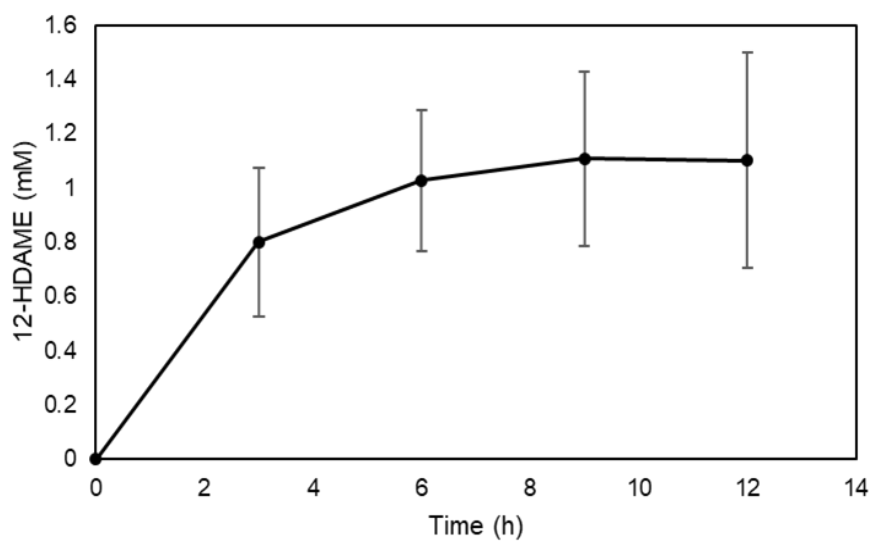
Figure 2. 1 Reaction with cell extracts BW25113(DE3)Δ*fadD* carrying pCDF duet with alkB and alkL and pET duet with alkG and alkT

Table 2.2 Sequence information of signal peptides used in this study

Enzyme	Signal peptide sequence
AlkL	MSFSNYKVIAMPVLVANFVLGAATAWA
FadL	MSQKTLFTKSALAVAVALISTQAWS
OmpW	MKKLTVAALAVTTLLSGSAFA
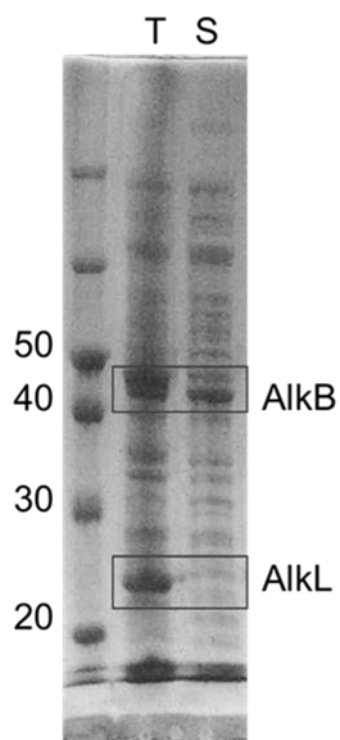
Figure 2. 2 SDS−PAGE (12%) analysis of recombinant *E. coli* BW25113 (DE3) Δ*fadD* carrying pCDF duet with alkB and alkL. Total fraction (lane T) and soluble fraction (lane S), respectively
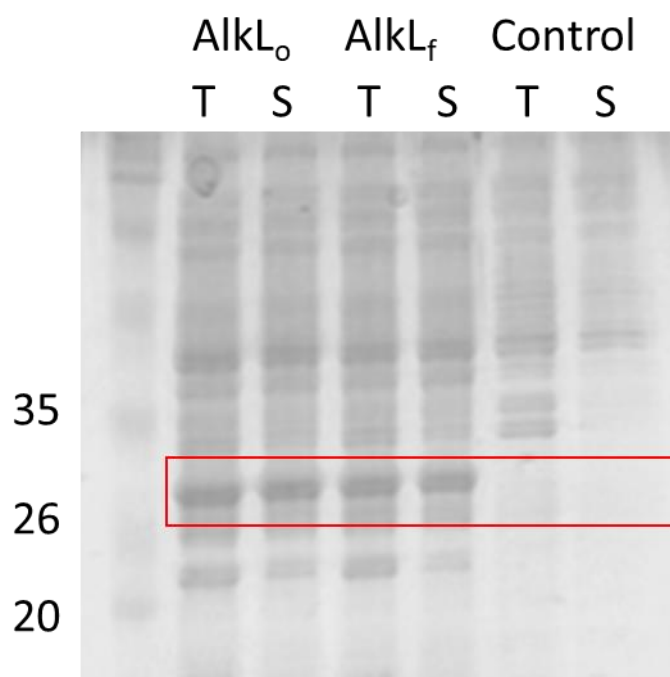
Figure 2. 3 SDS−PAGE (12%) analysis of recombinant *E. coli* BW25113 (DE3) *ΔfadD* carrying pCDF duet with AlkLf or AlkLo. Total fraction (lane 1) and soluble fraction (lane 2) for $AlkL_o$ and total fraction (lane 3) and soluble fraction (lane 4) of $AlkL_f$
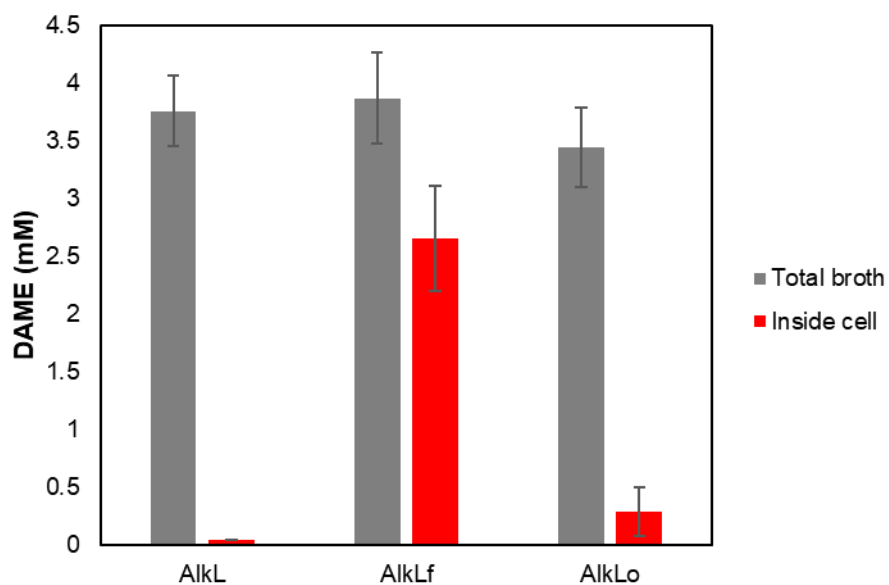
Figure 2. 4 Resting−cell activity assays related to transporter activity toward DAME by comparing the concentration of DAME in total broth and inside cell to check transporter activity. Gray square means DAME concentration in total broth and white square means DAME concentration in inside the cells.

2.3.2 Promoter optimization for efficient expression of the enzymes

In order to control efficient expression levels of the proteins and thereby the optimal hydroxylation of DAME, promoter optimization work was performed. For the promoter optimization, T7 library was generated by introducing two promoters, with 60% (FC097) and 20% (FC109) activity of the T7 promoter, respectively (Chizzolini et al. 2013). AlkL$_f$ transporter and AlkBGT monooxygenase system were cloned in MCS1 and MCS2 sites of the pCDF duet vector, respectively. In the case of AlkBGT, it was introduced as an operon and ribosome binding site (RBS) was added to each gene to maintain the expression level (Figure 2.5). The constructs were named combining the abbreviation of promoter strength (S for T7, M for FC097, W for FC109) according to the order of MCS. For example, the plasmid having the combination of FC109 promoter for *alkL$_f$* and the promoter FC097 for *alkBGT* was named as WM (Table 2.3). A library of 9 plasmids, each having different promoter combination, was constructed and transformed into *E. coli* BW25113(DE3) *ΔfadD* to compare the hydroxylation

performance toward 4 mM DAME. It was observed that the promoter system MS (having FC097 promoter for *alkL$_f$* and T7 promoter for *alkBGT*) showed the highest product concentration (3.0 ± 0.2 mM), which was ~3.5-fold higher than that by the SS construct (having T7 promoter for *alkL$_f$* and T7 promoter for *alkBGT*) after 6 hours. (Figure 2.5, Table 2.3). AlkB is an enzyme known to have overoxidation activity, for this reason 12-HDA is overoxidized to 1,12-dodecanedioic acid (DDA) by AlkB (Julsing et al. 2012). Therefore, we defined sum of concentration of 12-HDA and DDA as product concentration in this paper. Surprisingly, all of the products produced were in the form of 12-HDA and DDA from which the methyl group was removed. 12-HDA and DDA appear to be caused by hydrolysis of HDAME and DDAME by *E. coli* lipase and esterase (Kadisch, Schmid, and Bühler 2017).

Interestingly, it was also observed that concentration of products was higher when the transporter was weakly expressed than that of strong expression by the T7 promoter. In detail, AlkL$_f$ needs to be expressed using medium strength of a promoter, and AlkBGT operon need to be expressed using strong promoter. Owing to its highest concentration achieved in 4 mM reaction, efficiency of

the MS construct was evaluated with the increased substrate concentration (40 mM). Similar to that of 4 mM reaction, the MS construct achieved the highest product concentration of 13.2 ± 1.0 mM (Figure 2.6) which was about ~2.7-fold higher than the SS construct, attesting the importance of the expression level of monooxygenase. At this time, 8.5 ± 0.7 mM of 12-HDA and 4.7 ± 0.4 mM of DDA was produced because of over oxidation activity of AlkB.

 At the low and high substrate concentrations, the highest product concentration was observed with the MS construct. The overall tendency was also confirmed to be high when promoter for $alkL_f$ was FC097.

Aliphatic compounds can accumulate in membrane to cause toxicity to *E. coli*. Therefore, we think that strong promoter is not good for transporter expression because of toxicity of the cells. We think that the reason for relatively low yield when expressing the transporter as a T7 promoter is due to toxicity (Figure 2.6).

Also, the reason for the reaction comparison between FC097 and FC109 for $AlkL_f$, the reason for the more progress of the reaction in FC097 is that it did not have enough substrate when

using FC109. We think that sufficient DAME uptake in the absence of toxicity to cells would be good for yield improvement. Promoter for $alkL_f$ is better than FC097 when it is FC109, it is judged that it is because the DAME uptake is more active in FC097.

Overexpression of a recombinant protein can impose a metabolic burden to the host microorganism (Ahsan et al. 2018). Thus, optimization of expression levels for the heterologous proteins has been an area of research for numerous groups (Lee et al. 2013) To this end, various synthetic biology techniques have been developed to obtain the optimal amount of protein expressed and ultimately to improve the product concentration (Kim et al. 2018, Kadisch, Julsing, et al. 2017). Promoter, owing to its role in controlling the initiation of transcription of the associated genes, is one of the important key components of the expression system (Kaur, Kumar, and Kaur 2018). For instance, Kadisch et al., (Kadisch, Julsing, et al. 2017) reported the differential expression of AlkL using different promoters.

Heterologous overexpression of AlkL transporter also has been reported to impair the stability of the whole−cell biocatalysts (Grant et al. 2014, Julsing et al. 2012). It has been reported that

the facilitated transfer of hydrophobic substrates and their subsequent accumulation in the cell membranes causes membrane disintegration and permeabilization (Sikkema, de Bont, and Poolman 1994)

In the present study, heterologous overexpression of AlkL transporter using strong promoter also resulted in the lower overall outcomes of the biotransformations. To generalize, it can be stated that controlled expression of AlkL transporter can plausibly minimize the destabilizing effect and thus results in the better overall product concentration when AlkBGT operon was overexpressed using a strong promoter.
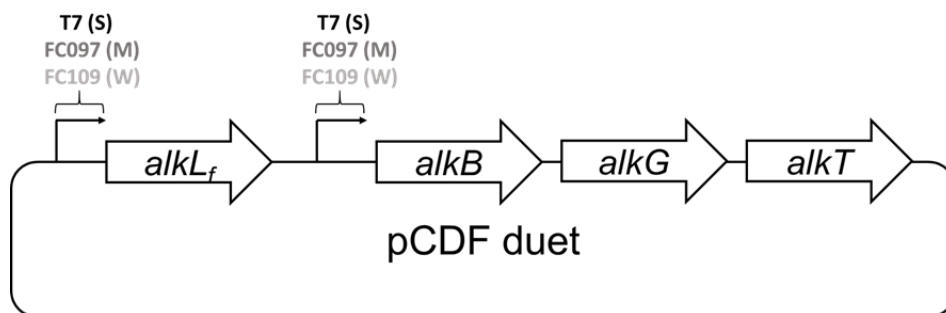
Figure 2. 5 Vector construction for the expression of enzymes

Table 2.3 Promoter construction of each strain and the amount of products after 6hours reaction with 4mM of DAME as substrate

Strain	Promoter (Relative strength % (Chizzolini et al. 2013))[a]		Product (mM)[b]
	For AlkL$_f$ expression	For AlkBGT expression	
SS	T7 (100)	T7 (100)	0.87±0.5
SM	T7 (100)	FC097 (60)	0.79±0.62
SW	T7 (100)	FC109 (20)	2.51±0.09
MS	FC097 (60)	T7 (100)	2.97±0.20
MM	FC097 (60)	FC097 (60)	2.37±0.51
MW	FC097 (60)	FC109 (20)	2.44±0.42
WS	FC109 (20)	T7 (100)	2.23±0.79
WM	FC109 (20)	FC097 (60)	2.55±0.60
WW	FC109 (20)	FC109 (20)	1.58±0.97

[a] See Figure 2.5

[b] Product means sum of concentration of 12-HDA and DDA.
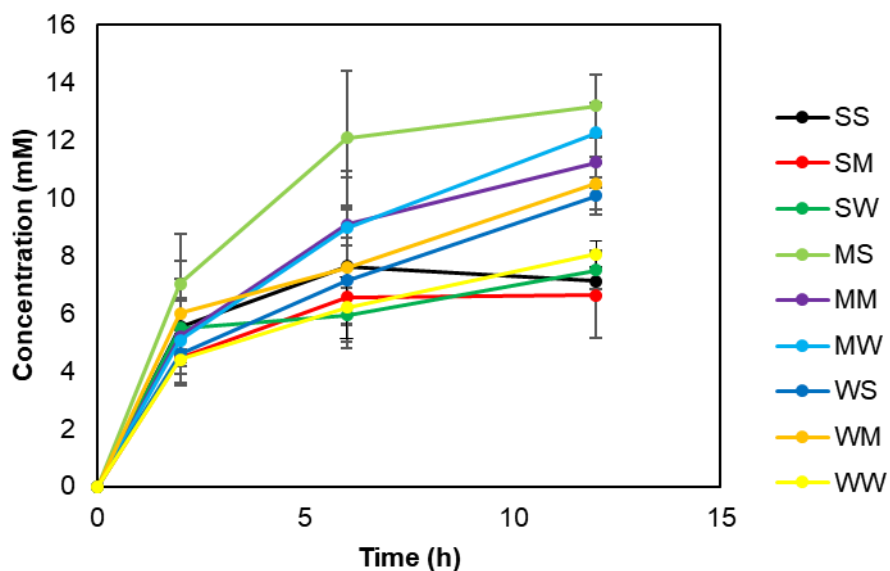
Figure 2. 6 Resting cell reaction profiles for the oxidation of DAME using various combinations of promoters with 40mM of DAME. The concentration is the sum of the concentrations of 12-HDA and 12-DDA produced in each time point. An annotation was performed in the order of promoter for alkf and alkBGT with T7 promoter : S, FC097 promoter : M, FC109 promoter : W.

2.3.3 Identification of new alkane monooxygenase

Bioinformatics tools have witnessed a surged interest for the identification of new enzymes and to gain the structural insights of already available enzymes (Patil et al. 2019, Kim et al. 2019, Patil, Grogan, and Yun 2018). In order to identify an alkane monooxygenase that is more active than AlkB, BLASTp search was performed using AlkB as a query sequence. We constructed a phylogenetic tree through MEGA7 after performing multiple sequence alignment with ClustalW for the sequences of 50 new monooxygenase candidates found through BLASTp (Figure 2.7). Among these enzymes, five enzymes were randomly selected and synthesized.

The genes encoding these putative enzymes were synthesized following the codon optimization, cloned in pCDFduet and the plasmids were transformed to *E. coli* BW25113(DE3) *ΔfadD* cells. For screening of newly identified alkane monooxygenases, FadL overexpressing *E. coli ΔfadD* strain was used as our group previously developed (Bae et al. 2014). AlkG and AlkT, which are electron partners of AlkB, were used as the electron partners also

for five new monooxygenases (Figure 2.8). Whole-cell biotransformations were carried out to examine the hydroxylation activity of six enzymes towards DAME substrate (5 mM). The results suggested PpAlkB completely converted DAME and achieved the highest product concentration, followed by AlkB (Figure 2.9). We were able to obtain about 4.6 ± 0.5 mM of products using PpAlkB, which was about 20% higher than AlkB producing 3.9 ± 0.5 mM of products. Analysis of the BLAST result exhibited that PpAlkB had 92% sequence similarity with AlkB. We surmised that the difference in reactivity would be due to the differential expression levels of the enzymes. Furthermore, to confirm the better hydroxylation efficiency of new monooxygenase PpAlkB, reactions were carried out using 40 mM substrate.

In this case, PpAlkB showed the highest product concentration of 11.9 ± 0.2 mM (8.4 ± 0.4 mM of 12-HDA and 3.5 ± 0.3 mM of DDA), which was 20% higher than that by AlkB which achieved 9.7 ± 2.0 mM (6.6 ± 1.6 mM of 12-HDA and 3.1 ± 0.4 mM of DDA) bioconversion of DAME after 12 hours from the start of the reaction (Figure 2.10). The better level of product concentration achieved by PpAlkB attested its better efficiency over AlkB for the

bioconversion of DAME. This result is consistent with the low concentration of the reaction. For better conversion of DAME to 12-HDA, we applied a biphasic reaction system based on experimental data using PpAlkB and AlkB.
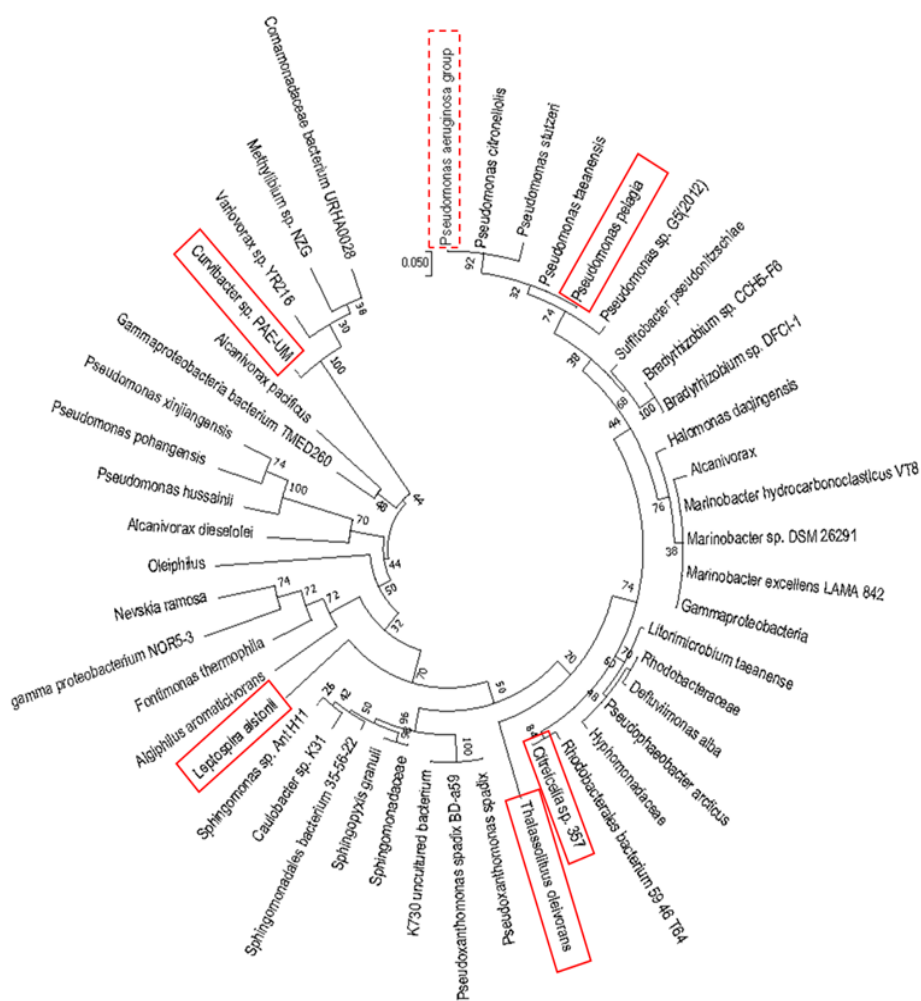
Figure 2. 7 Selection of novel monooxygenases from phylogenetic tree using AlkB as a query sequence. Sequence identity of AlkB with *Pseudomonas pelagia*, *Thalassolituus oleivorans*, *Curvibacter* sp. PAE-UM, *Citreicella* sp. 357, *Leptospira alstonii* are 92%, 73%, 55%, 77%, 67%, respectively. Dotted box shows AlkB, solid line boxes show newly identified monooxygenases
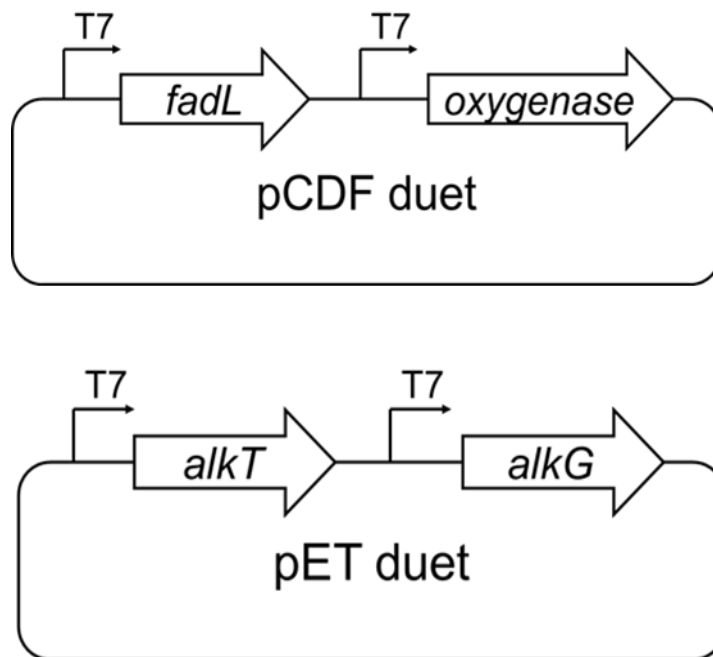
Figure 2. 8 Construction of vector system for
screening novel monooxygenase
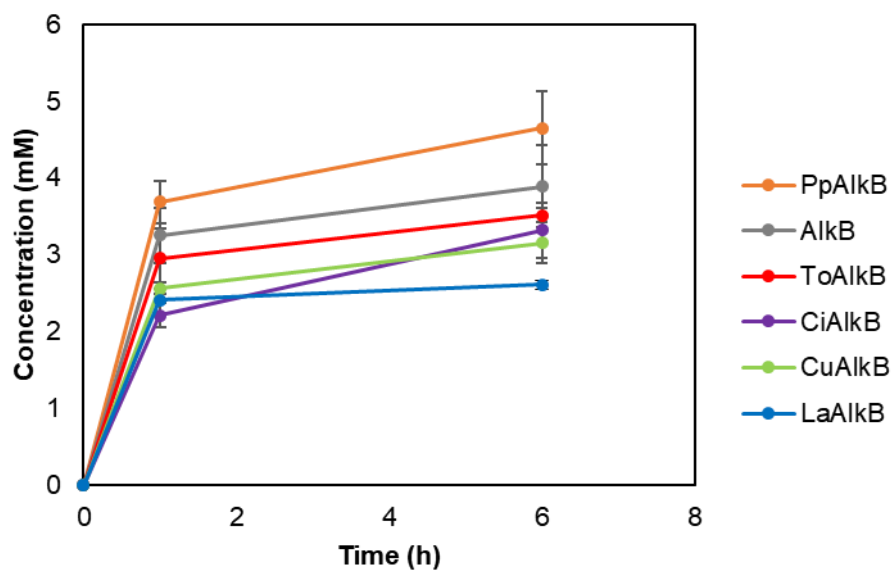
Figure 2. 9 Resting cell activity assays related to monooyxgenase activity toward DAME with 5mM of DAME. The concentration is the sum of the concentrations of 12-HDA and DDA produced in each time point
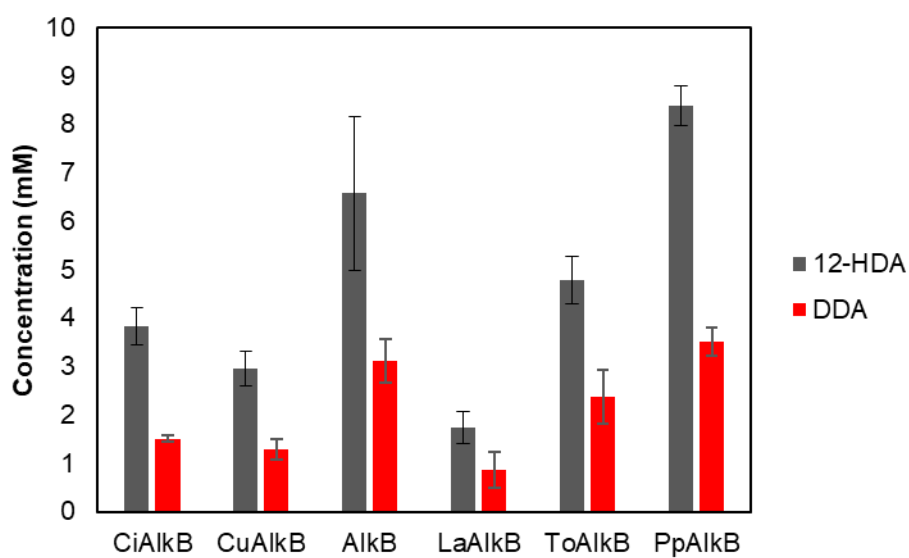
Figure 2. 10 Resting cell activity assays related to monooyxgenase activity toward DAME with 40mM of DAME as substrate.

2.3.4 Bioconversion of DAME to 12-HDA using a biphasic reaction system

Biphasic reaction systems are often advantageous in biocatalytic conversions to circumvent substrate and/or product inhibition (Patil et al. 2018, Jung et al. 2013). If DAME is used as an organic solvent to proceed with biphasic reaction, it has the advantage of continuous supply of substrate. It has been reported that AlkBGT catalyzed the bioconversion of DAME to 12-HDA using biphasic reaction system (Julsing et al. 2012). In the present study, we performed PpAlkB -catalyzed hydroxylation of DAME using biphasic reaction system with DAME as an orgnic solvent and substrate. For this experiments, two-plasmid one cell system was employed. Initially, the effect of ratio of organic solvent to aqueous layer was compared. Preliminary experiments suggested that more the organic layer, lower the degree of oxygen transfer and lesser the product concentration achieved. Thus, reactions were carried out using the ratios of 1 : 2 and 1 : 4 (organic layer : aqueous layer; Substrate conc. 4 M) (Figure 2.11, Figure 2.12). Products including 12-HDA and DDA were detected only in the organic phase but not in the aqueous layer. The product concentration in organic phase

achieved in both the biphasic systems (1 : 2 and 1 : 4) using PpAlkB -catalyzed reactions were better than that achieved by using AlkB-catalyzed reactions after 12 hours from the start of the reaction (Figure 2.11). This was further corroborated by better product concentration achieved in total reaction volume by both PpAlkB and AlkB-catalyzed reactions using biphasic system consisting the ratio of 1 : 2 were better than that of 1 : 4 (Figure 2.12). The amount of products obtained in 1 : 2 system with PpAlkB enzyme was 23.07 ± 2.7 mM (12.6 ± 1 mM of 12-HDA and 10.5 ± 1.5 mM of DDA). Nevertheless, the product concentration in total reaction volume was higher in PpAlkB -catalyzed reaction compared to that by AlkB. To further test the effect of increased organic layer, further reactions were carried out using 2 : 1 ratio of organic : aqueous layer. When comparing the amount of final product concentration only in the organic layer, the product concentration obtained by PpAlkB enzyme system was higher using 1 : 2 ratio of organic : aqueous layer. However, the corresponding amount of product in the total reaction mixture was highest using a cell system comprising of 2 : 1 organic : aqueous layer. (Figure 2.13, Figure 2.14). In this case, the product concentration achieved

was the highest about 63.7 ± 10.0 mM (44.8 ± 9.6mM of 12-HDA and 18.9 ± 1.3mM of DDA), which was 37% higher than that by AlkB. So far, it was confirmed that PpAlkB performed better than AlkB for the hydroxylation of DAME.

We reasoned that the highest production in the 2 : 1 ratio of organic : aqueous layer comes from the increased supply of the substrate supply. As the amount of substrate was increased relative to the amount of cells, the probability that each cell would uptake the substrate would increase. Therefore, we assumed that as the proportion of the organic layer increases, the amount of production also increases.

Then, we tried to combine developed systems which were chimeric transporter of AlkLf, promoter optimized construction, and biphasic process optimization using PpAlkB. The newly constituted promoter combinations for the transporter proteins were used in tandem with newly found efficient monooxygenase PpAlkB. Because the capacity of $AlkL_f$ (2.5mM in 4mM) for DAME uptake was ~31% higher than that of FadL(1.9 ± 0.5 mM in 4mM) (Figure 2.15), we used the MS construct harboring $AlkL_f$ and PpAlkB in with FC097 promoter and T7 promoter, respectively. Reaction catalyzed by

novel monooxygenase PpAlkB and transporter $AlkL_f$ achieved the highest product concentration of 76.0 ± 5.8 mM (44.8 ± 7.4 mM of 12-HDA and 31.8 ± 1.7 mM of DDA) using a biphasic reaction system consisting of 2 : 1 organic : aqueous layer (Figure 2.16) which was 31% higher than by FadL and AlkB system.

The hydroxy fatty acid can also be chemically synthesized. Yokota et al., described their method of producing hydroxy fatty acid via a metal catalyst. They made 7.4mmol of 12-hydroxy dodecanoic acid from 20mmol of barium salt of dodecanedioic acid monomethyl ester. Although increasing the amount of substrate would result in a steady increase in production with the aforementioned chemical reaction, the method requires large amount of metal catalysts and high reaction temperature of 254 °C (Yokota and Watanabe 1993). Unlike the chemical method, the biotransformation method described in this study can produce hydroxy fatty acid in a more environmentally friendly manner and under a mild condition that requires less energy consumption.

Generally, the approaches to hydroxylate various fatty acids by bio-catalyst are either to identify novel oxygenase systems (Malca et al. 2012) or to optimize the expression systems for those

already available (Yu et al. 2014). AlkB and AlkL are well known monooxygenase and alkane transporter, respectively. In the present study, we identified a novel monooxygenase from *Pesudomonas pelagia* (*co192_13285*) with 92% homology to AlkB showing 20% increased hydroxylation activity toward DAME. In the case of AlkL, the signal peptide FadL improved the expression in the soluble form and it was confirmed that the transporter protein facilitated the uptake of DAME.

The construction of the chimeric transporter and regulating the expression of the newly discovered oxygenase enzyme allowed us to obtain 76.0 ± 5.8 mM of products. (44.8 ± 7.4 mM of 12-HDA and 31.8 ± 1.7 mM of 12-DDA)
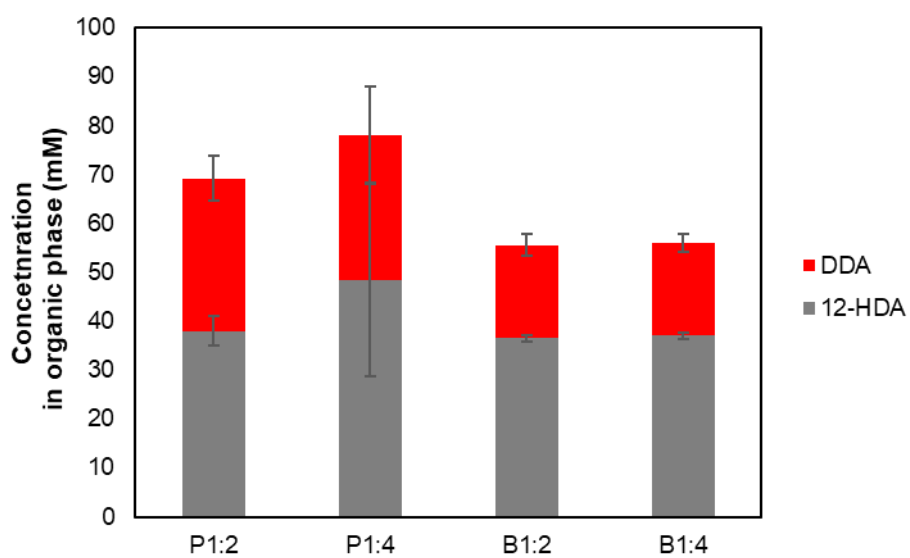
Figure 2. 11 Effect of volume ratio of organic (DAME) : aqueous layer on the hydroxylation of DAME as substrate. Product concentrations in the organic phase
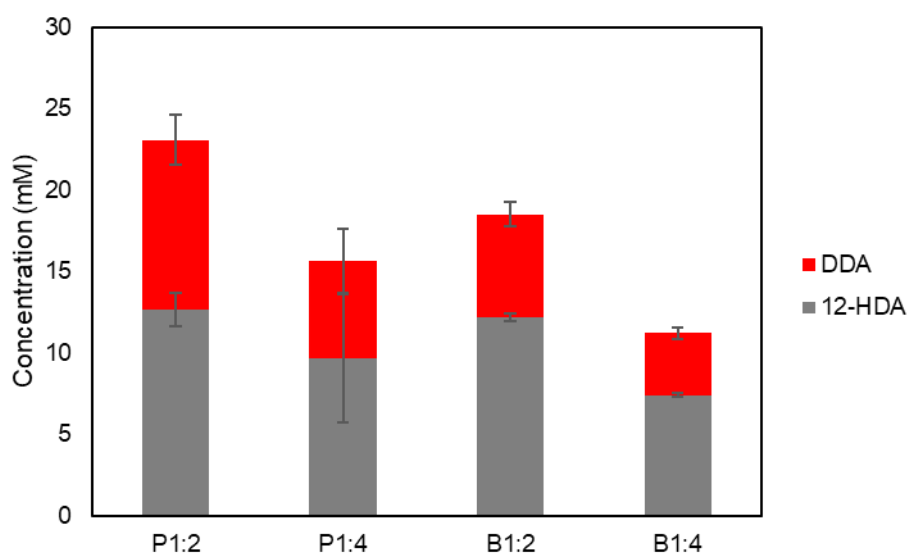
Figure 2. 12 Effect of volume ratio of organic (DAME) : aqueous layer on the hydroxylation of DAME as substrate. Product concentrations in the calibrated to full reaction volume to each product concentration.
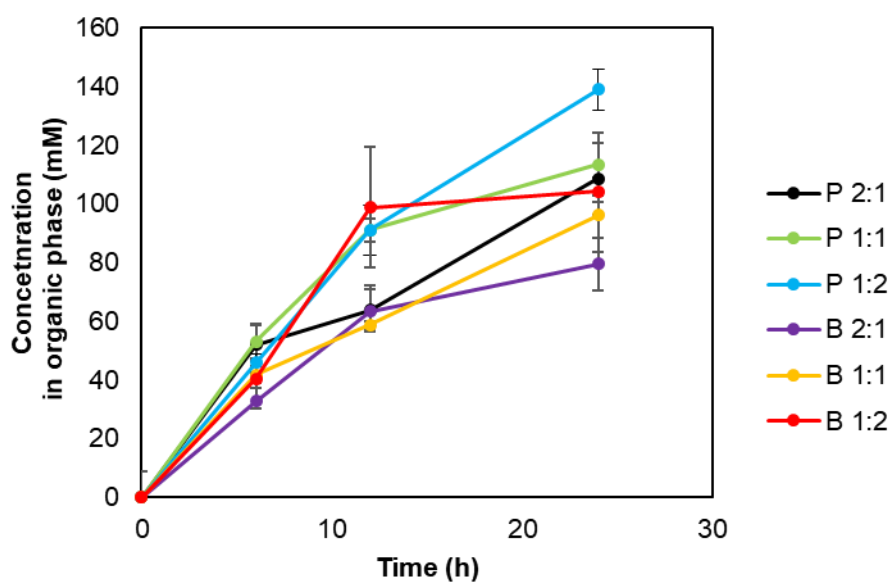
Figure 2. 13 Effect of volume ratio of organic (DAME) : aqueous layer on the hydroxylation of DAME as substrate. Product concentrations in the organic phase
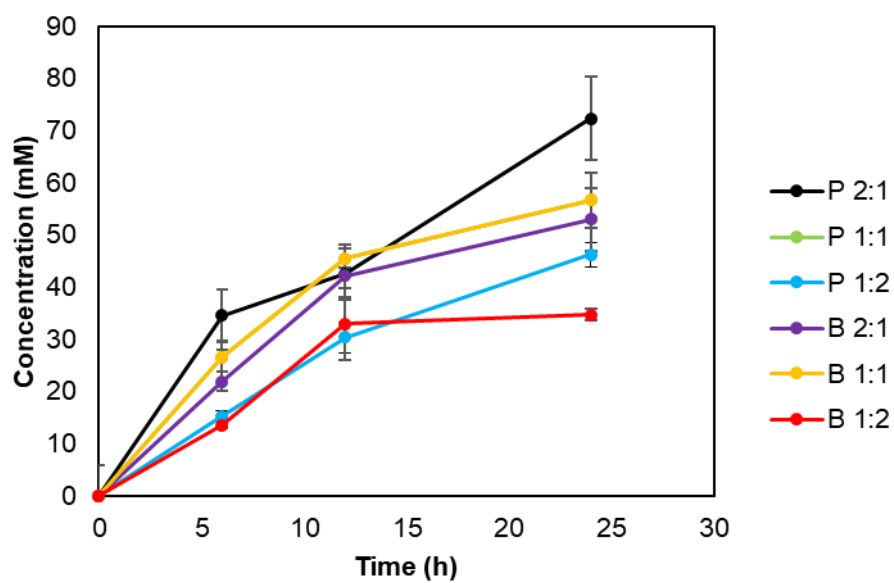
Figure 2. 14 Effect of volume ratio of organic (DAME) : aqueous layer on the hydroxylation of DAME as substrate. Product concentrations in the calibrated to full reaction volume to each product concentration.
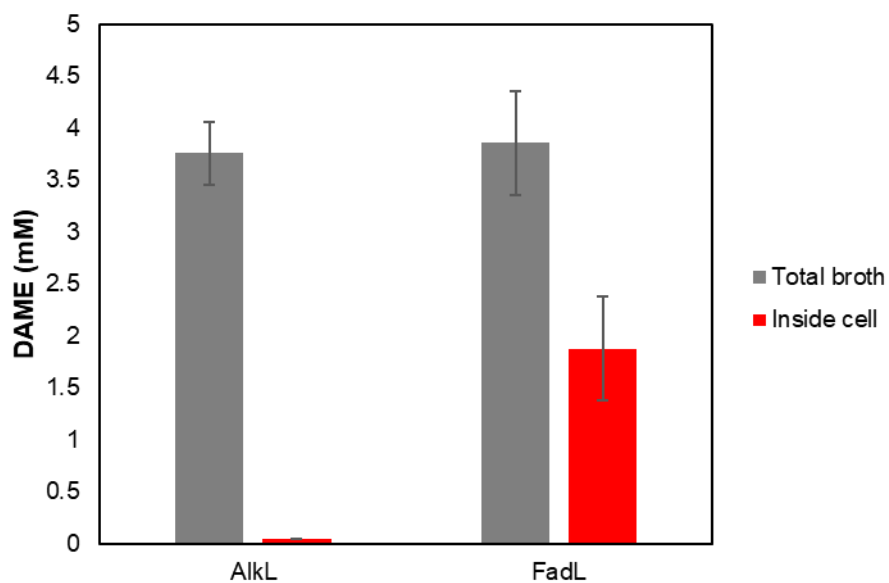
Figure 2. 15 Resting-cell activity assays related to transporter activity toward DAME between AlkLf and FadL. Gray square means DAME concentration in total broth and red square means DAME concentration in inside the cells
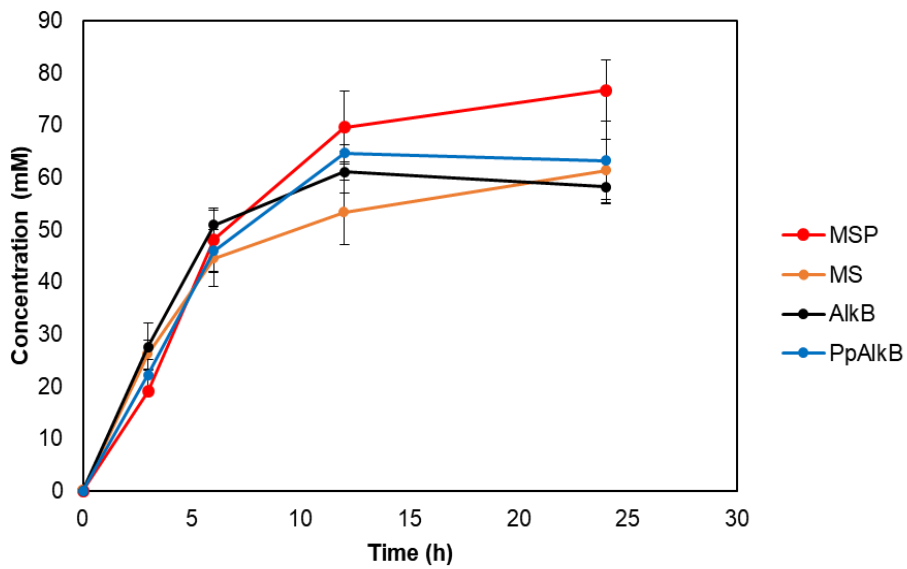
Figure 2. 16 Biphasic reaction with organic (DAME) : aqueous layer of 2 : 1 ratio with fully induced *E. coli* BW25113 carrying the expression plasmids. The concentration is the sum of the concentrations of 12-HDA and DDA produced in each time point. MSP : MS construct with PpAlkB ; Pp : two plasmid system with PpAlkB; MS : MS construct with AlkB; AlkB : two plasmid system with AlkB.

2.4 Conclusions

12-HDA is a precursor of many FA derived oleochemicals. In the present study 44.8 ± 7.4 mM of 12-HDA and 31.8 ± 1.7 mM of DDA was obtained by the identification of novel monooxygenase, development of chimeric transporter, and optimization of protein expression in *E. coli*. There are many reports on the formation of hydroxy fatty acid through monooxygenase in *E. coli*. The identification of a novel oxygenase and construction of a chimeric transporter which is better expressed in *E. coli* and facilitates the uptake of DAME opens a new avenue for syntheses of fatty acid derivatives.

Chapter 3. Multi-enzymatic cascade reactions with *Escherichia coli*-based modules for synthesizing various bioplastic monomers from fatty acid methyl esters

3.1 Introduction

With the recent energy shortage and increasing CO_2 levels, exacerbating the global warming effect, there has been great interest in the use of renewable resources, especially from biomass, to produce energy and industrial chemicals in eco－friendly production processes.(Sung et al. 2015, Zorn et al. 2016, Ahsan et al. 2018) Global demand for bio－based polymers is quickly increasing, mostly driven by the need for reducing environmental pollution, the shift to renewable resources, and the rise in consumer awareness of sustainability issues.(Fedorchuk et al. 2020) Due to the ubiquitous nature of polyamide functional groups and polyester precursors (amino, carboxyl, and hydroxyl), total synthesis via biocatalysis or fermentation is considered possible.(Fedorchuk et al. 2020, Schaffer and Haas 2014)

Among renewable feedstock, lipids such as animal fats and plant oils are abundant in nature and biodegradable.(Song et al. 2009) Since they contain hydrocarbon chains resembling the structure of petroleum components, lipids can be a

promising renewable resource alternative to petroleum−based products.(Lee et al. 2018) Medium−chain polyamides or polyester monomers can be obtained from lipids using multiple enzyme cascade catalysis.(Jiang and Loos 2016a) Multiple studies have optimized protocols to produce saturated dicarboxylic acids.fi(Chae et al. 2020) For example, 92.5 g/L of dodecanedioic acid was produced from dodecanoic acid methyl ester (DAME) using *Wickerhamiella sorbophila* as a host strain and up to 210 g/L of tetradecanedioic was produced from methyl myristate using *Candida tropicalis* as a host strain.(Lee et al. 2018, Picataggio et al. 1992) However, production of medium−chain bioplastic monomers, such as $\omega-$ amino fatty acid ($\omega-$AFA), $\alpha,\omega-$diamine, and $\alpha,\omega-$diol remains challenging. Current studies have only been able to generate 1.4 g/L of 1,12−dodecanediol from 12−hydroxy dodecanoic acid (12−HDA), 1.72 g/L of 1,10−diaminodecane from 1,10−decanediol, and 46.6 g/L of 11−amino undecanoic acid from ricinoleic acid in *Escherichia coli*.(Klatte and Wendisch 2014, Ahsan et al. 2017, Kim et al. 2020)

To produce various plastic monomers, including $\alpha,\omega-$

diol and α, ω −diamine, efficient production of ω −hydroxy fatty acid (ω −HFA) is key.(Zhang et al. 2020, Patil et al. 2018) Moreover, unlike unsaturated fatty acids such as ricinoleic acid and oleic acid, saturated fatty acids have been used as starting materials in few studies due to the difficulty of functionalizing the non−activated carbon on the substrate. Renewable unsaturated fatty acids are converted into esters by multiple enzymes, including hydratase, alcohol dehydrogenase, and Baeyer − Villiger monooxygenase, which are then hydrolyzed to ω −HFA and fatty acids by esterase or lipase.(Seo et al. 2019) ω −HFAs are further converted into biopolymer monomers using multiple enzymes; the hydrolyzed fatty acid is considered the by−product.(Seo et al. 2018, Jang et al. 2016) In comparison, saturated fatty acids can be converted directly using P450 or AlkBGT.(Jung et al. 2016, He et al. 2019) This reaction step is simple with high atomic economy. Further, due to the broad substrate specificity of monooxygenase, various carbon chain products can be produced from saturated fatty acids,(Malca et al. 2012) whereas the chain number of final products from unsaturated

fatty acids is constrained by the availability of double bonds in the molecule.(Ji-Won Song 2020) Therefore, saturated fatty acids offer several advantages as biotransformation substrates in the production of biopolymer monomers.

In establishing bio-based processes, microbial cell factories play a key role in converting renewable feedstocks into desired chemicals and materials by optimizing metabolic fluxes or enzyme expression toward desired products.(Chae et al. 2020) For biopolymer monomer production, multiple enzymes need to be heterologously expressed in *E. coli*.(Nuland et al. 2017) However, due to resource limitations and metabolic burden on the host, high protein production usually exerts a negative effect on the cell density of the bacterial culture.(Horga et al. 2018) Therefore, many studies have examined the potential of multi-enzyme cascade reactions to overcome these issues.(Lee et al. 2017, Lin and Tao 2017) Among them, construction of an in vivo multi-enzymatic cascade was demonstrated to offer many advantages over in vitro approaches, including elimination of costly steps (e.g., enzyme purification, addition of expensive

cofactors, etc.).(France et al. 2017)

In this study, we devised a multi−enzyme cascade system for the synthesis of ω−AFA, α,ω−diol, and α,ω−diamine (Fig. 1) with the following capabilities: (i) to use saturated fatty acids as substrates for biopolymer monomer synthesis; (ii) to synthesize multiple reaction products while limiting reaction by−products; and (iii) to use saturated fatty acids of various chain lengths as substrates. For the multilayer enzyme cascade system, a hydroxylation module (cell−H^m), an amination module (cell−A^m), and a reduction module (cell−R^m) were constructed to produce biopolymer monomers (Fig 1). Various biopolymer monomers were biosynthesized via combination of cell based modules, suggesting this as an effective model system for the production of biopolymer monomers.

Table 3.1. Representative examples of biopolymer monomers produced from aliphatic substrates in *E. coli*

Substrate	Enzyme	Product	Titer (g/L)	Refs
Dodecanoic acid methyl ester	AlkB from *P. putida*, ADH from *P. putida*, ω−TA from *C. violaceum*	12−amino dodecanoic acid methyl ester	0.1	(Ladkau et al. 2016)
Dodecanoic acid	P450 from *M. aquaeolei*, ADH from *G. stearothermophilus*, ω−TA from *C. violaceum*	12−amino dodecanoic acid	1.1	(Ge et al. 2020)
Ricinoleic acid	BVMO from *P. putida*, ADH from *M. luteus*, ChnD from *Acinetobacter* sp., ω −TA from *R. pomeroyi*	11−amino undecanoic acid	46.6	(Kim et al. 2020)
1−octanol	P450 from *Acinetobacter*	1,8−octanediol	0.72	(Sakagami et al. 2013)
12−hydroxy dodecanoic acid	CAR from *M. luteus*	1,12−dodecandiol	1.4	(Ahsan et al. 2017)
1,10−decanediol	ω−TA from *V. fluvialis*, ADH from *B. stearothermophilu*	1,10−diaminodecane	1.72	(Klatte and Wendisch 2014)
1,10−decanediol	ω−TA from *S. pomeroyi*, AHR from *Synechocystis* Sp. Strain PCC 6803	1,10−diaminodecane	9.76	(Sung et al. 2018)

1,12-dodecandiol	ω-TA from *S. pomeroyi*, AHR from *Synechocystis* Sp. Strain PCC 6803	1,12-diaminododecane	7.8	(Sung et al. 2018)
Dodecanoic acid methyl ester	AlkB from *P. pelagia*, ω-TA from *S. pomeroyi*	12-amino dodecanoic acid	9.95	This study
Dodecanoic acid methyl ester	AlkB from *P. pelagia*, CAR from *M. luteus*	1,12-dodecandiol	5.46	This study
Dodecanoic acid methyl ester	AlkB from *P. pelagia*, ω-TA from *S. pomeroyi*, CAR from *M. luteus*	1,12-diaminododecane	4.3	This study

3.2 Material and methods

3.2.1 Bacterial strains and materials.

E. coli DH5α was used for genomic manipulation, and BW25113 (Δ*fadD*, DE3) was used for protein expression and whole cell reaction. Chloroform was obtained from Junsei (Tokyo, Japan). N,O－bis－(trimethylsilyl) trifluoroacetamide (BSTFA) and N－Methyl－N－(trimethylsilyl) trifluoro－acetamide (MSTFA), Pyridine, every aliphatic substrate or products without DAME, 8－amino－1－octanol, 10－amino－1－decanol were purchased from Sigma－Aldrich Chemical Co.(St. Louis, MO, USA). Bacteriological agar, Luria Bertani (LB) broth, and terrific broth (TB) media were purchased from BD Difco (Franklin Lakes, NJ, USA). DAME, 8－amino－1－octanol, 10－amino－1－decanol was purchased from Tokyo Chemical Industry (Tokyo, Japan).

3.2.2 Cultivation and protein expression

For expression of each module system, plasmids harboring the corresponding genes were transformed to *E. coli* B

W25113 (DE3) $\varDelta fadD$ and the transformants were grown overnight in Luria-Bertani medium containing 100 μg/mL of ampicillin or 50 μg/mL streptomycin for cell-H^m and 100 μg/mL of ampicillin or 50 μg/mL kanamycin for cell-A^m and cell-R^m at 37 ° C. This seed culture was used to inoculate to Terrific-Broth and the cells were cultivated at 37 ° C until the cell concentration reached an optical density with 1 cm of path length, at 600 nm (OD$_{600}$) of 0.6. UV absorbance at 600 nm was measured with Multiskan spectrum (Thermo scientific, USA). The protein expreesion was induced by adding 0.05 mM isopropyl-thio-β-D-galactopyranoside (IPTG) for cell-H^m and 0.1 mM for cell-A^m and cell-R^m at 18 ° C for 18 hours.

3.2.3 Concurrent reaction system in shake flask.

For concurrent reaction, cells were harvested by centrifugation, washed with potassium phosphate buffer (pH 7.5, 100 mM) or Tris buffer (pH 8.0, 100 mM). The concurrent reaction was initiated by adding appropriate

concentration of substrate from 1M stock in ethanol and glucose to 10mL of cell resuspension in a 100 mL flask. in the case of $\alpha,\omega-$diamine compounds biosynthesis, amino donor was supplied and 10 mM $MgCl_2$ was supplied for the biosynthesis of $\alpha,\omega-$diol. All reactions were carried out at 30℃ and 200 rpm, and pH was titrated through 5M NaOH every 6 hours.

3.2.4 Carbon source optimization for 1,12-diol biosynthesis in shake flask.

For the optimization of carbon source glucose, glycerol and buffer+TB, the cells were diluted in potassium phosphate buffer (pH 7.5, 100 mM) with 30 OD_{600} of cell$-$H^m and cell$-$R^m, respectively. The corresponding concentration of glucose, 1%(w/v) glycerol and 1%(w/v) TB were added to proceed reaction at 30℃ 200rpm for 24 hours. For the comparison of complex media, the cells were diluted in LB, TB and RB respectively for the biosynthesis of 1,12-diol. The reaction condition to produce 1,12-diol was same with concurrent reaction.

3.2.5 Sequential reaction system in shake flask

In order to produce α,ω-diamine and α,ω-aminol by sequential reaction, α,ω-diol was produced by cell-H^m and cell-R^m beforehand with 100 mM DAME with 10 mL of reaction solution in 100 mL shake flask. After 24 hours, 120 OD_{600} cell-A^m, 400 mM benzyl amine and 1% DMSO were added to the reaction media, and the total volume was adjusted to 15 mL. The reaction was conducted at 30℃ and 200 rpm for 24 hours.

3.2.6 Whole-cell biotransformation in the reactor with constant pH control

Whole-cell biotransformation in the reactor with constant pH control was performed in 916 Ti-Touch with magnetic stirrer (Metrohm, Switzerland) pH controller. The reaction media for the biosynthesis of each product was the same condition with that of in the shake flask, and the total volume was 40 mL. In the case of Sequential reaction final volume of the reaction solution was 45 mL. The pH was kept constant at 7.5 or 8.0 through a pH controller, and

the pH was adjusted by 2M NaOH. The reaction was carried out at the same reaction conditions as the above experiments

3.2.7 Analysis by gas chromatography

The quantitative analysis of products were determined as previously described.(Yoo et al. 2019, Sung et al. 2018) Quantitative analysis was performed using a gas chromatography instrument with a flame ionization detector (GC/FID) fitted with an AOC−20i series auto sampler injector (GC 2010 plus Series, Shimadzu Scientific Instruments, Kyoto 604−8511, Japan). Analyzed using a nonpolar capillary column (Agilent J&W HP−5 column 30 m×320 μm i.d. 0.25 μm film thickness). To analysis of ω−HFA and α,ω−diols, the products were extracted with double volume of CHCl3 after vigorous vortexing for 1 min. After centrifugation, the organic phase was transferred to an Eppendorf tube and samples converted to their trimethylsilyl derivatives by incubation at 50 ° C for 20 min with an excess of BSTFA. We used Injector 260° C; flow 1.5 mL/min; Temperature program 50° C/hold 1 min. and 10° C per min to 250 ° C / hold 0 min and 30° C per min to 280 ° C / hold 5 min. For analysis of ω−amino fatty

acid and α,ω-diamines, samples were evaporated and pyridine was used for dilution of the samples. After 10min of sonication, the samples were then mixed with an equal volume of MSTFA by vigorous vortexing for 1 min and converted to the trimethylsilyl derivatives by incubation at 50 ° C for 20 min. After 3min centrifugation, supernatant was injected to GC/FID with Injector 230° C; flow 1.5 mL/min; Temperature program 90° C/hold 0 min; 15° C per min to 200 ° C/ hold 0 min and 5° C per min to 280° C / hold 5 min respectively. Each peak in GC chromatogram was identified by comparison with that of an authentic sample. In the case of 10-amino decanoic acid, standard curve of 12-ADA was used for quantification due to unavailability of the authentic sample. The qualitative analysis of products were determined with GC/MS analysis. GC/MS analysis was carried out using a Finnigan MAT system (gas chromatograph model AG3000 Trace GC Ultra ITQ1100) connected to an ion trap mass detector (Figure 3.33~3.43). Each sample preparation and analysis conditions were carried out under the same conditions as GC/FID.

3.2.8 Purification of 12-ADA with Boc protection

12-ADA was biosynthesized with cell-H[m] and cell-A[m] in the reactor with constant pH control for 48 hours (40mL). After completion of the reaction, the reaction media were heated at 80℃ for 30 minutes to stop the reaction. To remove organic compound such as excess benzyl amine and remained substrate, the heated reaction media was extracted with ethyl acetate (2 x 40mL) and the aqueous layer was collected. Since 12-ADA was insoluble in ethyl acetate and water, it precipitated and separated together with the aqueous layer. Next, equal volume of tert-butanol, NaOH (1.1 eq) and Di-tert-butyl dicarbonate (Boc-anhydride 2.0 eq) was added to the aqueous layer and stirred at room temperature for 18 hours. After the resulting reaction solution was extracted with ethyl acetate and washed with brine, and dried with $MgSO_4$. To enhance purity of the purified product, the resulting solution was purified with silica column chromatography with Hexane and ethyl acetate. Finally, the purified Boc-protected 12-ADA was concentrated in vacuum to obtain desired product. The isolation yield was 66.5% (390mg of Boc protected 12-ADA). The purified product was confirmed by ^{1}H NMR (Figure 3.44).

^{1}H NMR of Boc protected 12-ADA

Boc-protected 12-ADA ^{1}H NMR (400 MHz, CDCl$_3$): 1.26 (m, 16H), 1.48 (s, 9H), 1.64 (m, 2H), 2.35 (t, J = 12, 2H), 4.17 (t, J = 8, 2H), 4.88 (s, 1H), 10.05 (s, 1H)

3.3 Results and disccusion

3.3.1 Construction of cell-H^m, cell-A^m, and cell-R^m modules for the multilayer enzyme cascade system

Three cell modules (cell-H^m, cell-A^m and cell-R^m) were designed to produce biopolymer monomers from fatty acid methyl ester (FAME) by a multilayer cascade enzyme reaction. There are a number of advantages for the multi-enzymatic cascade reaction with cell modules, such as (i) reduction of the redox constraints or protein expression burden through distribution of the enzymatic pathway across the cell modules, (ii) parallel construction or optimization of the expression system in each cell module, (iii) ability to adjust the reaction solution concentration in each cell module to increase productivity through beneficial interactions between cell modules, and (iv) ability to combine cell modules to generate the desired product.(Wang et al. 2020) Since β-oxidation is activated by acyl-CoA synthetase (FadD) in *E. coli*, BW25113 ($\Delta fadD$, DE3) was selected as the host strain to reduce loss of the substrate (Bae et al. 2014).

Cell-H^m contains a monooxygenase to catalyze hydroxylation

of FAME to its corresponding ω-HFA. Cell-A^m consists of an aldehyde reductase (AHR) that catalyzes the oxidation of alcohols to ketones and ω-transaminase (ω-TA), which mediates the conversion of aldehydes to amine compounds. Cell-R^m contains carboxylic acid reductase (CAR) for the conversion of the carboxyl group to hydroxyl group (Figure 3.1). The AlkBGT system was selected as the hydroxylation system of cell-H^m, since it is known to produce more 12-HDA from DAME than the P450 system in *E. coli*.(Julsing et al. 2012, Scheps et al. 2013) To construct cell-H^m, various monooxygenases and FadL from *E. coli* were cloned in a pCDF duet vector, and AlkG and AlkT from *Pseudomonas putida* GPo1 were cloned in a pET duet vector. In addition to AlkB from *Pseudomonas putida* GPo1, five additional non-heme alkane monooxygenases from *Pseudomonas pelgia* (PpAlkB), *Curvibacter* sp. PAE-UM (CuAlkB), *Citreicella* sp. 357 (CiAlkB), *Thalassolituus oleivorans* (ToAlkB), and *Leptospira alstonii* (LaAlkB), which are known to have activity toward DAME,(Yoo et al. 2019) were cloned into the pCDF duet vector with FadL for monooxygenase screening (Figure 3.2). After FAME was converted to ω-hydroxy fatty acid methyl ester by the AlkBGT system, it was hydrolyzed to ω-HFA

by endogenous hydrolases such as lipase or esterase in *E. coli* (Figure 3.1).(Kadisch, Schmid, and Bühler 2017) Cell-A^m was composed of AHR and ω-TA. To construct cell-A^m, AHR from *Synechocystis* sp. PCC 6714 was cloned into the pET duet vector and ω-TA was cloned into pET28a. Further, four ω-TAs from *Silicibacter pomeroyi* (SpTA), *Vibrio fluvialis* JS17 (VfTA), *Chromobacterium violaceum* (CvTA), and *Agrobacterium tumefaciens* (AtTA),(Sung et al. 2018) which are known to have activity toward oxo-fatty acids, were cloned into pET28a for transaminase screening (Figure 3.2). The hydroxyl groups of fatty alcohols or ω-HFA were converted to aldehydes by AHR, followed by subsequent amination using ω-TA (Figure 3.1). Finally, cell-R^m was composed of CAR and Sfp. Recently, CAR from *Mycobacterium marinum* (MmCAR) was reported to exhibit selective reduction of the carboxylic acid functional group of ω-HFAs to corresponding aldehydes and high catalytic efficiency of Sfp from *Bacillus subtilis* on a separate plasmid since loading of a phosphopantetheine group onto CAR enzymes is essential for CAR activity (Figure. 3.1).(Akhtar, Turner, and Jones 2013, Venkitasubramanian, Daniels, and Rosazza 2007) Hence, Cell-R^m

was constructed by cloning CAR from *M. marinum* into the pET duet vector and Sfp from *B. subtilis* into pET24ma (Figure 3.2). CAR converted the carboxyl group of the fatty acid into an aldehyde; subsequently, endogenous aldehyde reductases of *E. coli* converted the aldehyde to its corresponding alcohol. Aldehydes in *E. coli* are known to be rapidly converted to their less toxic corresponding alcohols by endogenous enzymes.(Kunjapur, Tarasova, and Prather 2014)
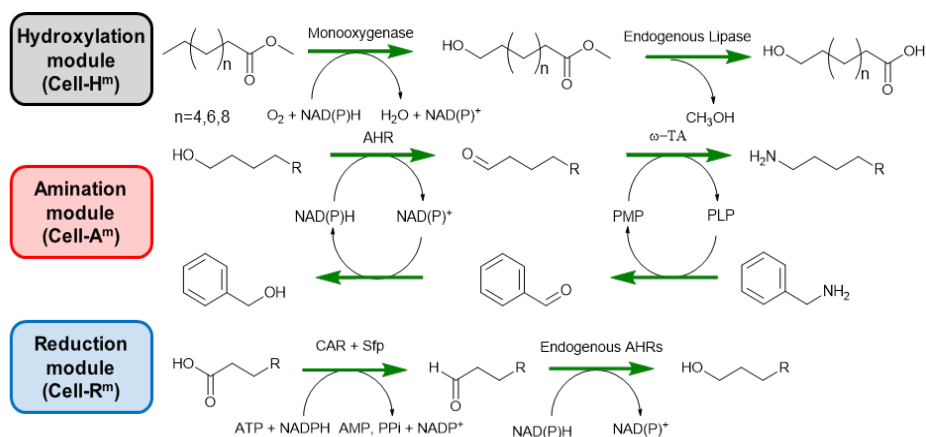
Figure 3. 1 Description of the reaction of each cell module. The hydroxylation module (cell－H^m; black), composed of monooxygenase; redox partners AlkG and AlkT; and FadL as a transporter, attaches hydroxyl group to the end of the fatty acid. The amination module (cell－A^m; red), composed of AHR and ω－TA, converts hydroxyl group of hydroxy fatty acid and aliphatic alcohol into amide group. The reduction module (cell－R^m; blue), composed of CAR and phosphopantetheinyl transferase (Sfp), converts the carboxyl group of fatty acids into aldehyde. Subsequently, endogenous aldehyde reductases inside *E. coli* convert aldehyde to its corresponding alcohol.
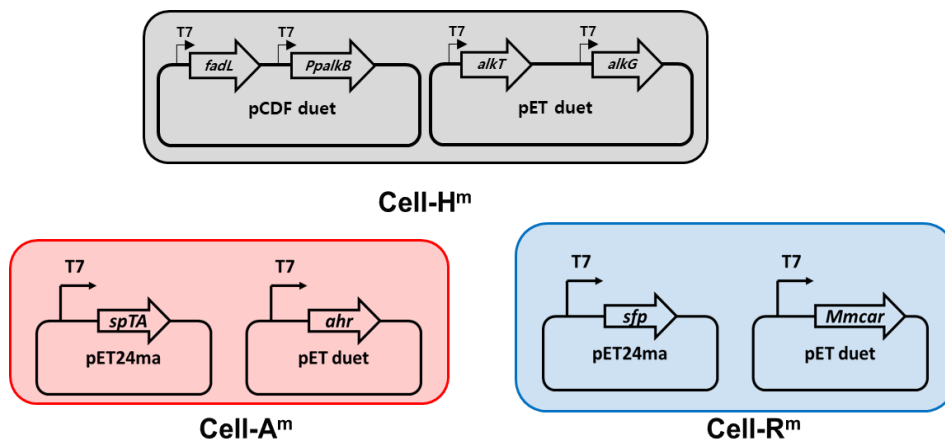
Figure 3. 2 Co−expression plasmid diagram of each cell module in BW25113 (Δ*fadD*, DE3).

3.3.2 Biosynthesis of ω－AFA using cell－H^m and cell－A^m cascade reaction system

Nylon 12 is used as a braking systems and coating for fuel in most automobiles due to its excellent heat, abrasion, chemical, UV, and scratch resistance, and 12－amino dodecanoic acid (12－ADA) is known as a monomer for Nylon 12 synthesis.(Ladkau et al. 2016, Wilding et al. 2015) Due to the importance of the Nylon 12 monomer, DAME was used as the model substrate to synthesize various ω－AFA from FAME. In the cascade reaction, 12－HDA was produced from DAME by cell－H^m, followed by further conversion into 12－ADA via aldehyde by AHR and ω－TA in cell－A^m (Figure 3.3). First, in a monooxygenase screening of cell－H^m, various monooxygenases (AlkB, PpAlkB, LaAlkB, ToAlkB, CuAlkB, and CiAlkB) were examined in the presence of SpTA, which is reported as the best enzyme for the conversion of 12－HDA to 12－ADA.(Sung et al. 2018) (S)－α－Methylbenzylamine ((S)－α－MBA) was selected as an amino donor, and 1% (w/v) glucose was supplied every 6 hours to regenerate NAD(P)H in the reaction media. Among them, PpAlkB produced the largest amount of

product (3.2 mM), whereas 2.1 mM of 12-ADA was produced with AlkB (Figure 3.4). Therefore, PpAlkB was selected as the monooxygenase of cell-H^m. Next, ω-TA biosynthesis ability was compared in cell-A^m using four reported enzymes (SpTA, VfTA, CvTA, and AtTA).(Sung et al. 2018) Similar amounts (around 2.8 mM) of 12-ADA were produced with the four ω-TAs (Figure 3.5). Therefore, cell-H^m with PpAlkB and cell-A^m with SpTA were selected for further optimization experiments.

When performing a multilayer enzyme cascade reaction, the concentration ratio of cells in the reaction media is an important factor in determining the amount of product.(Ricca, Brucher, and Schrittwieser 2011) Therefore, the ratio in each module using a fixed amount of cells [final optical density at 600 nm (OD$_{600}$) was 60] was optimized. At a 2:1 ratio in cell-H^m and cell-A^m, 3.08 mM of 12-ADA was produced (Figure 3.6). By contrast, only 1.35 mM of 12-ADA was produced at a 1:2 ratio of cell-H^m and cell-A^m (Figure 3.6). Glucose was used to regenerate NAD(P)H for the PpAlkB reaction in cell-H^m. Additionally, glucose will be converted into pyruvate through glycolysis, which is known as a universal amino acceptor for ω-TA.(Han, Jang, and Shin 2019) Therefore,

to optimize the amount of glucose in the reaction media, 0.5-8% (w/v) of glucose was supplied every 6 hours, and 2% (w/v) of glucose was found to produce 4.3 mM 12-ADA (Figure 3.7). Removal of the deaminated amino donor (acetophenone) is crucial for the efficient ω-TA reaction.(Park and Shin 2013) In the previous report, benzylamine served as amino donor to the ω-TA and on the other hand after deamination to benzaldehyde also as oxidant by AHR to benzyl alcohol which might minimizing the inhibition of the ω-TA by benzaldehyde.(Sung et al. 2018) In the previous report, benzyl amine served as amino donor to the ω-TA and on the other hand after deamination to benzaldehyde also as oxidant by AHR to benzyl alcohol which might minimizing the inhibition of the ω-TA by benzaldehyde and about 91.5 mM of 12-ADA was produced from 100 mM 12-HDA with 200 mM benzyl amine as amino donor.(Sung et al. 2018)   Therefore, benzyl amine was used as an amino donor, and the deaminated amino donor (benzyl aldehyde) was utilized by AHR for conversion into benzyl alcohol with NAD(P)H regeneration (Figure 3.1). After a 12-hour reaction, 4.88 mM of 12-ADA was produced, which was an 18% increase compared to $(S)-\alpha$-MBA as an amino donor (Figure 3.8).

The optimal pH of AlkB is known to be 7.5,(Schrewe et al. 2011) while that of SpTA is 8.0.(Sung et al. 2018) The pH of the reaction should be carefully determined to balance enzyme activities. Tris buffer (100 mM, pH 8.0) was evaluated as a reaction buffer. In brief, 4.96 mM 12-ADA was produced from 10 mM DAME with Tris buffer (100 mM, pH 8.0), which is a 13% increase compared to the reaction with potassium phosphate buffer (100 mM, pH 7.5) (Figure 3.9). To synthesize higher concentrations of 12-ADA, the reaction was optimized using 100 mM DAME, which produced 30.4 mM of 12-ADA after 12 hours (Figure 3.10). In the cascade reaction for the biosynthesis of 12-ADA, the amount of intermediates (such as 12-HDA) in the reaction solution was negligible (Figure 3.10). 12-HDA is known to have inhibitory effects in monooxygenase-based reactions(Lundemo et al. 2016). To investigate the inhibitory effect of 12-HDA against PpAlkB, 12-HDA inhibition was examined using 10 mM DAME as a substrate and different initial concentrations (0, 5, 10 mM) of 12-HDA. PpAlkB lost nearly 25% of its activity in the presence of 10 mM of 12-HDA. (Figure 3.11). Since almost no 12-HDA was accumulated in the reaction solution, suggesting that biosynthesis and consumption of 12-HDA were almost balanced,

the inhibitory effect of 12-HDA on PpAlkB in cell-H^m might have been minimized. In addition, since 12-HDA is not detected in the reaction media (Figure 3.10) and the production amount of 12-ADA is increased when the ratio of cell-H^m is increased (Figure 3.6), biosynthesis of 12-HDA from cell-H^m could be considered to a rate limiting step of a multi-enzyme cascade reaction that produces 12-ADA from DAME. Following the successful biosynthesis of 12-ADA from DAME as a model system, the applicability of this system to synthesize a wide range of ω-AFAs was examined. To produce ω-AFAs with various chain lengths, FAMEs with diverse carbon numbers (C8~C12) were tested as substrate. Due to the importance of efficient production of ω-AFAs with various carbon numbers, multiple monooxygenases in cell-H^m were examined to determine the most suitable monooxygenase for each carbon number. The highest biosynthesis of 12-ADA (30.5 mM) and 8-amino octanoic acid (29.1 mM) was obtained by cell-H^m with PpAlkB, whereas that of 10-amino decanoic acid (37 mM) was obtained by cell-H^m with ToAlkB (Figure 3.12). On the contrary, the lower amount of product formation was obtained for 6-aminohexanoic acid (1.5 mM) using cell-H^m with AlkB.

Despite the importance of Nylon 12, few studies have been conducted to examine the 12-ADA produced from saturated fatty acids. 0.46 mM 12-amino dodecanoic acid methyl ester was produced from DAME, and 4 mM 12-ADA was produced from dodecanoic acid in *E. coli* (Table 3.1).(Ladkau et al. 2016, Ge et al. 2020) In this study, not only 30.4mM of 12-ADA was produced, but also ω-AFA of various carbon lengths was produced. Therefore, this system might have beneficial applications for biosynthesis of the nylon 12 monomer.
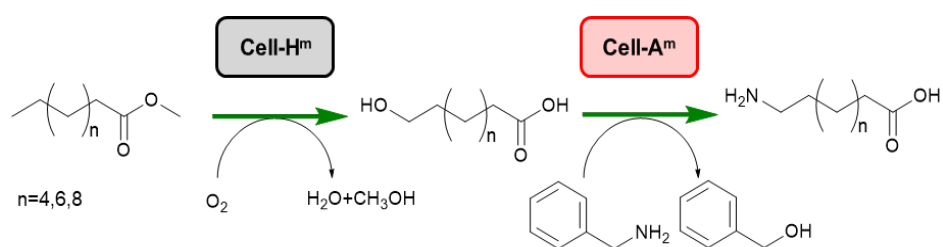
Figure 3. 3 Schematic illustration of ω−AFA biosynthesis by cell−H^m and cell−A^m in one−pot reaction system from FAME.
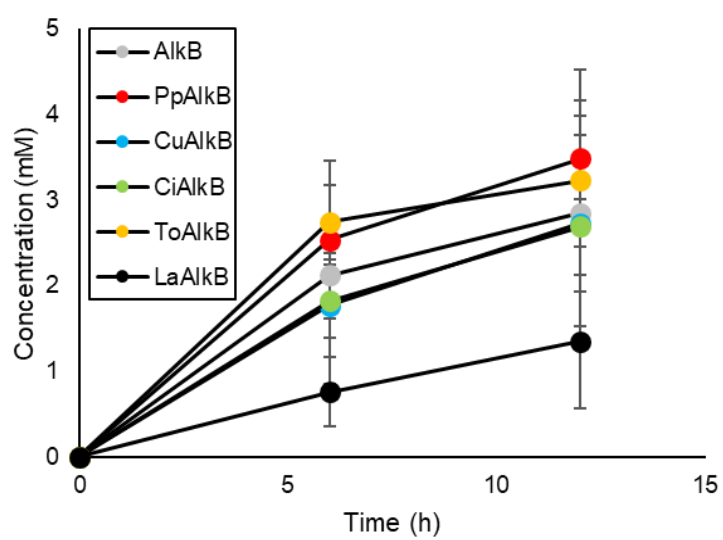
Figure 3. 4 Monooxygenase screening of cell－H^m for 12－ADA
production through concurrent system with SpTA as ω－
Transaminase of cell－A^m
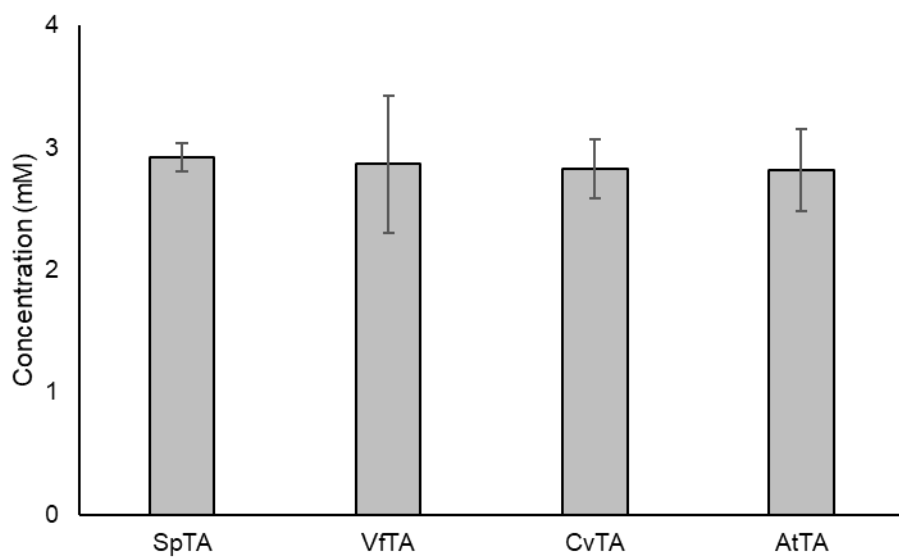
Figure 3. 5 ω−Transaminase screening of cell−A^m to produce 12−ADA reaction with PpAlkB as monooxygenase of cell−H^m.
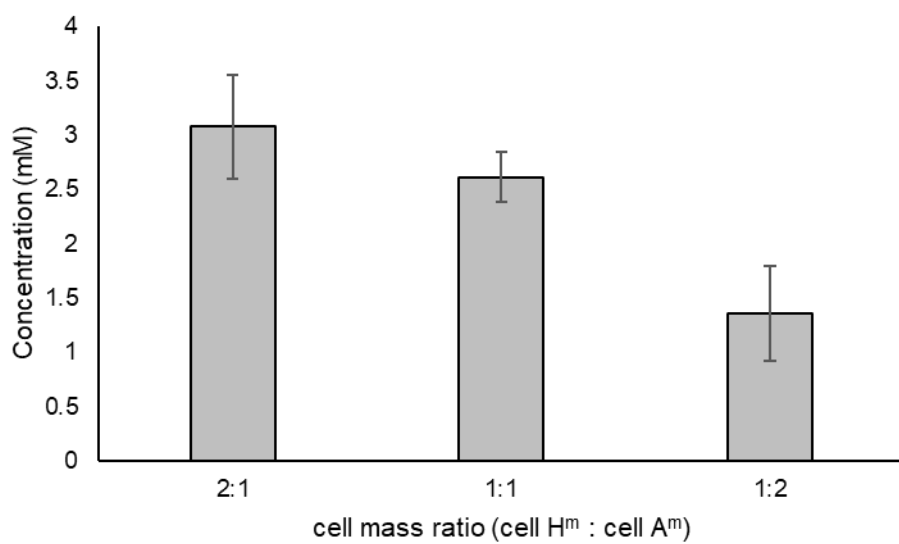
Figure 3. 6 Optimization of cell mass ratio of H^m and A^m to increase the prodcution of $12-ADA$. Sum of total OD600 of cell-H^m and cell-A^m is fixed as 60
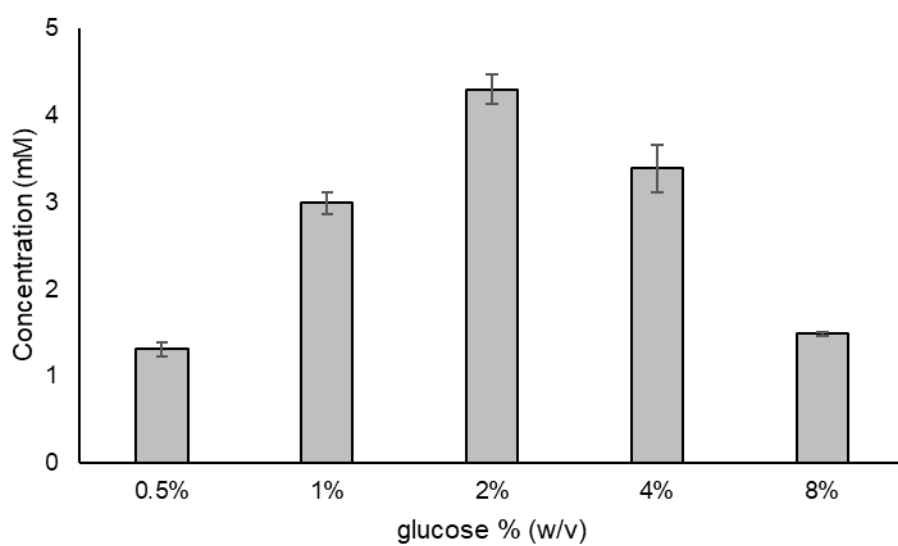
Figure 3. 7 Optimization of glucose concentration to increase the prodcution of 12-ADA. Each concentration of glucose was fed to the reaction media every 6 hours;
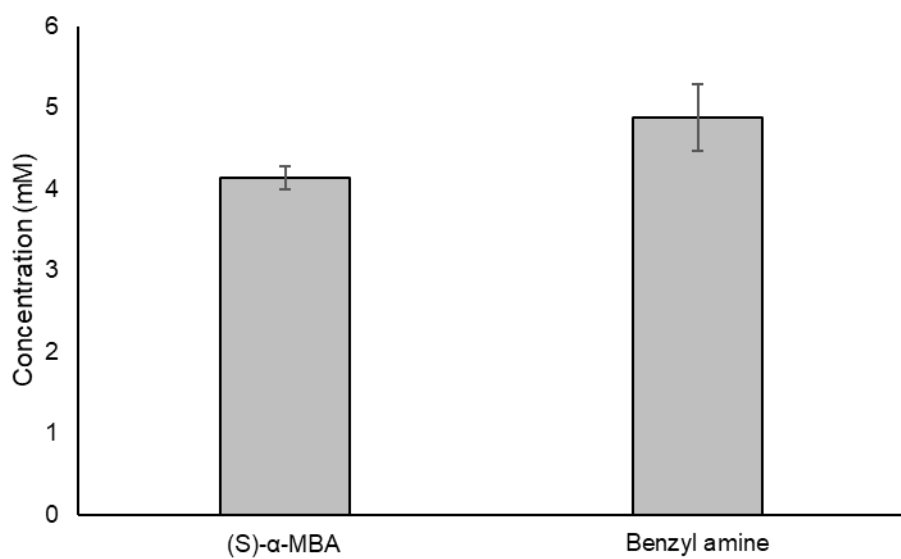
Figure 3. 8 Amino donor optimization to increase the production of 12-ADA
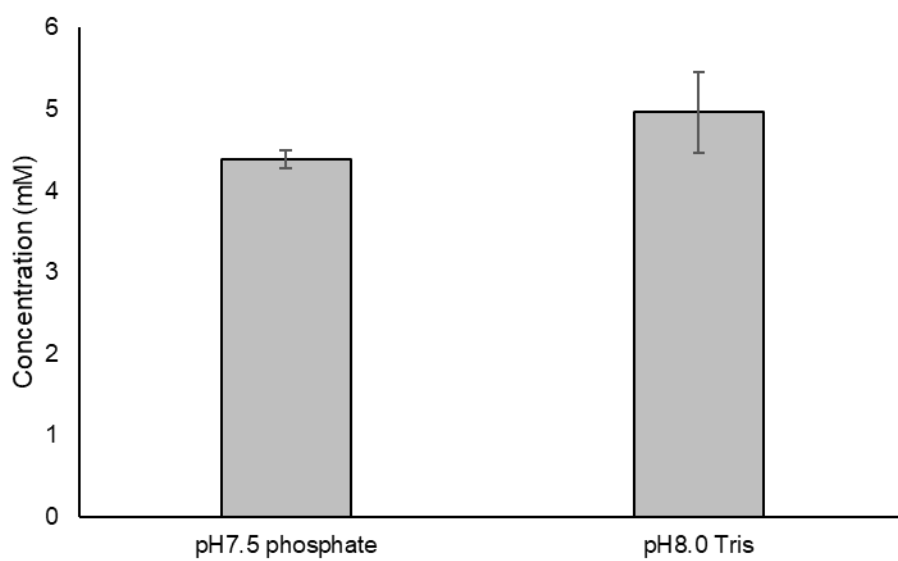
Figure 3. 9 Reaction buffer optimization to increase the production of 12-ADA.
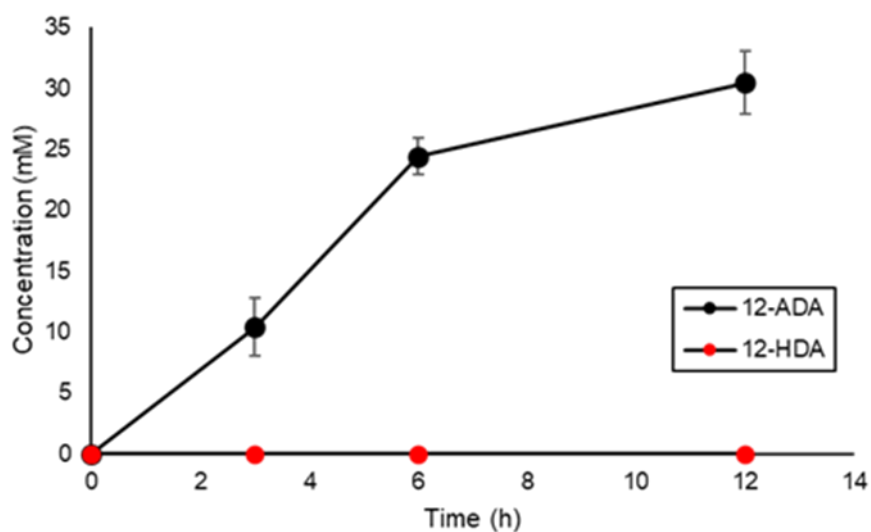
Figure 3. 10 Time profile of 12-ADA production by multi-enzyme cascade reaction performed in Tris buffer (100 mM, pH 8.0) supplemented with 40 OD_{600} cell-H^m and 20 OD_{600} cell-A^m, 100 mM DAME, 200 mM benzyl amine at 30℃ and 2% (w/v) glucose was supplied every 6 hours. Black and red circles indicate 12-ADA and 12-HDA
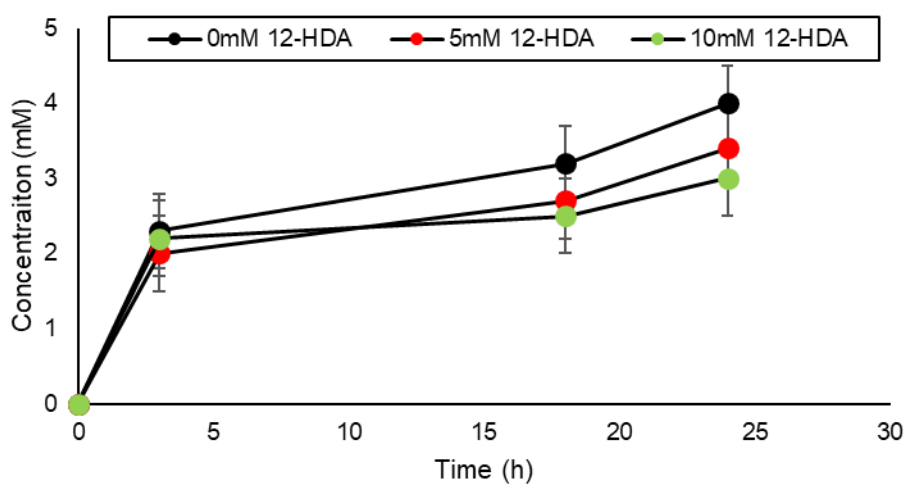
Figure 3. 11 Inhibitory effects of the concentrations of 12-HDA on monooxygeanse activity in the biotransformation of DAME. The reaction were performed with 10 mM of substrate and different initial concentrations (0, 5, 10 mM) of 12-HDA in potassium phosphate buffer (100 mM, pH 7.5).
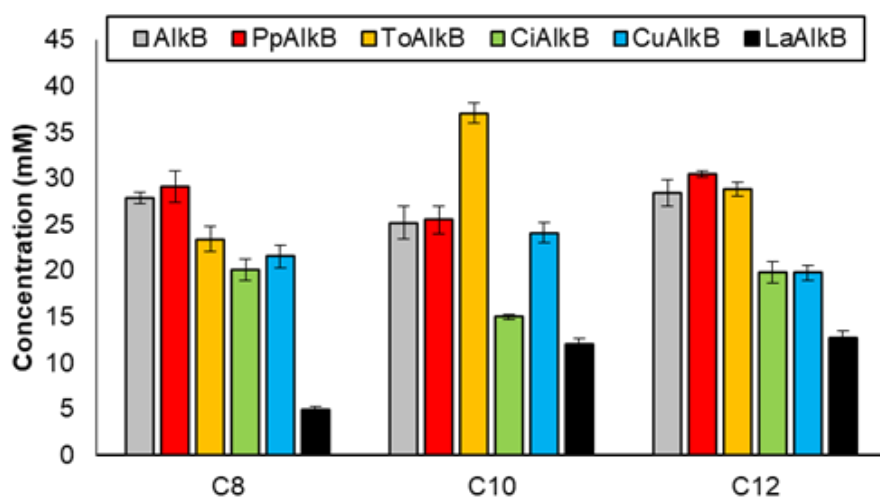
Figure 3. 12 Production of ω−AFA, respectively, with various carbon chain lengths FAME (C8, C10 and C12) and six monooxygenases in cell−H^m. The reaction was performed with the same condition for 12 hours.

3.3.3 Biosynthesis of α,ω-diol in cell-H^m and cell-R^m cascade reaction system

α,ω-diols are used as monomers of polyesters and polyurethanes.(Kawaguchi, Ogino, and Kondo 2017, Sakagami et al. 2013) Currently, industrial-scale manufacturing is limited to short-chain diol biosynthesis, whereas biosynthesis of medium-chain α,ω-diols (C8–C12) has not been extensively studied.[48] Here, DAME was selected as a model substrate to produce α,ω-diol from FAME in a multi enzyme cascade reaction using cell-H^m and cell-R^m (Figure 3.13).

In this study, the highest concentration of 12-ADA was produced by cell-H^m expressing PpAlkB (Figure 3.4). CAR from *M. marinum* (MmCAR) has been reported to cause selective reduction of carboxylic acid to corresponding aldehydes with Sfp from *B. subtilis*. Therefore, a multi-enzymatic cascade reaction was conducted using cell-H^m with PpAlkB and cell-R^m with MmCAR. First, a multi-enzyme cascade reaction was conducted to produce 1,12-dodecanediol (1,12-diol) with 100 mM DAME. The optimal pH of AlkB and MmCAR is 7.5; hence, potassium phosphate buffer

1 1 3

(100 mM, pH 7.5) was used.(Schrewe et al. 2011, Ahsan et al. 2017) Further, the concentrations of cell-H^m and cell-R^m were both fixed at OD$_{600}$ of 30. After 24 hours, 16.3 mM of 1,12-diol was produced (Figure 3.14). In the cascade reaction for the biosynthesis of 1,12-diol from DAME, both NAD(P)H and ATP regeneration are essential to enhance enzyme cascade catalysis in both cell-H^m and cell-R^m reactions. Cellular carbon metabolism is a well-known process to regenerate NAD(P)H or ATP during biotransformation. Therefore, to investigate the effects of the various types of carbon sources on 1,12-diol biosynthesis from DAME, a multi-enzymatic cascade reaction was carried out in the presence of 1% (w/v), 5% (w/v), 10% (w/v) of glucose, 1% (w/v) glycerol, and 1% (w/v) Terrific broth (TB) in potassium phosphate buffer (100 mM, pH 7.5). In addition, complex media suitable for ATP regeneration in *E. coli*, such as Luria-Bertani broth (LB), Terrific broth (TB), and Riesenberg media (RB), were selected since ATP was the main cofactor for the CAR reaction in cell-R^m. In brief, 30 OD$_{600}$ cell-H^m and 30 OD$_{600}$ cell-R^m were resuspended in the potassium phosphate buffer (100 mM, pH 7.5) or complex media for the reaction. When 5% (w/v) glucose was used as C-

source, 17 mM of 1,12-diol was produced (Figure 3.15). Moreover, supplementation of 1, 2.5, 5, and 7.5% (w/v) glucose to the reaction mixture every 6 hours were examined, and 18.1 mM of 1,12-diol was detected when 2.5% (w/v) glucose was supplied every 6 hours (Figure 3.16). Therefore, all subsequent experiments were performed by supplying 2.5% (w/v) glucose every 6 hours. After carbon source optimization, the concentration of each cell module was optimized. Results showed a slower reaction in cell-H^m than cell-R^m since 12-HDA was not accumulated in the reaction solution (Figure 3.14). Therefore, cell-H^m concentration optimization was examined in the presence of 30 OD_{600} of cell-R^m at various concentrations (OD_{600} of 30, 60, 90, 120) of cell-H^m, for which 60 OD_{600} produced 23.1 mM of 1,12-diol in cell-H^m (Figure 3.17). 12-HDA was present in a trace amount in the reaction media (Figure 3.14). In addition, when the OD_{600} of cell-H^m was increased from 30 to 60, the production amount of 1,12-diol was increased (Figure 3.17). In view of this, it could be considered that the limiting step of the enzyme cascade reaction to produce 1,12-diol from DAME is to produce 12-HDA from cell-H^m. This is the same

pattern as when 12-ADA is produced from DAME using cell-H[m] and cell-A[m].

To increase variety of biopolymer monomers, production of α,ω-diols at various chain lengths is important.(Kawaguchi, Ogino, and Kondo 2017) Therefore, α,ω-diol production was measured using various carbon chain lengths of FAME (C8 to C12) as the substrate. In brief, 8.3 mM 1,8-octanediol, 11.2 mM 1,10-decanediol, and 17.6 mM 1,12-diol were produced (Figure 3.18). Further, the amount of biopolymer monomer produced was found to be dependent on the monooxygenase in cell-H[m] (Figure 3.4, Figure 3.12). Therefore, α,ω-diol production might be maximized using different monooxygenases in cell-H[m]. Production of short chain α,ω-diols by chemical production is well established. However, biosynthesis of medium chain α,ω-diols has not been studied extensively.(Jiang and Loos 2016b) 4.94 mM of 1,8-octanediol from 1-octanol and 6.48 mM of 1,12-diol from 12-HDA in *E. coli* (Table 3.1).(Ahsan et al. 2017, Fujii et al. 2006) In this study, 23.1 mM of 1,12-diol was produced from DAME, which might be attributed to the progress of biopolymer monomer research.
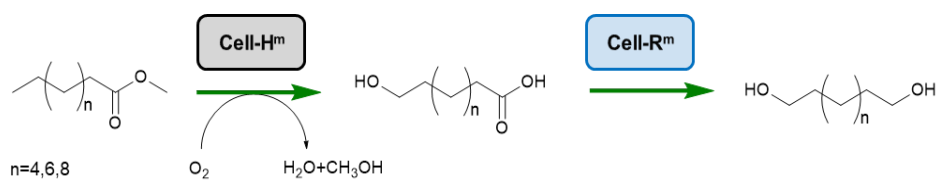
Figure 3. 13 Schematic illustration of α,ω−diol biosynthesis from FAME as substrate by cell−H^m and cell−R^m in one−pot reaction system.
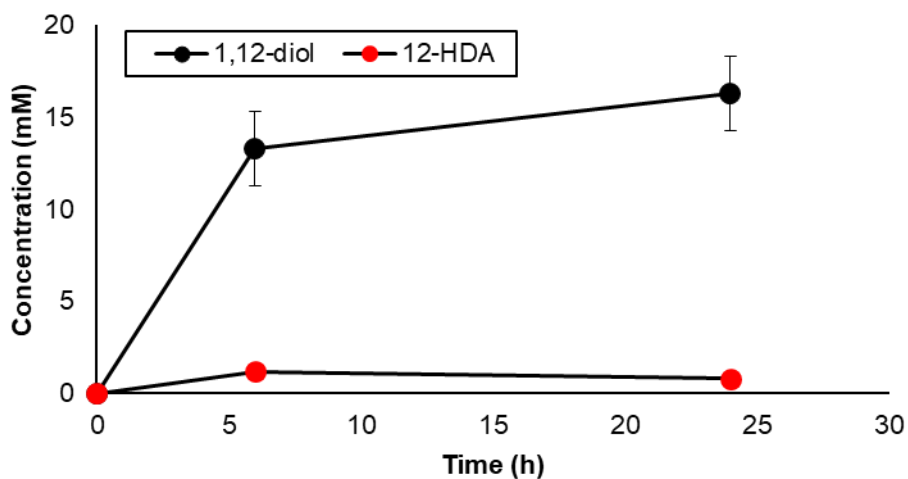
Figure 3. 14 1,12-diol production through 100 mM of DMAE as substrate. 30 OD_{600} of cell-H^m and cell-R^m, 100 mM DAME, 1%(w/v) glucose was used for the reaction in potassium phosphate buffer (100 mM, pH 7.5). The reaction was performed in potassium phosphate buffer (100 mM, pH 7.5) with 100 mM DAME, 10 mM $MgCl_2$ as substrate at 30 ℃ with 200 rpm for 24 hours reaction. Black circle indicates 1,12-diol and red circle indicates 12-HDA.
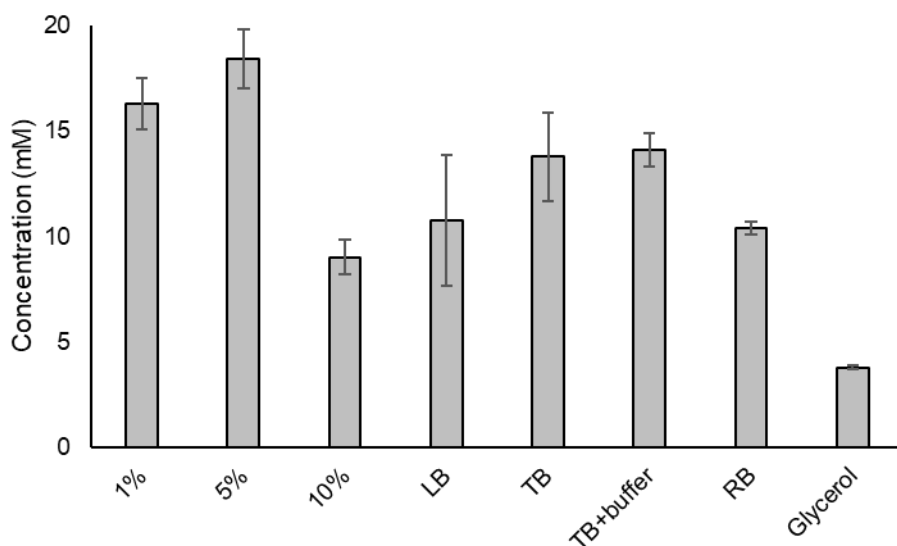
Figure 3. 15 Carbon source optimization to 1,12-diol production, in which 1, 5 and 10% indicate glucose concentration. Comparison of the various glucose concentrations, glycerol and TB+buffer, and potassium phosphate buffer (100 mM, pH 7.5) supplemented with 30 OD_{600} in cell-H^m and cell-R^m to 100 mM DAME, 10 mM $MgCl_2$ with 1, 5, 10% (w/v) glucose, 1% (w/v) glycerol, 1% (w/v) TB at 30℃ for 24 hours. To compare complex media, cells were diluted in each complex media with 100 mM 30 OD_{600} of cell-H^m and cell-R^m, 100 mM DAME, and 10 mM $MgCl_2$ and the reaction was conducted at 30℃ for 24 hours. Abbreviations: LB: Luria-Bertani broth, TB: Terrific broth, RB: Riesenberg media.
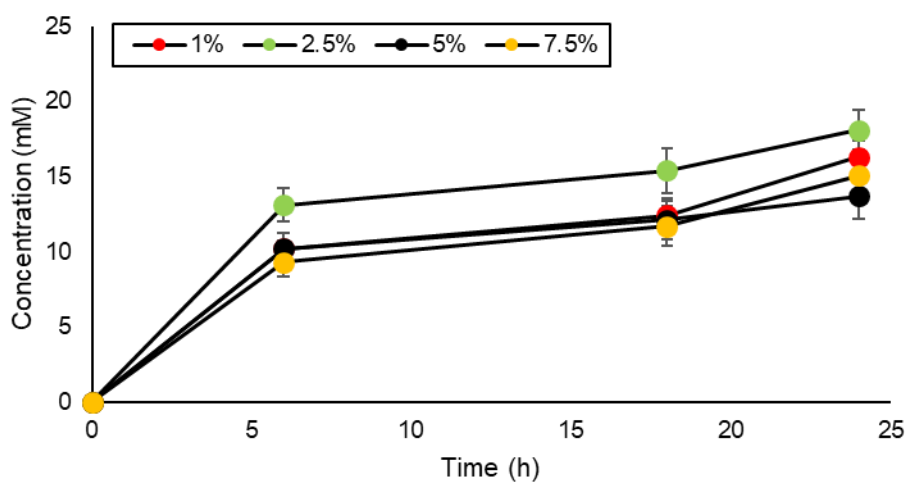
Figure 3. 16 Glucose optimization to produce 1,12−diol with cell−H^m and cell−A^m. Optimization of glucose concentration supplied every 6 hours. Each glucose concentration indicates %(w/v) value. Glucose optimization was performed in potassium phosphate buffer (100 mM, pH 7.5) with 100 mM DAME ase substrate at 30 ℃ with agitation of 200 rpm for 24 hours reaction.
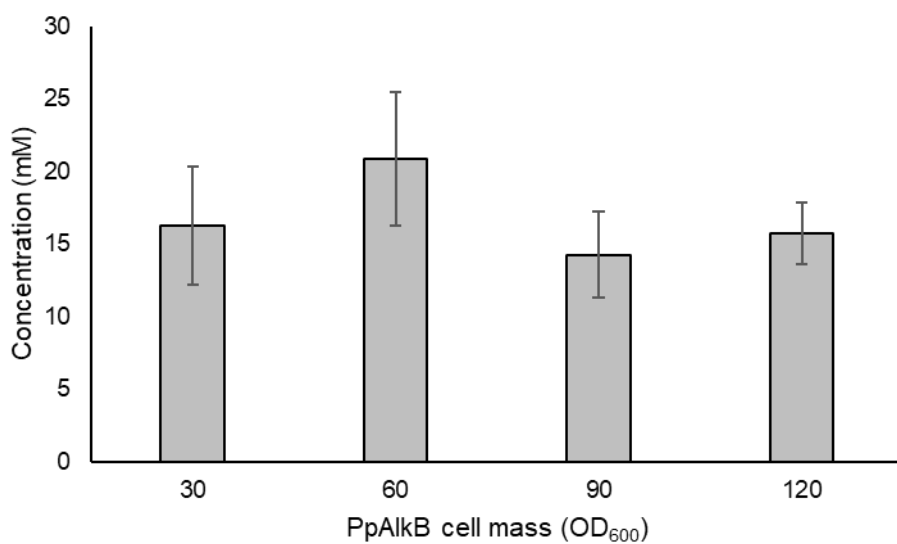
Figure 3. 17 Optimization of 1,12-diol production by optimizing the concentration of cell-H^m and cell-R^m. The cell concentration of cell-R^m was fixed to 30 OD$_{600}$ and only the concentration of cell-H^m was changed to OD$_{600}$ of 30, 60, 90 and 120. Cell concentration optimization was performed in potassium phosphate buffer (100 mM, pH 7.5) with 100 mM DAME, 10 mM MgCl$_2$ as substrate at 30 ℃ with 200 rpm for 24 hours reaction.
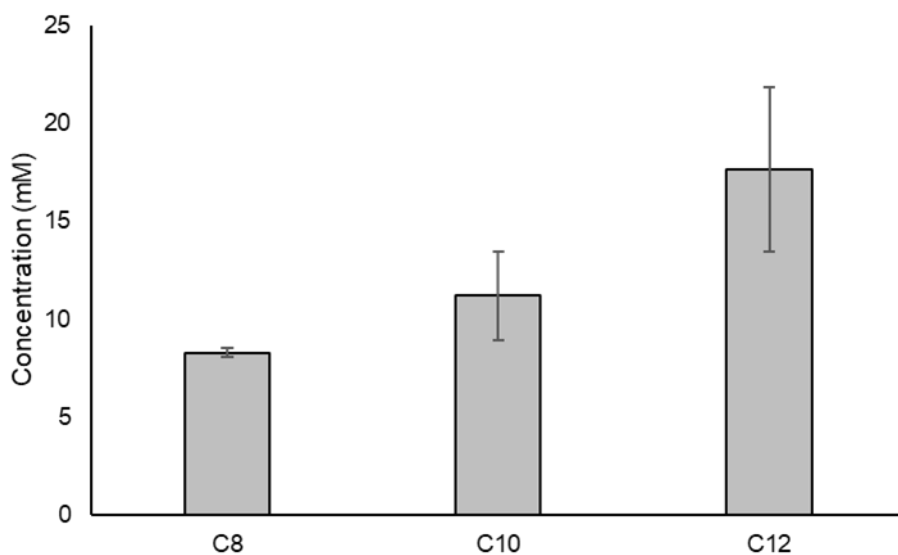
Figure 3. 18 Production of α,ω−diols by various carbon chain lengths with FAME as the substrate. The reaction was performed in potassium phosphate buffer (100 mM, pH 7.5) supplemented with 60 OD_{600} of cell−H^m and 30 OD_{600} of cell−R^m, 100 mM FAME, 10 mM $MgCl_2$ at 30℃ for 24 hours

3.3.4 Biosynthesis of aliphatic amine using cell−H^m, cell−R^m, and cell−A^m in cascade reaction system

Medium−chain α,ω−diamines are used as monomers for polyamides with low moisture absorption and high mechanical resistance.(McKeen 2012) However, fermentative production of medium−chain diamines from renewable carbon sources has not been reported yet. In this study, DAME was selected as a model substrate to produce α,ω−diamine in a multi−enzymatic cascade reaction. Enzyme cascade reactions can be classified as concurrent or sequential reactions. In a concurrent reaction, reaction conditions do not change between successive steps, and no new reagents are added after the initial step. By contrast, in sequential reactions, the second catalyst or a specific major reagent can be added only after the first step has been completed.(Rudroff et al. 2018) To classify the optimal reaction for 1,12−diaminododecane (1,12−diamine) production using three modules (Figure 3.19), both concurrent and sequential reactions were conducted.

In brief, a sequential reaction was conducted to measure 1,12-diamine production from DAME using three cell modules. First, to synthesize 1,12-diamine by sequential reaction, 1,12-diol was produced from DAME in the presence with 60 OD_{600} of cell-H^m and 30 OD_{600} of cell-R^m for 24 hours. In the second step, 120 OD_{600} of cell-A^m and 400 mM benzyl amine were added to the reaction solution to produce 1,12-diamine (Figure 3.20). After 24 hours, 0.74 mM 12-amino-1-dodecanol (1,12-aminol) and 2.35 mM 1,12-diamine were produced by sequential reaction (Figure 3.21). Next, since 1,12-diol has poor solubility in water, 1% DMSO was added to increase its solubility in the reaction solution, after which 3.6 mM of 1,12-aminol and 10.3 mM 1,12-diamine were produced (first step: 24 hours, second step: 24 hours) (Figure 3.22). Subsequently, a concurrent reaction system was conducted to produce 1,12-diamine from DAME (Figure 3.19). After a 24-hour reaction, 8.3 mM 1,12-diamine and 4.1 mM 1,12-aminol were produced from 100 mM DAME (Figure 3.22). Notably, the concurrent reaction system with cell-H^m, cell-A^m, and cell-R^m combined generated a total 12.4 mM (4.1 mM 1,12-

aminol and 8.3 mM 1,12-diamine), whereas 32 mM of 12-ADA was produced using the cell-H^m and cell-A^m combined reaction system. This finding might be due to the complexity of the multi-enzymatic cascade reaction with three modules. Although the reaction using the sequential reaction produced slightly more products than the concurrent reaction, a concurrent reaction was a reaction that proceeds for 24 hours, and a sequential reaction was a reaction that proceeds for 48 hours (24 hours for 1,12-diol production and 24 hours for 1,12-diamine production) (Figure 3.22). Therefore, the productivity was 0.52 mM/h with the concurrent reaction, which was about 2 times better than the productivity of 0.29 mM/h with the sequential reaction. In the industrial production of bioplastic monomer, titer increase is important, but productivity is also a very important consideration. Therefore, further experiments were conducted with concurrent reactions. To increase production amounts, optimization of reaction conditions was conducted by adjusting the glucose and amino donor concentrations in the reaction solution. First, the glucose concentration was optimized for cofactor regeneration in the

reaction. The reaction was conducted with 1% (w/v), 5% (w/v), and 10% (w/v) glucose. Both 1% (w/v) and 5% (w/v) glucose were added at the start of the reaction, whereas in the case of 10% (w/v), 2.5% (w/v) of glucose was supplied every 6 hours. The highest amount of products was obtained with 5% (w/v) of glucose, yielding 14.3 mM (7.8 mM of 1,12−diamine and 6.5 mM of 1,12−aminol) of amine compounds after 24 hours. Results with 10% (w/v) glucose were similar, yielding 14.2 mM (7.6 mM of 1,12−diamine and 6.6 mM of 1,12−diamine) of products (Figure 3.23). Therefore, reaction solution containing 5% (w/v) glucose was selected for the concurrent reaction. After optimization of glucose concentration, the concentration of benzyl amine was varied from 50 mM to 400 mM, resulting in production of 5.1 mM of 1,12−aminol and 8.4 mM of 1,12− diamine with 400 mM of initial benzyl amine. By contrast, 16.2 mM of 1,12−aminol and only 0.2 mM of 1,12−diamine were produced with 50 mM of initial benzyl amine (Figure 3.24). Total amount of products remained unchanged when varying amino donor concentration, but the ratio between 1,12−aminol and 1,12−diamine was altered with various concentration of

benzyl amine. Therefore, the product ratio might change, depending on the amino donor concentration. However, as the total amount of production was higher when the concentration of Benzyl amine was 50mM than when 400mM was used, it can be seen that the high concentration of benzyl amine had an effect on the reaction.

Based on the successful production of 1,12−diamine from DAME as model system, we further tested production of various chain lengths of α,ω−diamine using this system. FAME at various chain lengths (C8~C12) was used as a substrate for the concurrent reaction using the three cell modules. In brief, 9.6 mM (5.4 mM of 8−amino−1−octanol and 4.2 mM of 1,8−diaminooctane), 11 mM (4.9 mM of 10−amino−1−decanol and 6.1 mM of 1,10−diaminodecane), and 13.5 mM (5.1 mM of 1,12−aminol and 8.4 mM of 1,12−diamine) were produced by FAME with C8, C10 and C12 carbon chain lengths, respectively (Figure 3.25). The dependency of α,ω−diamine conversion on carbon chain length is similar to that of α,ω−diol production (Figure 3.18). After testing various chain lengths of α,ω−diamine in the three−cell module combined

reaction, efforts were made to maximize $\alpha,\omega-$aminol production by concurrent reaction. Since the ratio between 1,12$-$aminol and 1,12$-$diamine was changed by benzyl amine concentration (Fig. 3.24), 50 mM benzyl amine was supplied in the reaction media to maximize the ratio of $\alpha,\omega-$aminol for the concurrent reaction with FAME at various carbon chain lengths as the substrate. Production of $\alpha,\omega-$aminols increased with 50 mM benzyl amine, whereas production of $\alpha,\omega-$diamines decreased (Figure 3.26). The production of the biopolymer monomer showed the same pattern as above based on carbon chain length, even when produced by sequential reaction (Figure 3.27).

Recently, biosynthesis of short chain $\alpha,\omega-$diamines has been well studied.(Chae et al. 2020) However, few studies on producing medium chain $\alpha,\omega-$diamines in *E. coli* have been conducted, and most studies have produced $\alpha,\omega-$diamines from $\alpha,\omega-$diol as a substrate (Table 3.1).(Chae et al. 2020) Therefore, to produce bioplastic monomers using renewable resources such as food waste as a substrate, studies on the production of $\alpha,\omega-$diamine from saturated fatty acid are

required. In this study, 13.5 mM (5.1 mM of 1,12−aminol and 8.4 mM of 1,12−diamine) of amine compounds were produced from DAME in *E. coli*.
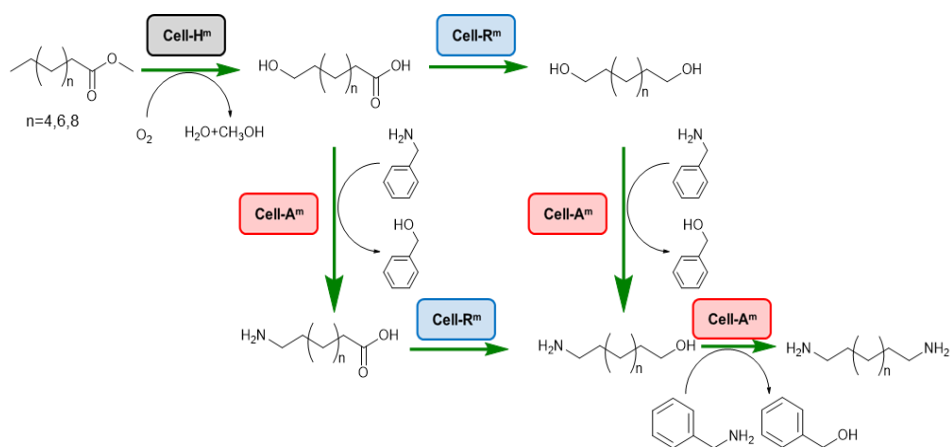
Figure 3. 19 Schematic illustration of α,ω−aminol and α,ω−diamine biosynthesis from FAME by concurrent reactions with three cell based modules in one−pot system.
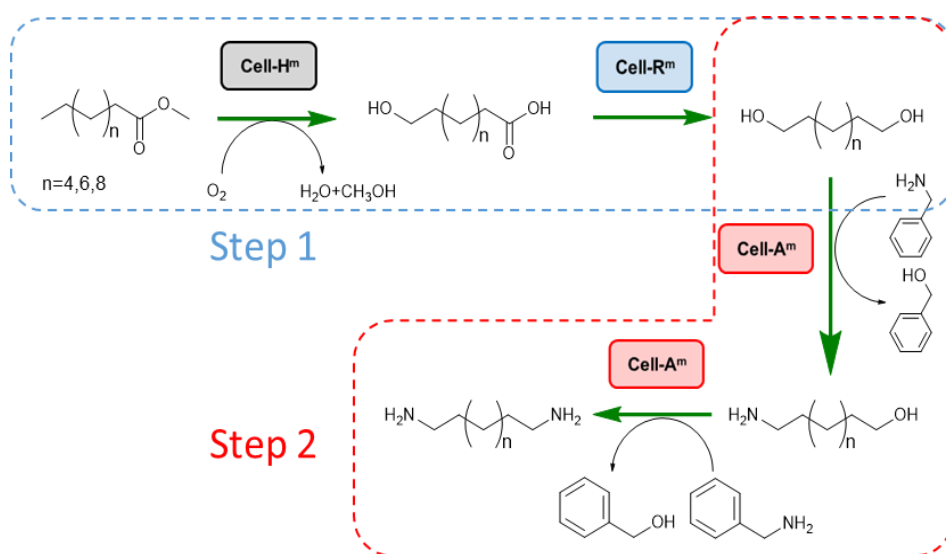
Figure 3. 20 Schematic illustration of α,ω−aminol and α,ω−diamine biosynthesis from FAME by sequential reactions with three cell based modules in one−pot system.
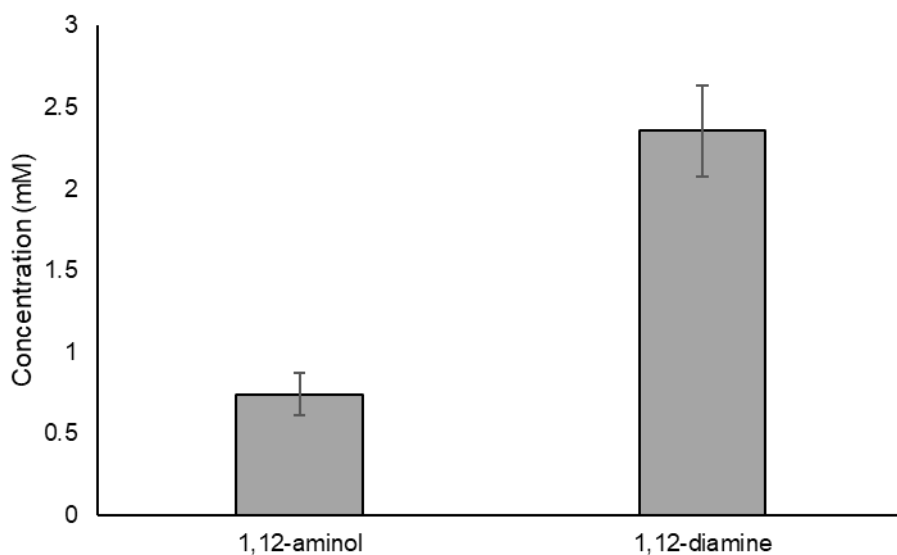
Figure 3. 21 Sequential reaction to produce 1,12−diamine without DMSO. 100 mM DAME, 10 mM of $MgCl_2$, 30 OD_{600} of cell−R^m, 60 OD_{600} of cell−H^m potassium phosphate buffer (100 mM, pH 7.5). The reactions were conducted at 30℃ and 200 rpm 24 hours beforehand and 400 mM of benzyl amine, 120 OD_{600} of cell−A^m was added to the reaction solution. The graph above is the production amount 24 hours after adding cell−A^m
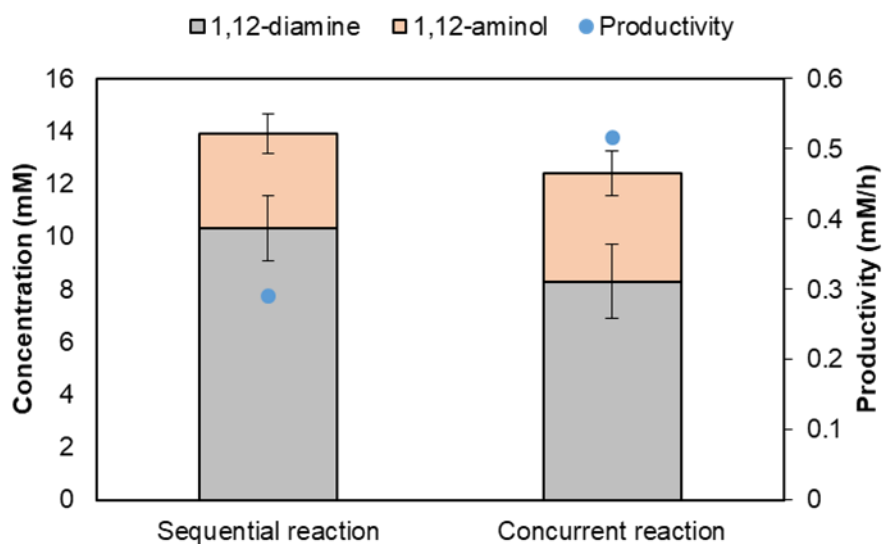
Figure 3. 22 Biosynthesis of α,ω−aminol and α,ω−diamine from FAME by cell−H^m, cell−R^m, and cell−A^m in one−pot reaction system. 1,12−aminol and 1,12−diamine production in concurrent (24 hours after start) or sequential reaction system (24 hours after the addition of cell A^m). Gray square indicates 1,12−diamine and orange square indicates 1,12−aminol.
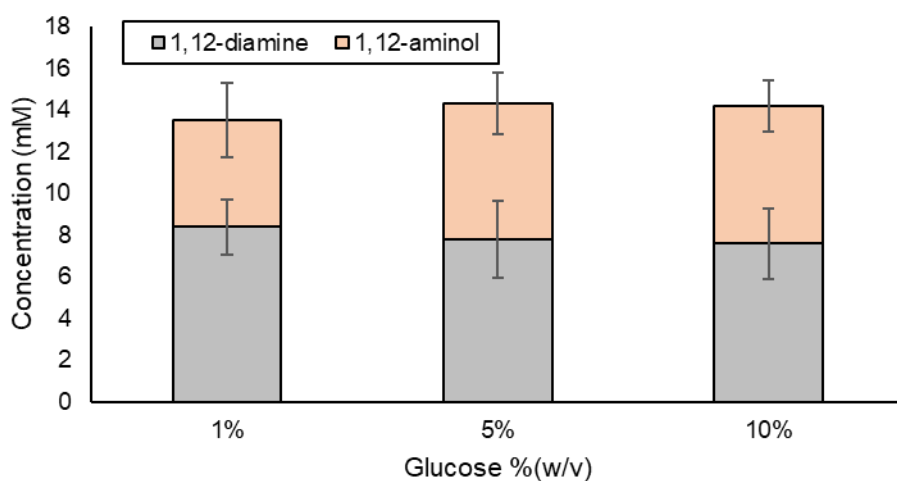
Figure 3. 23 Glucose optimization for concurrent reaction to produce 1,12-diamine. 1% (w/v), 5% (w/v) glucose at the start of reaction and final 10% (w/v) glucose (as a final concentration) was repeatedly supplied to the reaction mixture every 6 hours. Gray square indicates 1,12-diamine and orange square indicates 1,12-aminol.
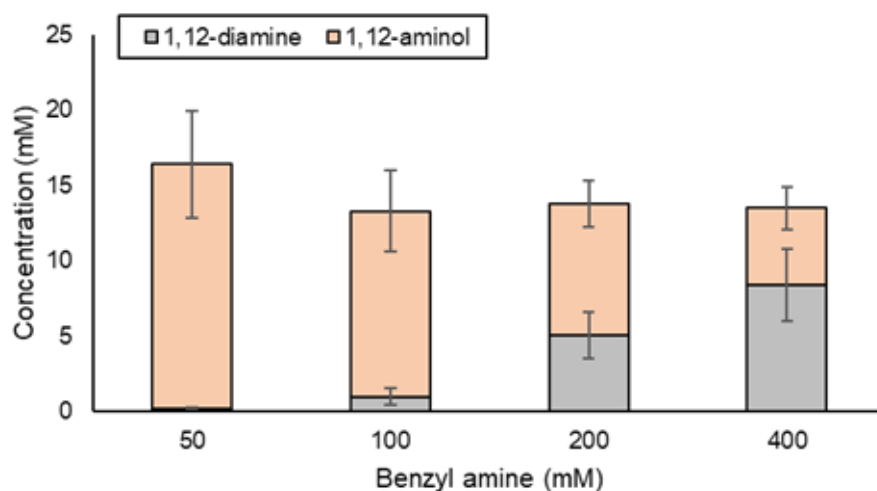
Figure 3. 24 Benzyl amine optimization for 1,12-aminol and 1,12-diamine production. The reaction was performed in potassium phosphate buffer (100 mM, pH 7.5) supplemented with 60 OD_{600} of cell-Hm, 120 OD600 of cell-A^m, and 30 OD_{600} of cell-R^m, 100 mM DAME, 10 mM $MgCl_2$, 1% DMSO, 5%(w/v) glucose, and various concentration of benzyl amine at 30℃ for 24 hours. Gray square indicates 1,12-diamine and orange square indicates 1,12-aminol.
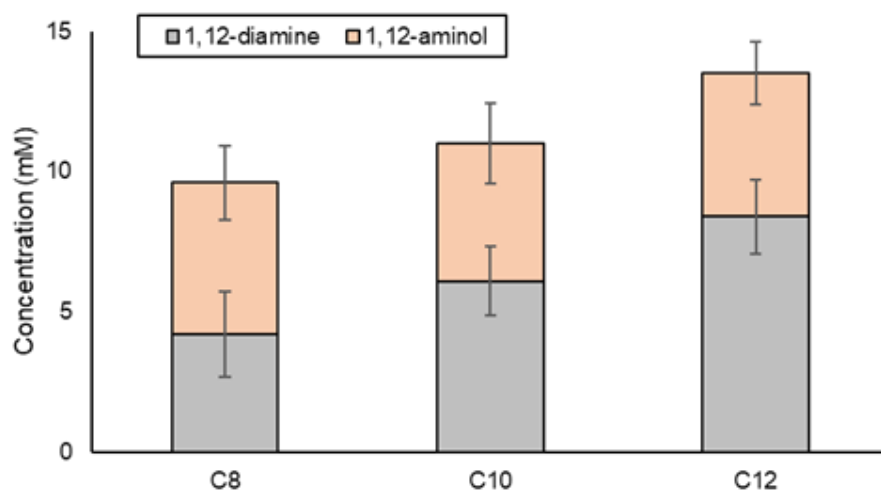
Figure 3. 25 Production of α,ω−aminol and α,ω−diamine by various carbon chain lengths of FAME as the substrate in the presence of 400 mM benzyl amine. Orange square indicates α,ω−aminol, and gray square indicates α,ω−diamine.
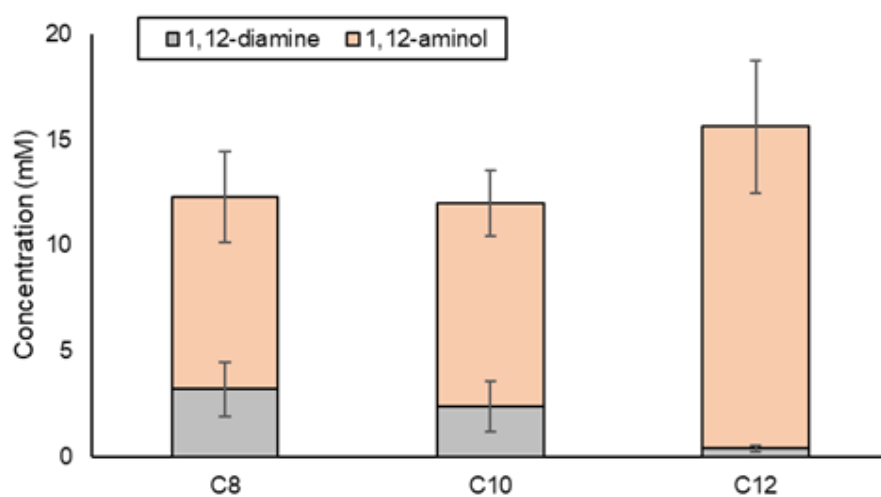
Figure 3. 26 Production of α,ω－aminol and α,ω－diamine by
various carbon chain lengths of FAME as the substrate in the
presence of 50 mM benzyl amine. Orange square indicates α,ω－
aminol, and gray square indicates α,ω－diamine.
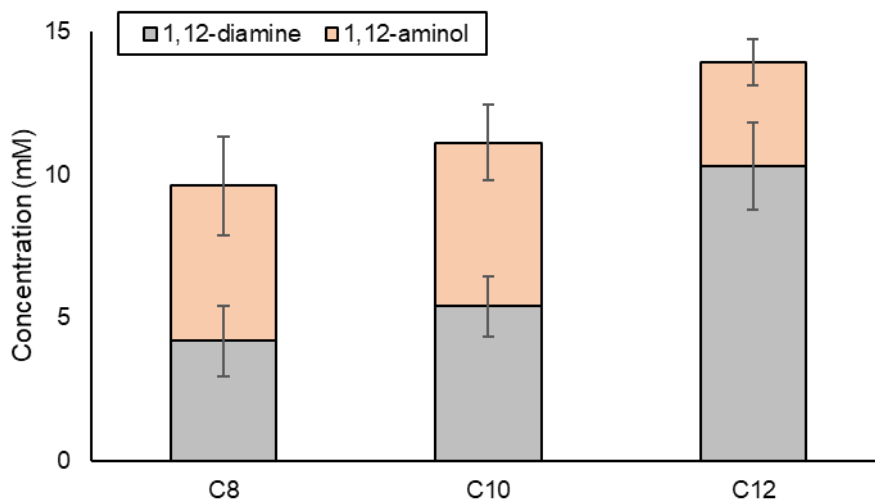
Figure 3. 27 Sequential reaction to produce various carbon chain length α,ω−diamine with 400 mM benzyl amine in shake flask. The reaction was peformed in potassium phosphate buffer (100 mM, pH 7.5) supplemented with 60 OD_{600} cell−H^m and 30 OD_{600} cell−R^m, 5% (w/v) glucose, 100 mM FAME, 10 mM of $MgCl_2$ at 30℃ and 200 rpm 24 hours for α,ω−diol production beforehand. After 24 hours for the α,ω−diol production, 120 OD_{600} cell−A^m and 400 mM benzyl amine, 1% DMSO were added to the reaction media for the production of α,ω−diamine. Gray square indicates 1,12−diamine and orange square indicates 1,12−aminol.

3.3.5 Efficacy of one-pot reaction system in reactor with constant pH control

pH is a factor that can significantly affect enzymatic reactions both in vitro and in vivo. In the whole-cell biocatalyst with high substrate concentrations, it can be difficult to make manual adjustments to pH in the reaction. When producing biopolymer monomers in a shake flask, pH of the reaction media is often manually adjusted every 6 hours. In this study, the pH of the reaction solution was around 6.0 before adjusting pH after 6 hours, and the decrease was offset using 5M NaOH during 1,12-diol production in the shake flask. Therefore, the use of a pH-stat system for continuous maintenance of the initial pH would be beneficial for the reaction. The reaction was carried out using the same reaction conditions as the above mentioned experiments, in a total reaction volume of 40 mL in the reactor and constant pH control (pH controller). First, concurrent reactions to produce 12-ADA or 1,12-diol were carried out in the pH controller using 100 mM DAME. After 48 hours, 46.3 mM of 12-ADA and 27 mM of 1,12-diol were produced from 100 mM DAME (Figure 3.28, Figure

3.29). Thus, the constant pH control showed a positive effect on biopolymer monomer production. Next, 1,12-aimnol and 1,12-diamine were produced from DAME in a concurrent reaction using the pH controller. After 48 hours, 4.2 mM of 1,12-aminol and 14 mM of 1,12-diamine were produced from 100 mM DAME and 400 mM benzyl amine (Figure 3.30). Additionally, 29.12 mM of 1,12-aminol and 2.56 mM of 1,12-diamine were produced using 50 mM benzyl amine to maximize 1,12-aminol production (Figure 3.31). There are two pathways to produce 1,12-diamine in this system (Figure 3.19). We hypothesized that if 1,12-diol was produced preferentially by cell-H^m and cell-R^m, and the activities of the two modules were decreased, 1,12-diamine conversion would increase in the sequential reaction. After producing 1,12-diol for 48 hours with cell-H^m and cell-R^m in 40 mL of final reaction solution, cell-A^m, benzyl amine, and DMSO were added to the reaction media for achieve 45 mL of final reaction solution volume. In the sequential reaction, 21.5 mM of 1,12-diamine and 7.93 mM of 1,12-aminol were produced (Figure 3.32). However, 1,12-aminol was still accumulated in the reaction media, even though activity of the modules in the first reaction was decreased. This might be due to

the higher activity of SpTA in cell−A^m toward 1,12−diol compared that of 1,12−aminol suggesting that a transaminase with higher activity toward 1,12−aminol might increase the production ratio of 1,12−diamine. Constant pH control of the reaction media is important in biotransformation. In this study, higher amounts of products (1,12−ADA, 1,12−diol, 1,12−diamine) were produced using a pH controller compared to the biotransformation produced in a shake flask. Specifically, 46.3 mM of 12−ADA, 27 mM of 1,12−diol, and 29.43 mM (7.93 mM 1,12−aminol and 21.5 mM 1,12−diamine) of amine compounds were produced. Finally, the 12−ADA as model compound was isolated and purified by established protocol(Sarak et al. 2021) using tert−butyloxy carbonyl (*Boc*) protection with overall isolated yields varying from 66.5%. The final product was characterized and confirmed by 1H NMR spectroscopy (Fig. S15†).

Figure 3. 28 12−ADA production with pH controller. The reaction was performed in Tris buffer (100 mM, pH 8.0) supplemented with 40 OD_{600} of cell−H^m, 20 OD_{600} of cell−A^m, 100 mM DAME, 200 mM benzyl amine, 0.5 mM of PLP, and 2% (w/v) glucose for every 6 hours at 30℃ for 48 hours.
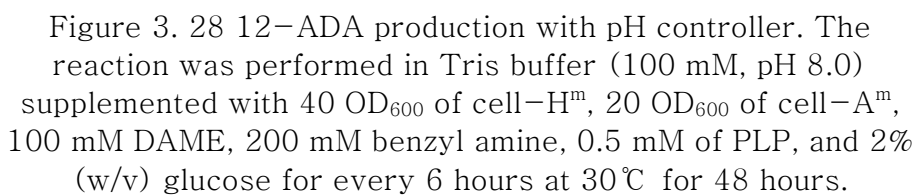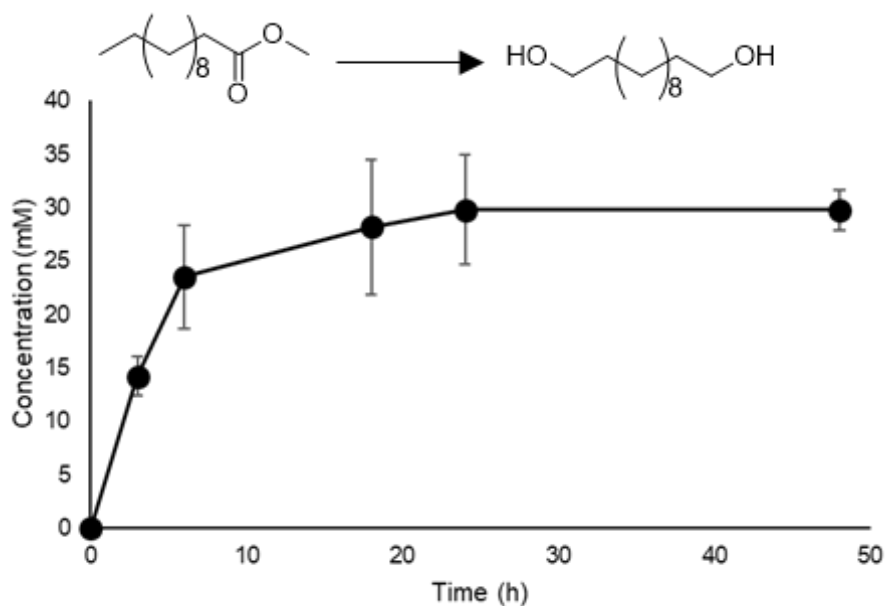
Figure 3. 29 1,12-diol production reaction in pH controller. The reaction was conducted in potassium phosphate buffer (100 mM, pH 7.5) supplemented with 60 OD_{600} of cell-H^m, 30 OD_{600} of cell-R^m, 100 mM DAME, 10 mM $MgCl_2$, and 2.5% (w/v) glucose were added for every 6 hours at 30℃ for 48 hours.
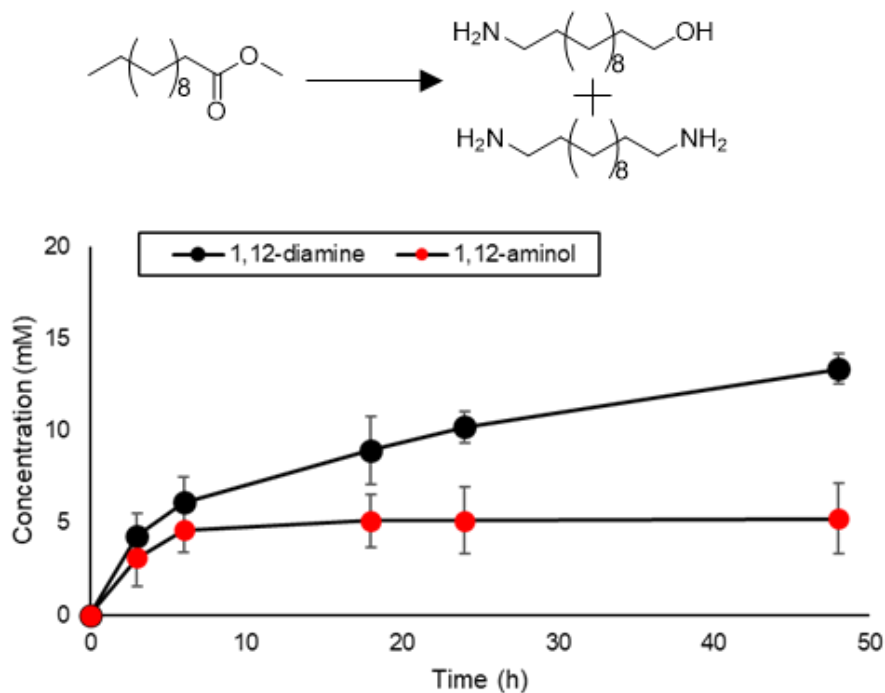
Figure 3. 30 Concurrent reaction to produce 1,12-diamine with 400 mM of benzyl amine. The reaction was conducted in potassium phosphate buffer (100 mM, pH 7.5) supplemented with 60 OD_{600} of cell-H^m, 30 OD_{600} of cell-R^m, 120 OD_{600} of cell-A^m, 100 mM DAME, 400 mM benzyl amine, 10 mM $MgCl_2$, 5% (w/v) glucose, 0.5 mM PLP, and 1% DMSO at 30℃ for 48 hours. Red circle indicates 1,12-aminol, and black circle indicates 1,12-diamine
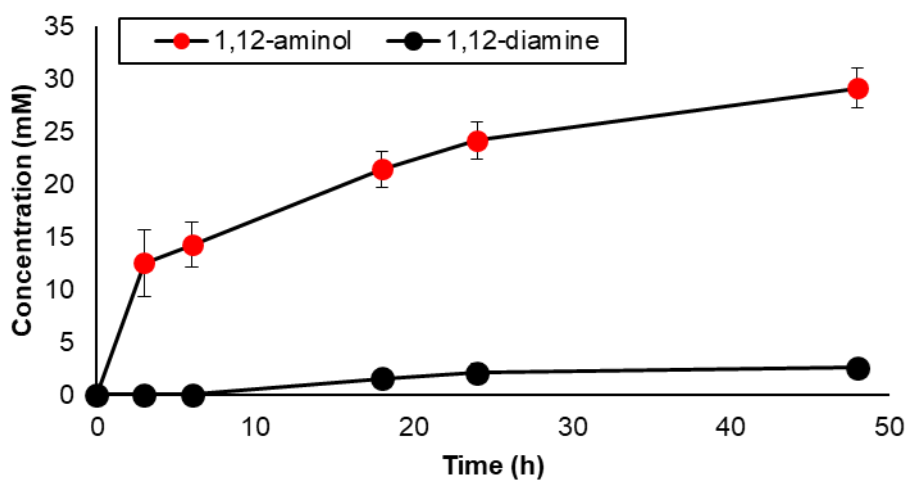
Figure 3. 31 Concurrent reaction to produce 1,12−diamine with 50 mM of benzyl amine in pH controller. 100 mM DAME, 50 mM of benzyl amine, 0.5 mM of PLP, 10 mM of $MgCl_2$, 1% DMSO, 30 OD_{600} of cell−R^m, 60 OD_{600} of cell−H^m, 120 OD_{600} of cell−A^m in potassium phosphate buffer(100 mM pH7.5.) The reactions were conducted at 30℃ and 200 rpm. Red circle indicates 1,12−aminol and black circle indicates 1,12−diamine.
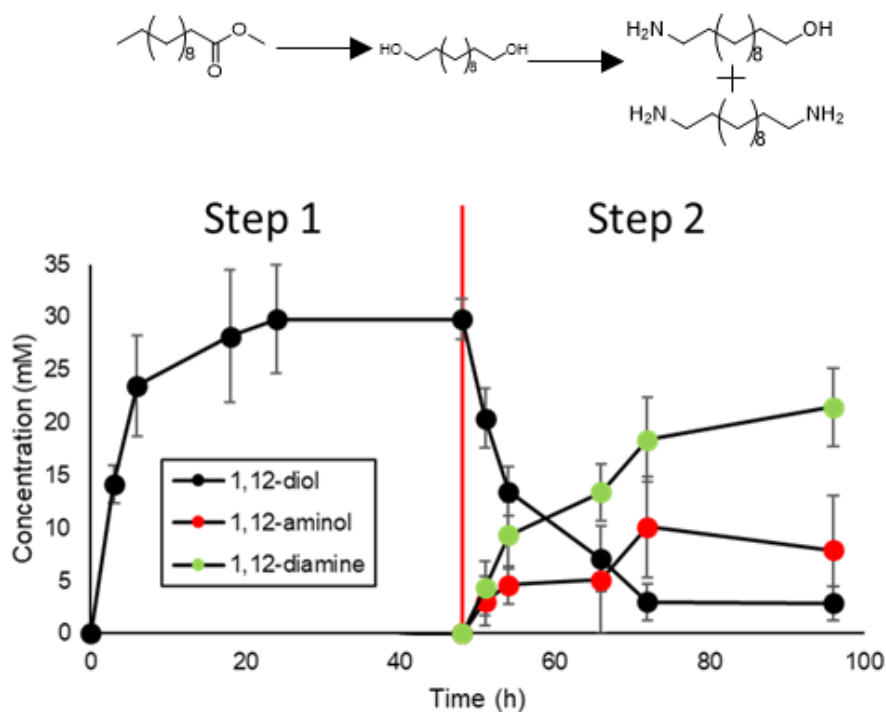
Figure 3. 32 Sequential reaction to increase the proportion of 1,12-diamine. 1,12-diol was produced with cell-H^m and cell-R^m for 48 hours beforehand, and 120 OD$_{600}$ of cell-A^m, 400 mM benzyl amine, 5% (w/v) glucose, 0.5 mM PLP, and 1% DMSO at 30℃ for 48 hours. Red circle indicates 1,12-aminol, black circle indicates 1,12-diol, and green circle indicates 1,12-diamine.
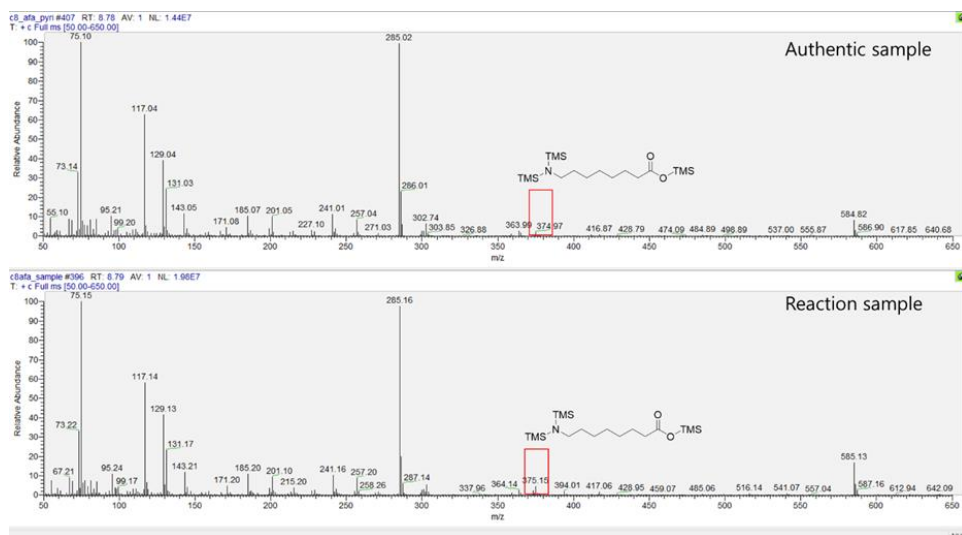
Figure 3. 33 GC/MS analysis of 8-amino ocatanoic acid
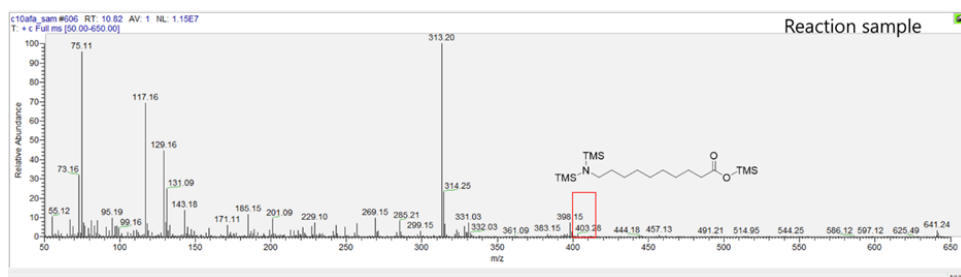
Figure 3. 34 GC/MS analysis of 10-amino decanoic acid
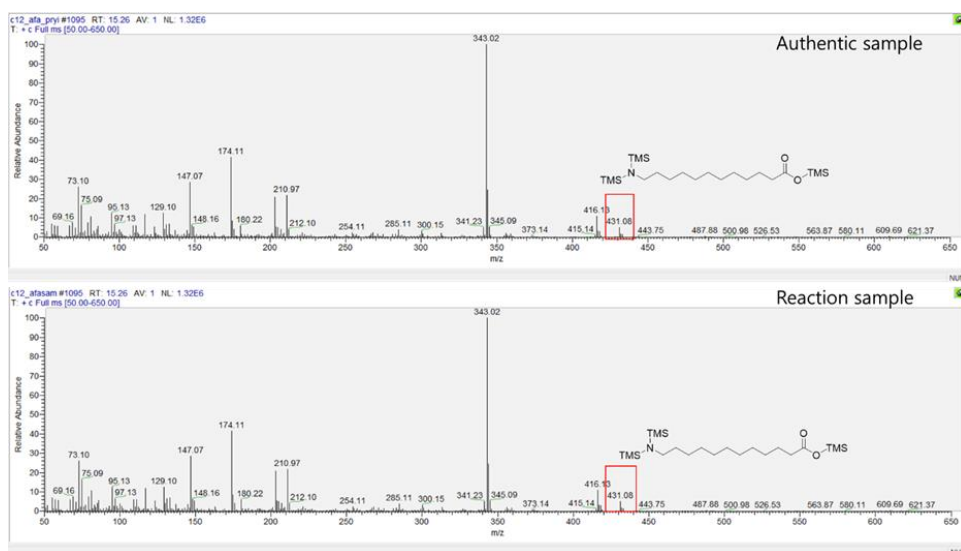
Figure 3. 35 GC/MS analysis of 12−amino dodecanoic acid
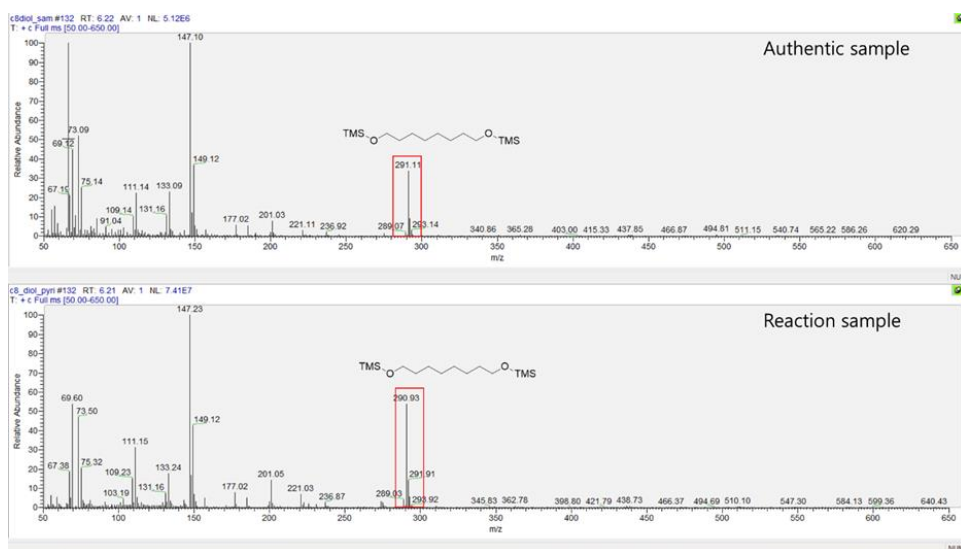
Figure 3. 36 GC/MS analysis of 1,8-octanediol
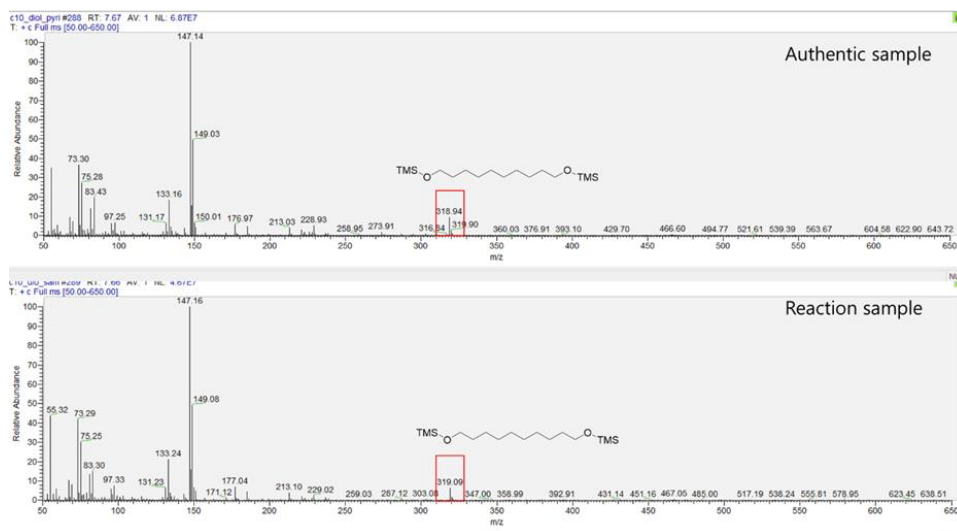
Figure 3. 37 GC/MS analysis of 1,10-decanediol
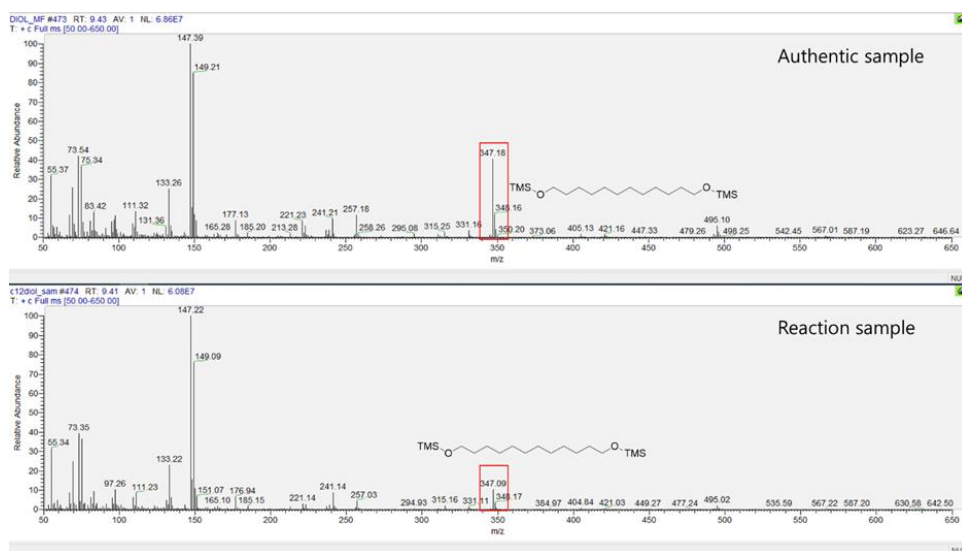
Figure 3. 38 GC/MS analysis of 1,12-dodecanediol
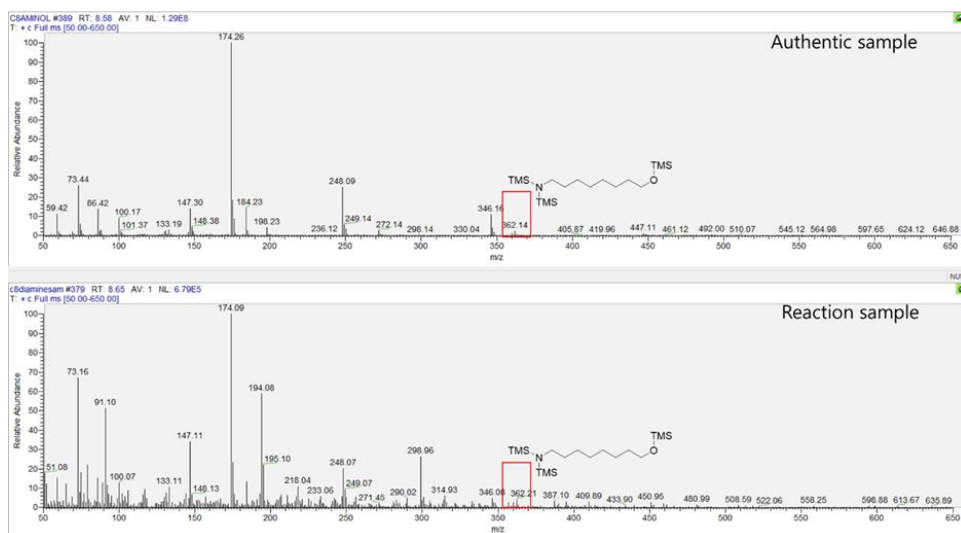
Figure 3. 39 GC/MS analysis of 8-Amino-1-octanol
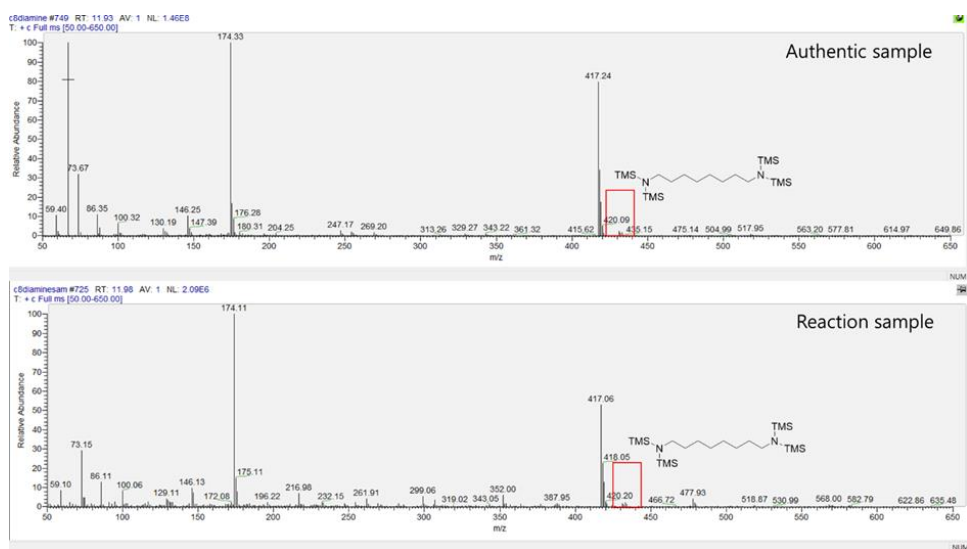
Figure 3. 40 GC/MS analysis of 1,8-diaminooctane
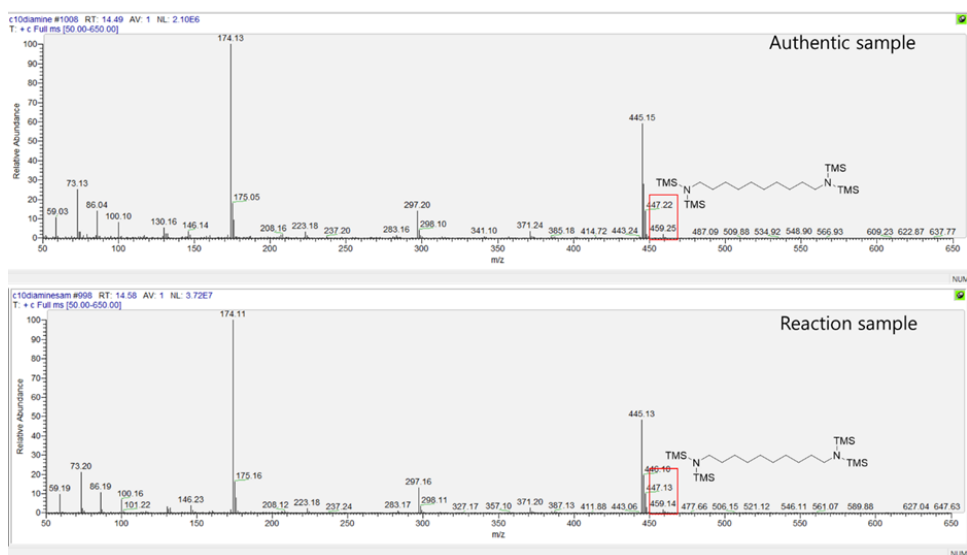
Figure 3. 41 GC/MS analysis of 1,10-diaminodecane

Figure 3. 42 GC/MS analysis of 12-amino-1-dodecanol
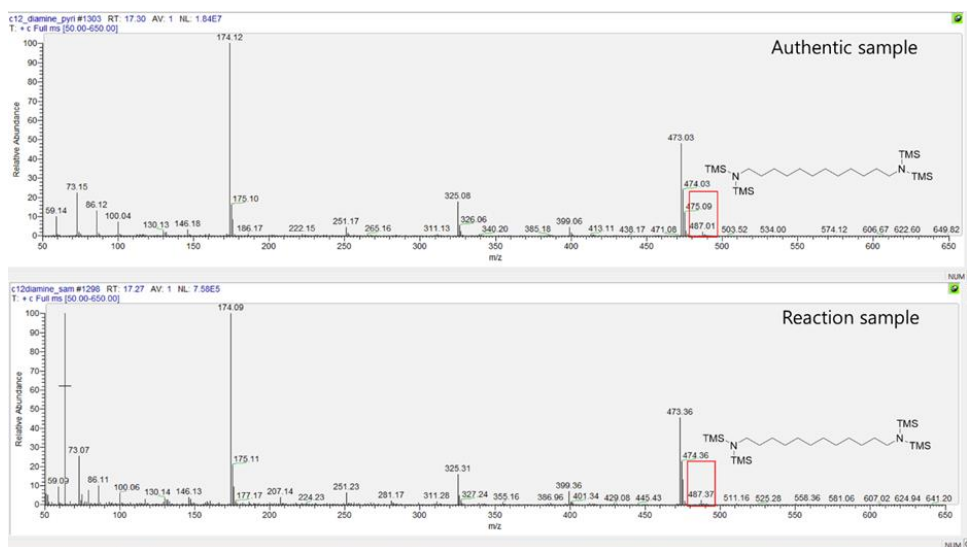
Figure 3. 43 GC/MS analysis of 1,12-diaminododecane
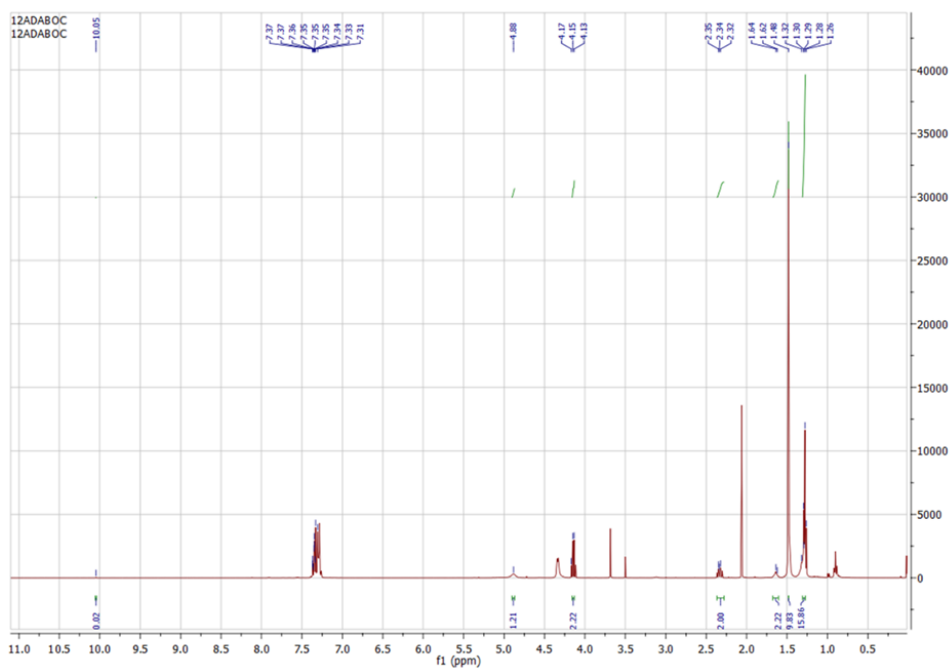
Figure 3. 44 NMR Data of Boc-protected 12-amino dodecanoic acid

3.4 Conclusions

In this study, *E. coli* based three cell modules (cell−H^m, cell−A^m, and cell−R^m) were designed and constructed and various biopolymer monomers were synthesized by the product specific module combinations. Biopolymer monomers with various carbon chain lengths (C8, C10 and C12) were efficiently produced with the multi−enzymatic cascade reaction such as ω−AFA, α,ω−diol, α, ω−aminol and α,ω−diamine. The present study demonstrates the potential application of multi−enzymatic cascade reactions for one−pot synthesis of high−value biopolymer monomers in an environmentally friendly biocatalyst−based process.

Chapter 4. Engineering of non-heme alkane monooxygenase with in vivo screening system

4.1 Introduction

Enzyme engineering is a powerful tool to improve the properties of enzymes (Newton et al. 2018). Therefore, many studies have examined to improve activity or stability through enzyme engineering (Leveson-Gower, Mayer, and Roelfes 2019).

Various methods such as error-prone PCR and saturation mutagenesis had been developed to generate enzyme mutant libraries (Quaglia et al. 2017). In order to identify improved mutants from large population of the libraries, it is important to devise relevant enzyme screening methods. If the screening method is not properly established, selection of the improved mutants will be extremely difficult. High-throughput screening strategy can dramatically reduce the time and effort for tedious screening process by allowing us to test large libraries in a short period of time (Canavaci et al. 2010).

There are two types of screening systems: *in vitro* and *in rvivo*. In the case of *in vitro* screening, addition of cofactors, substrates, and additional enzymes are necessary to confirm the activity (Jung et al. 2016). However, *in vivo* enzyme screening

system requires minimal human interference for the screening process since cofactors and additional enzymes required for the assay are already present in the cell. In addition, the activity measured *in vitro* does not always match the activity measured *in vivo* (van Eunen and Bakker 2014). Therefore, it is favorable to develop an *in vivo* enzyme screening system.

Non-heme di-iron alkane monooxygenases allow bacteria to utilize alkanes as the carbon source (Beilen and Funhoff 2005). Non-heme di-iron alkane monooxygenase from *Pseudomonas putida* Gpo1 (AlkB) is the representative enzyme which catalyzes hydroxylation of medium chain length alkanes (van Beilen, Kingma, and Witholt 1994, Van Beilen et al. 2005). Since rational engineering of AlkB was difficult due to the lack of PDB structure, researches were carried out to elucidate the structure of AlkB and its active site. However, the exact 3D structure is still not yet clear (Alonso et al. 2014, de Sousa et al. 2017). The topology of AlkB was suggested that the AlkB is composed of six transmembrane domains and N-terminus and C-terminus are located in the cytoplasm according to the analysis of the hydrophobicity and gene fusions study with β-galactosidase and alkaline phosphatase (Van

Beilen, Penninga, and Witholt 1992). Sequence alignment and alanine scanning studies revealed that AlkB contains two iron molecules and eight conserved histidine residues (H138, H142, H168, H172, H173, H312, H315 and H316) which are essential for holding the iron molecules (Shanklin and Whittle 2003). Also, AlkB can oxidize medium chain length(C6 to C12) linear alkanes (Witholt et al. 1990).

There are several mutational studies reported for the AlkB. Van Beilen *et al.* reported that the side chain of Trp55 blocks the bottom of the substrate binding pocket, which limits the entrance of long chain fatty acids and W55S or W55C mutant allows oxidation of tetradecane and hexadecane respectively (Van Beilen et al. 2005). Also, mutant V129M, L132V and I233V proximal to the histidine containing sequence motif A ($H_{138}EXXHK_{143}$) exhibited higher rates of 1-butanol production from butane (Koch et al. 2009).

In this study, we devised an antibiotic resistance gene based in vivo screening system to search for *Pseudomonasa pelagia* AlkB (PpAlkB) mutants with increased activity toward dodecanoic acid methyl ester (DAME). In the previous report, in vivo screening system combined Free fatty acid-responsive transcription factor

FadR, tetracycline efflux pump (TetA), and synthetic promoter (P_{AR}) to find mutants that show minimal cell to cell variation for enhanced biosynthesis (Xiao et al. 2016). TetA is expressed by P_{AR}, a syntehtic promoter and FadR inhibits TetA expression by binding to PAR. If Escherichia coli produces a lot of fatty acids and the amount of fatty acyl−CoA in the cell increases, so that fatty acyl−CoA and FadR bind, FadR that binds to fatty acyl−CoA is separated from P_{AR}, and TetA is expressed by P_{AR} (Figure 4.1). To construct the screening module, we cloned FadR derived from Thermus thermophilus (TtFadR), which could bind lauroyl−CoA then insert putative binding sequence of TtFadR in the PAR (PARTt)(Agari et al. 2011, Lee, Um, and Van Dyke 2017). In vivo screening was designed to rely on the growth rate that if more dodecanoic acid was produced from dodecane by PpAlkB, E. coli could survive better in the presence of tetracycline due to the increased expression of TetA (Figure 4.2). As a result, it is possible to increase the production of many biopolymer monomers with non−heme alkane monooxygenase.
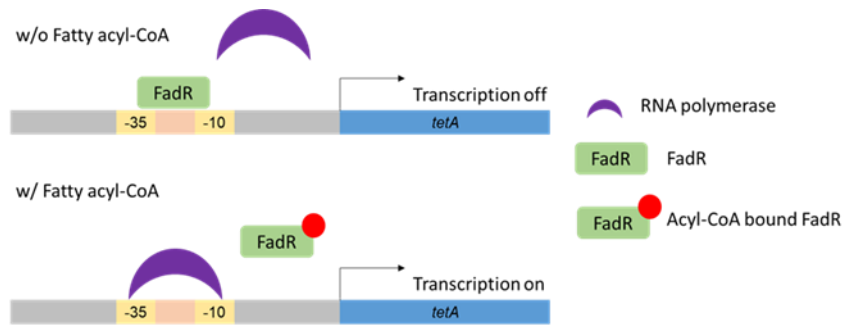
Figure 4. 1 Principle of fatty acyl－CoA biosensor
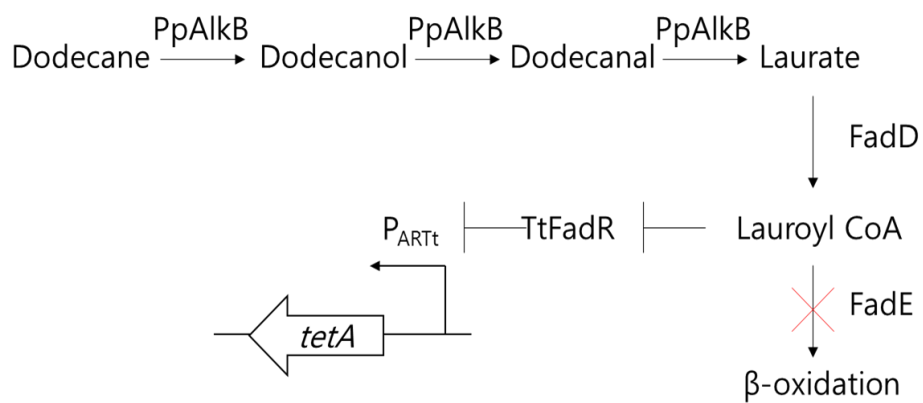
Figure 4. 2 Schematic diagram of the screening system method

4.2 Material and methods

4.2.1 Bacterial strains and materials

E. coli DH5α was used for genomic manipulation, and BW25113 ($\Delta fadE$, DE3) was used for in vivo screening system and BW25113 ($\Delta fadD$, DE3) was used for whole cell reaction. Chloroform was obtained from Junsei (Tokyo, Japan). N,O−bis−(trimethylsilyl) trifluoroacetamide (BSTFA). Dodecane was purchased from Sigma−Aldrich Chemical Co. Bacteriological agar, Luria Bertani (LB) broth, and terrific broth (TB) media were purchased from BD Difco (Franklin Lakes, NJ, USA). DAME was purchased from Tokyo Chemical Industry (Tokyo, Japan).

4.2.2 Construction of libraries

The library was constructed by carrying out error prone PCR of the PpAlkB gene. A 50−μL PCR reaction mixture was set up by adding 0.35mM of dATP, 0.4mM of dCTP, 0.2mM of dGTP, 1.35mM of dTTP, 2.5mM of $MgCl_2$, 0.5mM of $MnCl_2$, 10X Mg^{2+} free buffer, 50ng of template, 1U of rTaq DNA polymerase, 1mM of each primer. The protocol of error prone PCR was an initial denaturation step

(95℃ for 10 min), 30 amplification cycles (95℃ for 30 s, 55℃ for 30 s and 72℃ for 90 s) and a final extension step (72℃ for 5 min). The product of PCR was purified and double cut with *SacI* and *HindIII* restriction enzymes and inserted into a pQE80L vector using T4 ligase. The ligation product was transformed into DH5α.

4.2.3 Growth rate assay in LB media

E. coli BW25113 (Δ*fadE*, DE3) expressing screening module was grown in LB media with 25 μg/mL chloramphenicol overnight. The overnight cultured cells were diluted to the OD_{600} of 0.1 in LB media with 25 μg/mL chloramphenicol, 0.05 mM of IPTG, 0.1 % Triton−X 100 and each concentration of tetracycline and dodecanoic acid. For the test of growth rate with dodecane, The overnight cultured *E. coli* BW25113 (Δ*fadE*, DE3) with screeing module, assistance module, and library module were diluted to the OD_{600} of 0.1 in LB media with 12.5 μg/mL tetracycline, 33 μg/mL ampicillin, 16.6 μg/mL streptomycin, 8.3 μg/mL chloramphenicol, 0.05 mM IPTG and each concentration of dodecane. Total volume of LB broth was 10 mL in 100 mL baffled flask and each cells were grown in 30℃ 200rpm. UV absorbance at 600 nm was measured

with Multiskan spectrum (Thermo scientific, USA).

4.2.4 In vivo screening

150 ng of the PpAlkB mutant library DNA was transfromed to BW25113(Δ*fadE*, DE3). The transfromants were spread on LB plate containing 25 μg/mL tetracycline, 33 μg/mL ampicillin, 16.6 μg/mL streptomycin, 8.3 μg/mL chloramphenicol, 1 mM dodecane, 0.05 mM IPTG. After 48hr incubation at 30℃, 100 colonies were picked onto the same agar plate with 37.5 μg/mL tetracycline to secondary screening. After 48hr incubation at 30℃, the reaction proceeded by selecting 10 colonies with the largest size.

4.2.5 Biotransformations with resting cell reaction

For the screening of potential mutants, whole-cell biotransformations were performed by using dodecane or DAME as substrate, 1% (w/v) glucose and density of the cell suspension was adjusted to OD_{600} of 30 using potassium phosphate buffer (pH 7.5, 100mM) by dilution of concentrated cells. The final volume of the reaction mixture was 2 mL in test tube in 30℃ 200rpm.

4.2.6 Analysis by gas chromatography

Quantitative analysis was performed by gas chromatography (HP 6890 Series, Agilent Technologies, Santa Clara, CA, USA) with flame ionization detector (GC/FID). 5 μL of the sample was injected by split less mode (a split less time of 0.8 min) and analyzed using a nonpolar capillary column (5% phenyl methyl siloxane capillary 30 m×320 μm i.d. 0.25 μm film thickness, HP-5 MS).

The oven temperature started at 100 ˚ C for 1 min, and then increased by 15 ˚ C/min to 250 ˚ C, holding time at this temperature was 10 min. The temperature of the inlet was kept at 250 ˚ C, and the temperature of the detector was 280 ˚ C. The flow rate of the carrier gas was 1.0 mL/min, while flow rates of hydrogen, air, and helium in the FID were 45, 400, and 20 mL/min, respectively. Each peak in GC chromatogram was identified by comparison with that of an authentic sample. Errors in the analyses were corrected by using 0.5 mM hexadecane as an internal standard.

4.3 Results and discussion

4.3.1 Construction of screening module and assistance module

      for library screening

We constructed three plasmids for the library screening. i) containing FadR from *Thermus thermophilus* (TtFadR), and tetracycline resistance gene(TetA) with P_{AR} promoter in pACYC duet vector (screening module), ii) containing electron partner and transporter, alcohol dehydrogenase in pCDF duet vector (assistance module), iii) containing library of PpAlkB in pQE80L vector (library module) (Figure 4.3)

In the previous reports, continuously select for high performing *E. coli* which showed enhanced fatty acid production by FadR from *E. coli* and P_{AR} promoter with FadR binding sequence (Xiao et al. 2016). It is known that the FadR from *E. coli* (EcFadR) could be antagonized by fatty acyl-CoAs over 14 carbon atoms (Fujita, Matsuoka, and Hirooka 2007). The target substrate of this system is dodecanoic acid methyl ester (DAME). Therefore, screening with EcFadR is not possible. TtFadR, which is known to bind with lauroyl-CoA, was introduced into the screening

module.(Agari et al. 2011). In addition, a putative sequence known to bind to TtFadR was inserted at the location of the sequences which bind with EcFadR in P_{AR} promoter (Lee, Um, and Van Dyke 2017). There are two putative sequences (5´- TTRNACYNRGTNYAA-3´, 5´-TTANACT-(N6-7)-ARNNNAR- 3´) known to be able to bind with TtFadR. The K_d values of TtFadR and each sequence were 0.17 nM and 2.6 nM, respectively (Agari et al. 2011, Lee, Um, and Van Dyke 2017). Therefore, we used 'TTGGACTAAGTCCAA', which is known to be able to bind with TtFadR in previous papers, as the TtFadR binding sequence. To construct the screening module, TetA was cloned at the MCSI and TtFadR at the MCSII location of the pACYC duet vector. In addition, MCSI's T7 promoter and lac operator were replaced with a P_{AR} promoter with a putative sequence capable of binding to TtFadR (P_{ARtt}). When a protein was expressed with an inducible promoter, the amount of protein expression may not be constant by some factors such as leaky expression (Kang, Son, and Hoang 2007). Therefore, we changed the promoter of MCSII and the lac operator into the constitutive promoter, J23100 promoter, so that the protein of the screening module might be expressed consistently (Figure

4.3) (Kelly et al. 2009).

In order to hydrate DAME with AlkB, electron transfer by AlkG and AlkT is essential (Schrewe et al. 2014). In addition, to uptake DAME, AlkL, a transporter, is required (Julsing et al. 2012). It is known that AlkB convert DAME into dodecanedioic acid mono methyl ester (DDAME) by over-oxidation. The process of converting 12-hydroxy dodecanoic acid methyl ester (HDAME) to 12-oxododecanoic acid methyl ester (ODAME) in the process of over-oxidation is known as the limiting step, and the introduction of AlkJ, an alcohol dehydrogenase from *Pseudomonas putida* Gpo1, is known to support HDAME over-oxidation (Schrewe et al. 2014). In our previous reports, $AlkL_f$, which replaced the signal peptide of AlkL to that of FadL, had better uptake ability of DAME into the *E. coli* and hydroxylation of DAME was enhanced when $AlkL_f$ was expressed with an intensity of 60% of the T7 promoter (FC097) and AlkBGT was expressed with the T7 promoter (Yoo et al. 2019). Therefore, we cloned $AlkL_f$, AlkJ, AlkG, and AlkT into pCDF duet vector to construct assistance module to support AlkB reaction. The MCSI promoter of the pCDF duet vector was replaced to FC097, and $AlkL_f$ was inserted into the MCSI. In addition, AlkJ, AlkG, and

AlkT were inserted into MCSII, and each gene was designed to have its own RBS (Figure 4.3). Genes encoding AlkJ,G,T and L or AlkG,T and L were cloned by Circular Polymerase Extension Cloning (Quan and Tian 2011) and plasmids were verified using DNA sequencing.
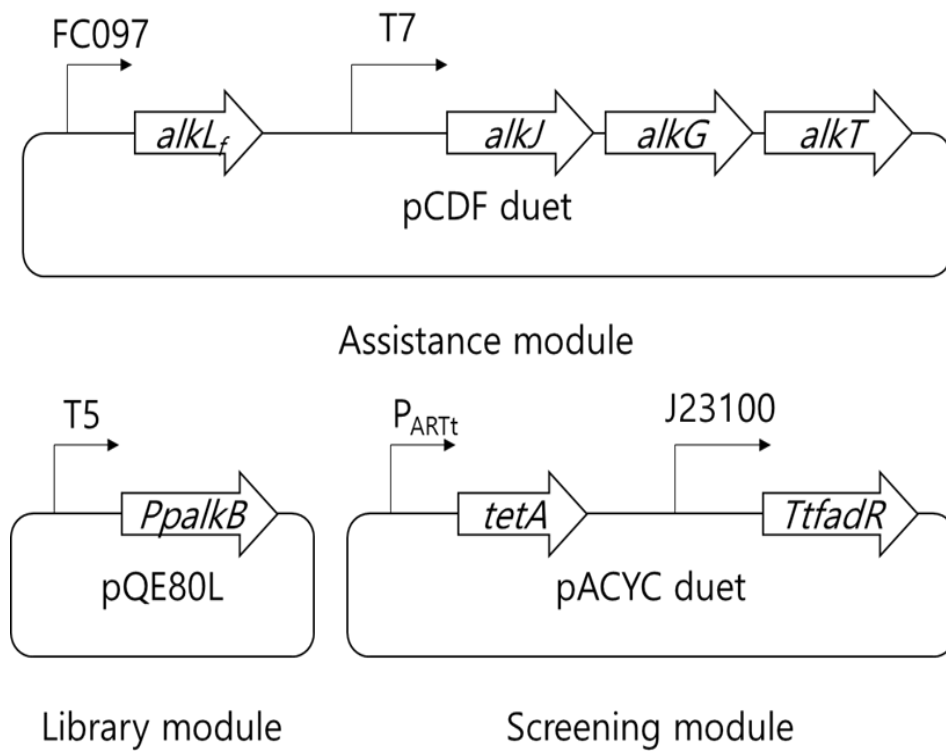
Figure 4. 3 Plasmid diagram of each cell module in
BW25113 (Δ*fadE*, DE3).

4.3.2 Growth test of *E. coli* with screening module in LB media

Although our ultimate goal is to find PpAlkB mutants with enhanced hydroxylation activity toward DAME, DAME was hydrolysis to dodecanoic acid inside the *E. coli* and binds to FadR directly (Kadisch, Schmid, and Bühler 2017). Therefore, libraries were tested with dodecane, which is considered structurally similar to DAME, as a substrate.

To test whether screening module could provide sufficient selection pressure for selecting mutants in *E. coli*, the growth rate of *E. coli* with different concentration of tetracycline was tested. First of all, we checked whether *E. coli* with a screening module could growth in a medium with tetracycline. We transformed the screening module into BW25113 (Δ*fadE*, DE3) and cultured the cells with 0 μg/mL, 6.25 μg/mL, 12.5 μg/mL, 25 μg/mL, 50μg/mL of tetracycline concentrations in LB media, respectively. The growth rate was decreased as the concentration of antibiotics increased (Figure 4.4). *E. coli* grew slowly even at 12.5 μg/mL, which seems to be due to leak expression of TetA. Next, the growth rate of BW25113 (Δ*fadE*, DE3) with the screening module with dodecanoic

acid was tested. The growth rate was confirmed by varying the concentration of dodecanoic acid from 0 to 1 mM with 12.5 μg/mL of tetracycline. The growth rate of *E. coli* increased as the concentration of dodecanoic acid increased (Figure 4.5). Finally, the cell growth rate of BW25113 (Δ*fadE*, DE3) with screening module, assistance module, and library module was tested depends on the concentration of dodecane. 0, 0.1, 0.5, 1, 2 mM of dodecane was added to each LB media and cultured at 30℃ with 12.5 μg/mL of tetracycline. The growth rate of *E. coli* increased as the concentration of dodecane increased (Figure 4.6).

The growth rate of *E. coli* with three screening modules was slower than that of *E. coli* with only screening module (Figure 4.4, Figure 4.6). The screening module is cloned into pACYC duet vector which containing the medium-copy-number origin but the assistance module and the library module is cloned into pQE80L vector which containing high-copy-number origin. In addition, the promoter expressing *tetA* was a constitutive promoter, while the assistance module and the library module expressed enzymes with the strong inducible promoter (Figure 4.3). Therefore, in the case of *E. coli* with three modules, the amount of *tetA* expression is less

than that of *E. coli* with only the screening module, so it is thought

that there is a difference in the growth rate.
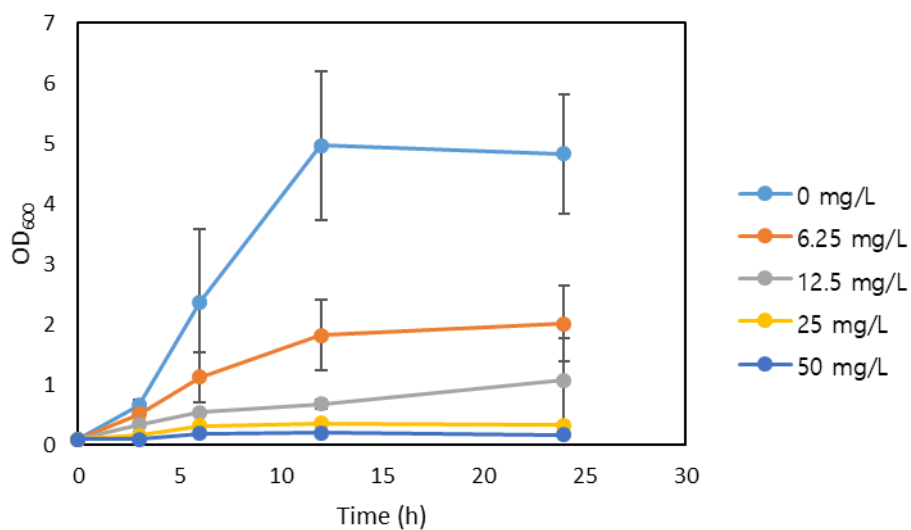
Figure 4. 4 Growth rate of BW25113 ($\Delta fadE$, DE3) with screeing module with different concentration of tetracycline in LB media. Initial OD_{600}: 0.1, 0.05 mM of IPTG, 30℃, 200rpm, 10mL in 100mL flask
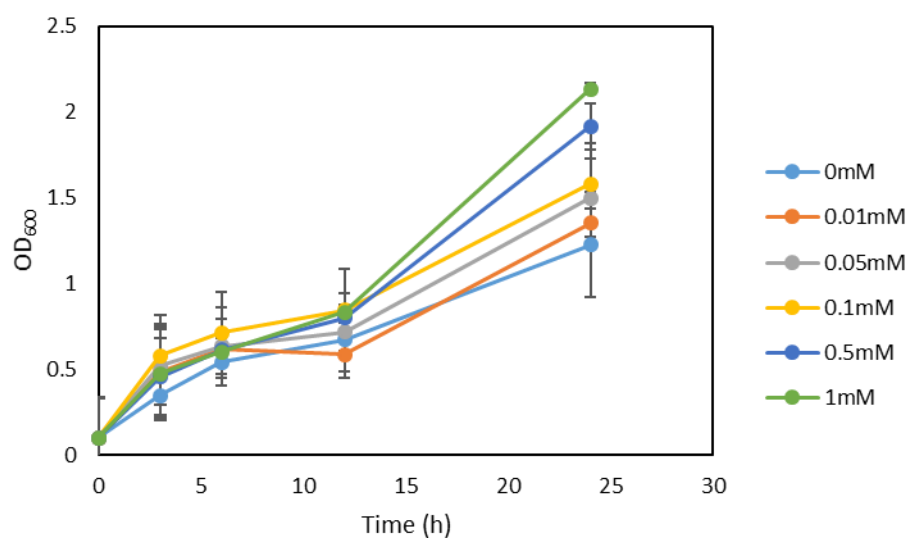
Figure 4. 5 Growth rate of BW25113 ($\Delta fadE$, DE3) with screeing module with different concentration of dodecanoic acid in LB media. Initial OD_{600}: 0.1, [Tetracycline] : 12.5 μg/mL, 0.05 mM of IPTG, 0.1 % Triton−X 100, 30℃, 200rpm, 10mL in 100mL flask
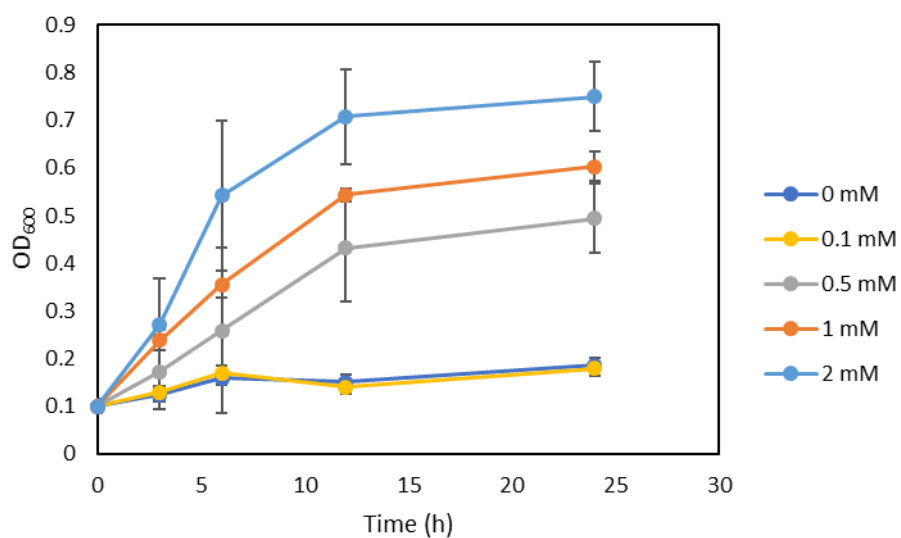
Figure 4. 6 Growth rate of BW25113 (Δ*fadE*, DE3) with three
modules with different concentration of dodecane in LB media.
Initial OD_{600}: 0.1, [Tetracycline] : 12.5 μg/mL, 0.05 mM of IPTG,
0.1 % Triton−X 100, 30℃, 200rpm, 10mL in 100mL flask

4.3.3 In vivo screening with dodecane

In order to find enhanced mutants from large-sized libraries, it is important to set the screening conditions in which most mutants could be washed out. Therefore, when screening is performed based on the growth rate of cells according to the concentration of antibiotics, screening should be performed under the condition in which *E. coli* with WT could not grow. *E. coli* with screening module was hardly grows at concentrations above 25 µg/mL tetracycline (Figure 4.4). Therefore, it was decided to proceed with the first screening at 25 µg/mL tetracycline and the second screening at 37.5 µg/mL tetracycline.

The size of the library was estimated by plating the transformed *E. coli* on LB agar plate. We obtained the library size of between around 4.93×10^6 [6,160 (number of colonies) x 0.8 (cloning efficiency) x 100 (dilution rate) x 10 (number of repetitions)]. BW25113($\Delta fadE$, DE3) with three modules were plated on LB agar plate containing 25 µg/mL tetracycline, 33 µg/mL ampicillin, 16.6 µg/mL streptomycin, 8.3 µg/mL chloramphenicol, 1 mM dodecane, 0.05 mM IPTG and cultured at 30℃. After 48 hours,

100 colonies with large colony size were picked from each plate into the plate with 37.5 μg/mL tetracycline for the second screening. After 48 hours, 10 large colonies were selected and the reaction was performed with 10 mM dodecane as a substrate in order to test whether the activity of PpAlkB was improved. Two mutants showed more than 50% higher activity than WT (Figure 4.7, Table 4.1). However, the reaction hardly proceeded in the two colonies, which is thought to be due to false-positive. As a result of comparing the growth rate of the *E. coli* with m1-3 and WT, the growth rate of *E. coli* with m1-3 was faster (Figure 4.8). Therefore, we repeated the above experiment with m1-3 as a control, and selected 100 additional colonies larger than m1-3 in the second screening. 14 colonies produced 20% higher concentration of products compared than m1-3 with 10 mM dodecane as substrate (Figure 4.9). The library module of each colony was purified to DNA sequencing (Table 4.2).
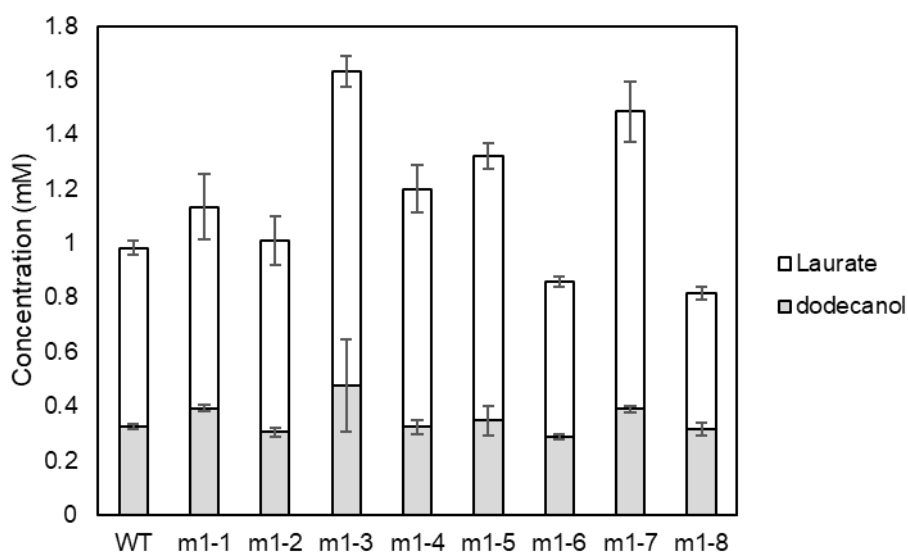
Figure 4. 7 Production of dodecanol and dodecanoic acid from 10 mM dodecane with BW25113($\Delta fadE$, DE3) with mutants. The reaction was performed in potassium phosphate buffer (100 mM, pH 7.5) supplemented with 30 OD_{600}, 10 mM dodecane, 1%(w/v) glucose at 30℃ for 12 hours
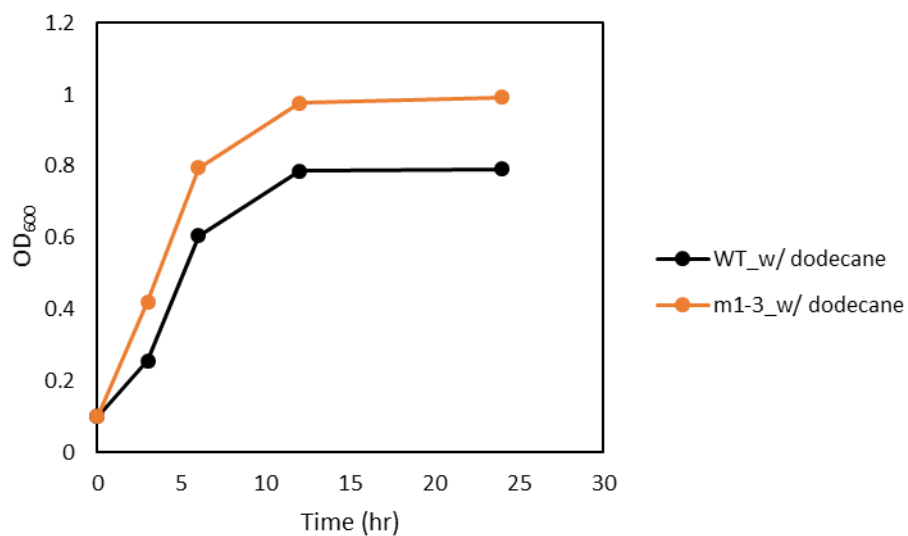
Figure 4. 8 Comparision of growth rate of BW25113(Δ*fadE*, DE3)with m1−3 and WT. Initial OD_{600} : 0.1, [Tetracycline] : 12.5 μg/mL, 0.05 mM of IPTG, [Dodecane] : 1 mM, 30℃, 200rpm, 10mL in 100mL flask

Table 4. 1 Sequence of mutant m1-1 to m1-8

	Mutation sequence
m1-1	I36T/M187I/A379T/D357N
m1-2	D181V/I191V/R226S/D375E
m1-3	R174C/S185N/I199T
m1-4	L24P/T52A/E118K/R312H
m1-5	V89D/V159I
m1-6	N135S/V158D/P340S
m1-7	A202T/A206P/A268S/M345V
m1-8	V109D/N169I/W222R

●
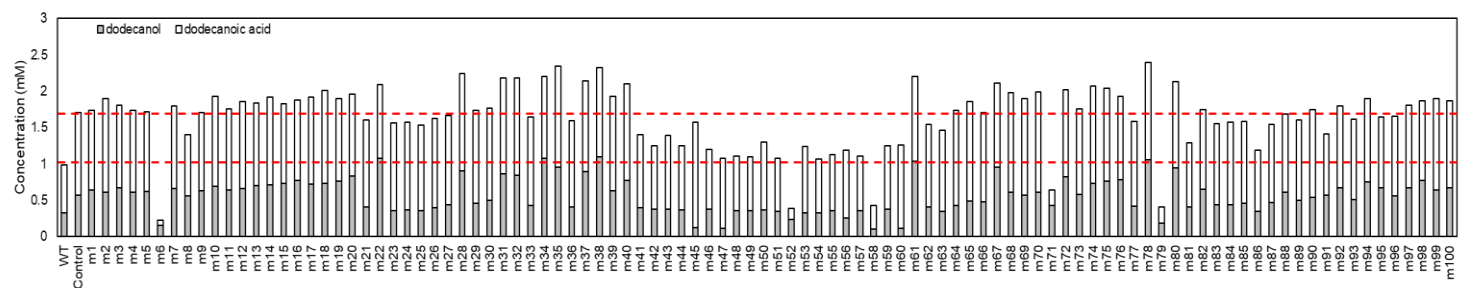
Figure 4. 9 Production of dodecanol and dodecanoic acid from 10 mM dodecane with BW25113（Δ*fadE*, DE3）with mutants. The reaction was performed in potassium phosphate buffer （100 mM, pH 7.5) supplemented with 30 OD_{600},10 mM dodecane, 1％(w/v) glucose at 30℃ for 12 hours. Gray box means dodecnaol and white box means dodecanoic acid. Control: PpAlkB with R174C/S185N/I199T.

Table 4. 2 Sequence of mutants sequence with enhanced activity
toward dodecane

	Mutation sequence
Control	R174C/S185N/I199T
22	L344Q/A401V
28	V89I/E211K/E227V/T235P/N303I
31	A39V/T42I/F246I/A244E/E372L/A379V
32	T94I/G120D/I271F/K280R/H318Y/W351R
34	H292L/D314G
35	Y86H/N130D/L254P/I348T
37	D16V/I382F
38	W44R/M65V/G160D/P182Q/R231C
40	L124Q/R213W/I256N
61	A133V/S325I/F343S
67	P12L/A30V/M33L/S369C
74	Y14N/G57S/P200Q/E210G
78	S115F/H292N
80	F53I/S313P

4.3.4 Mutant evaluation with DAME as substrate

The aim of this study was to find PpalkB with increased activity toward DAME. In order to check whether the mutants screened with dodecane have higher activity toward DAME than that of WT, the reaction was performed with DAME as a substrate. In order to confirm the activity of PpAlkB in fresh cells, we transformed the assistance module and library modules with each mutant into BW25113(Δ*fadD*, DE3) since the production of lauroyl-CoA by FadD was no longer required. AlkJ was removed from the assistance module to confirm the intrinsic activity of PpAlkB. As a result of the reaction with 10 mM DAME, it was confirmed that *E. coli* with including each mutant produced higher products than *E. coli* with WT (Figure 4.10). Although the patterns of production in dodecane and DAME of the mutant strains did not exactly match, every mutant showed higher production from DAME than WT. To find mutant with high activity at high concentration of DAME, we increased the concentration of the substrate to 100 mM. Concentration of products from DAME were increased by 58%, 57% and 56% compared to WT at m80, m40 and m35 respectively

(Figure 4.11).
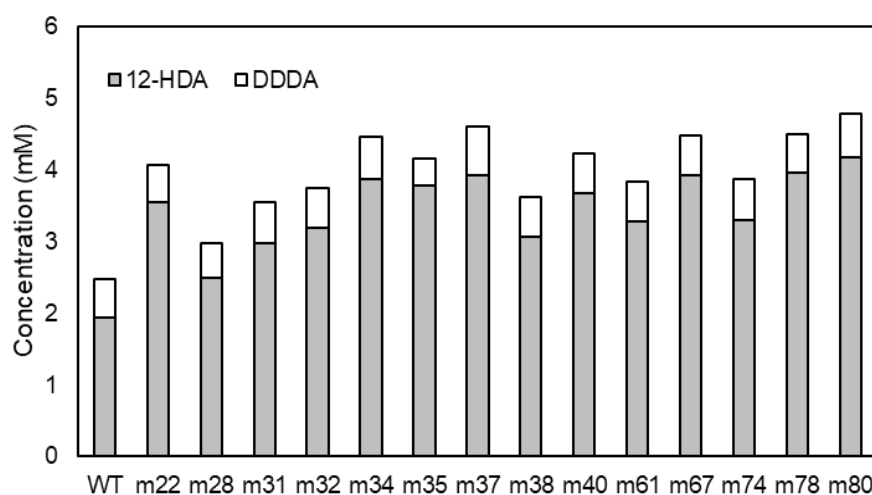
Figure 4. 10 Production of 12－HDA and DDDA from 10 mM DAME with BW25113(ΔfadD, DE3) with mutants. The reaction was performed in potassium phosphate buffer (100 mM, pH 7.5) supplemented with 30 OD_{600},10 mM DAME, 1%(w/v) glucose at 30℃ for 12 hours. Gray box means 12－HDA and white box means DDDA.
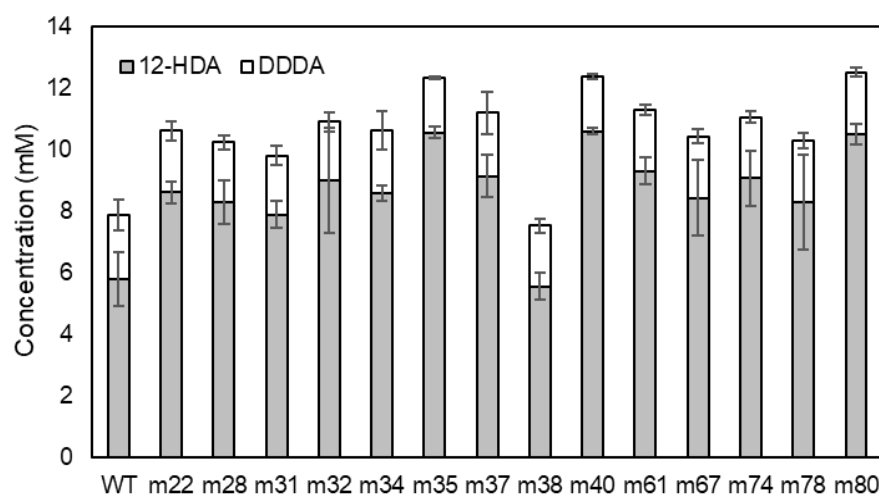
Figure 4. 11 Production of 12-HDA and DDDA from 100 mM DAME with BW25113(Δ*fadD*, DE3) with mutants. The reaction was performed in potassium phosphate buffer (100 mM, pH 7.5) supplemented with 30 OD_{600}, 100 mM DAME, 1%(w/v) glucose at 30℃ for 12 hours. Gray box means 12-HDA and white box means DDDA.

4.3.5 Identification of key residues of PpAlkB with single mutant evaluation

There was no overlapping sequence of the 14 mutants. Therefore, it is hard to know which site had a significant effect on the enhancement of PpAlkB activity toward DAME. We decided to test the activity by making each residue of the screened mutants as a single mutant. In the case of an enzyme mutant, multiple mutant exceeds the expectations from the additive effects of the individual mutations by synergetic effect (Pérez-Pérez, Candela, and Micol 2009). We produced a single mutant of mutants with 2 or 3 mutations because in the case of mutants with more than 4 mutations, it was difficult to find which site was an important site through a single mutant. Also, since m35 shows enhanced production ration (Figure 4.11), single mutant study for m35 was also conducted. A401V at the end of the PpAlkB C-term and S115F at the periplasm were excluded from the test (Figure 4.12, Table 4.3).

10.47 mM (7.26 mM of 12-HDA and 3.21 mM of DDDA) and 9.33 mM (6.20 mM of 12-HDA and 3.13 mM of DDDA) of products were produced with H292L and S313P single mutant (Figure 4.13).

In particular, the production with H292L was almost similar to that of multiple mutants (Figure 4.14). AlkB is known to oxygenate alkane by di-iron present in the cytoplasm. Both H292 and S313 are present in the cytoplasm and two residues are expected to be near iron ions from the topology structure of AlkB. S313 is the site which was in the histidine containing sequence motif D (L_{309}QRHXDHHA$_{317}$). Histidine containing sequence motif was known to be essential for the involvement in co-ordination of di-iron center (Alonso et al. 2014). As it is a residue in the conserved region that interacts with iron, it is expected to play an important role in the acitivity of enzymes.

Finally, H292L was introduced into m80 in order to make a mutant with higher activity. 12.95 mM (11 mM of 12-HDA and 1.96 mM of DDDA) of products was produced by PpAlkB with H292L/F253I/S313P mutation, while 12.51 mM (10.5 mM of 12-HDA and 2.01 mM of DDDA) of products was produced by m80 (Figure 4.15). After testing the activity of the mutant through 100 mM DAME reaction, a biphasic reaction was performed to maximize the production amount of 12-HDA. 12-HDA is known as a substance that inhibits the reaction of monooxygenase (Lundemo et

al. 2016). Biphasic reactions would help to circumvent the product inhibition (Sarak et al. 2021). Therefore, many studies have been conducted to produce 12-HDA through the biphasic reaction (Yoo et al. 2019, Julsing et al. 2012, Scheps et al. 2013). DAME, which exists in a liquid state at room temperature, could be used as an organic solvent in the biphasic reaction to produce 12-HDA. In particular, if DAME was used as an organic solvent, it has the advantage of not only removing product inhibition but also enabling continuous substrate supply. Therefore, biphasic reaction using DAME as a substrate and an organic solvent was conducted. According to a previous study, when process a biphasic reaction using DAME as an organic solvent and substrate, the most 12-HDA could be produced with the reaction proceeds in a ratio of organic phase: Aqueous phase = 2: 1 (Yoo et al. 2019). 54 mM and 48.4 mM of products were produced with E . coli containing F253I / H292L / S313P and F253I / S313P mutant. This is an increase of 43% and 33%, respectively, compared to WT which produced 33.9 mM (Figure 4.16).

Finding a mutant with improved activity is a research being conducted by many groups. In this study, our group performed in

vivo screening with TtFadR and antibiotic resistance gene as screening module. We found mutant with 64% enhanced activity toward DAME as substrate. This study could contribute to the study of alkane monooxygenase.
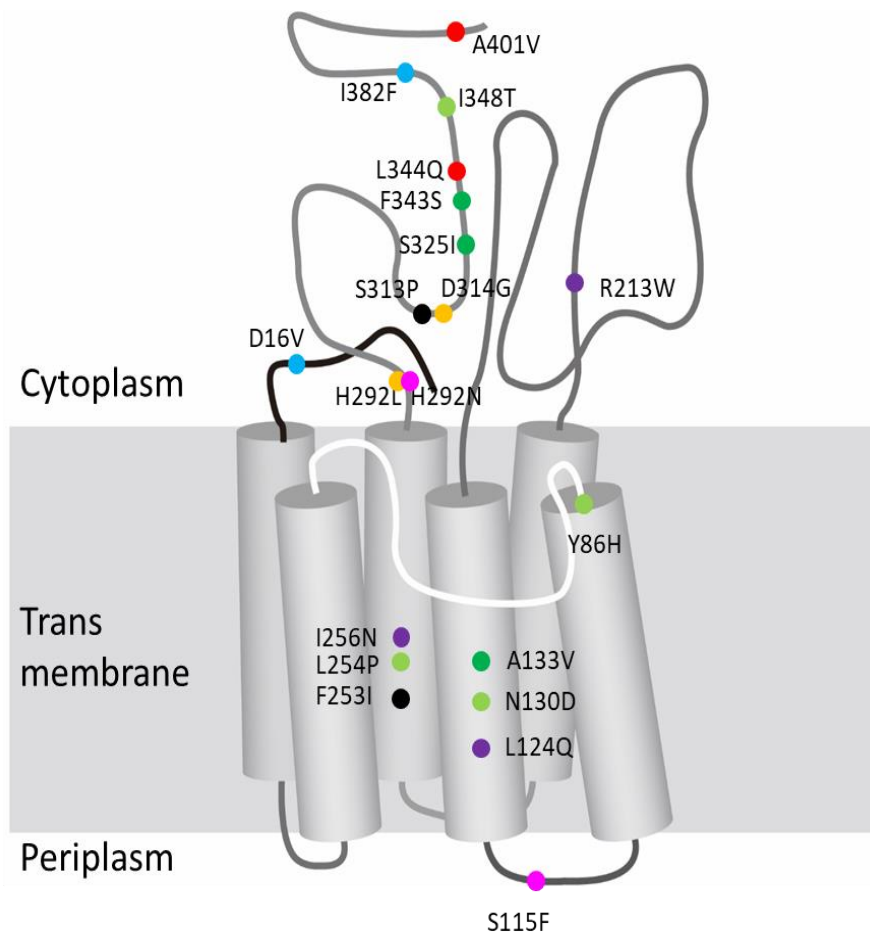
Figure 4. 12 Topological model of PpAlkB and approximate locations of each single mutant. Red circle : m22, orange circle : m34, yellow green circle : m35, blue circle : m37, purple circle : m40, green circle : m61, margenta circle : m78, black circle : m80

Table 4. 3 Locations of each single mutant residues

	Cytoplasm	Transmembrane	Periplasm
m22	L344Q A401V		
m34	H292L D314G		
m35	I348T	Y86H N130D L254P	
m37	D16V I382F		
m40	R213W	L124Q I256N	
m61	S325I F343S	A133V	
m78	H292N		S115F
m80	S313P	F253I	
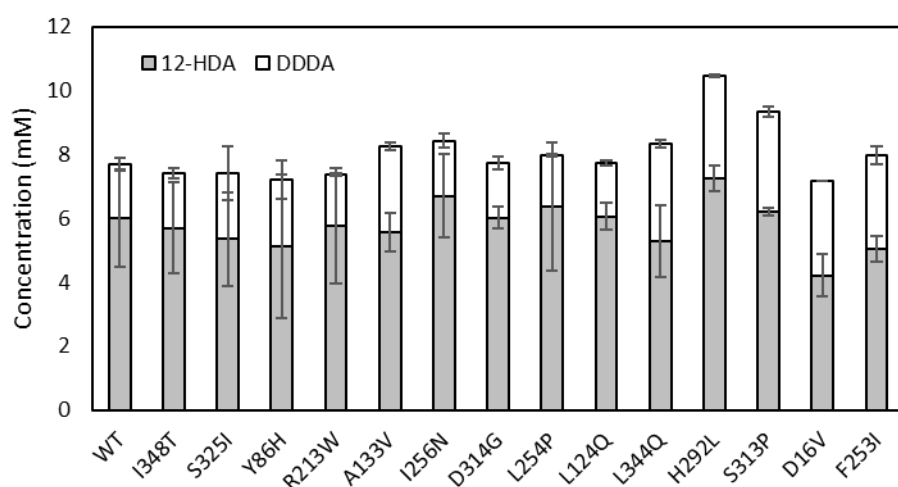
Figure 4. 13 Production of 12－HDA and DDDA from 100 mM
DAME with BW25113(Δ*fadD*, DE3) with single mutant. The
reaction was performed in potassium phosphate buffer (100 mM,
pH 7.5) supplemented with 30 OD_{600}, 100 mM DAME, 1%(w/v)
glucose at 30℃ for 12 hours. Gray box means 12－HDA and white
box means DDDA.
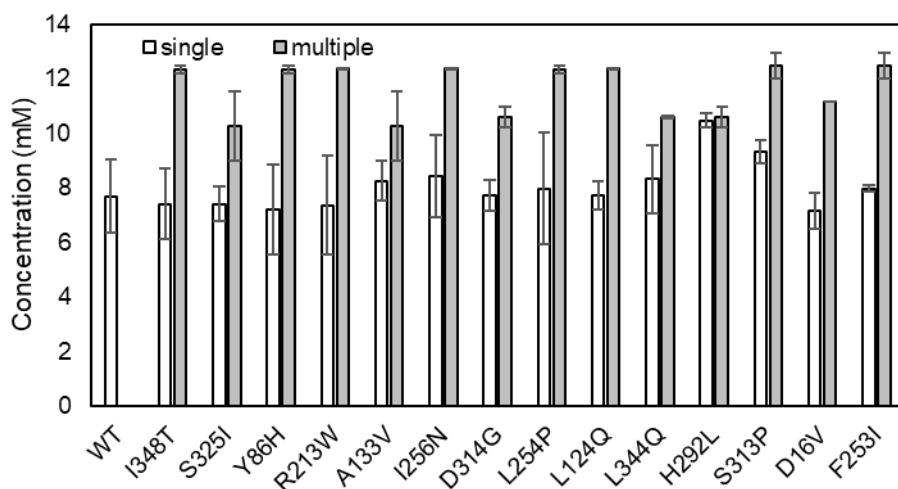
Figure 4. 14 Comparison of the concentration of products between ingle mutant and multiple mutant. The reaction was performed in potassium phosphate buffer (100 mM, pH 7.5) supplemented with 30 OD_{600}, 100 mM DAME, 1%(w/v) glucose at 30℃ for 12 hours. Gray box means 12-HDA and white box means DDDA.
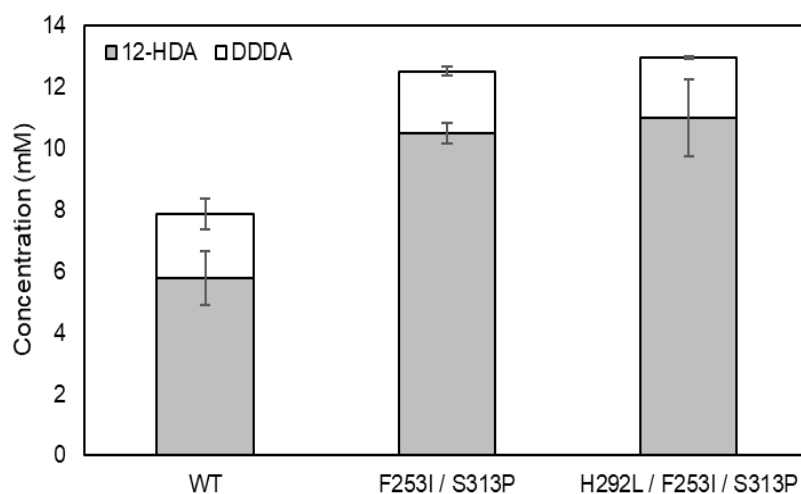
Figure 4. 15 Resting cell reaction for the production of 12-HDA and DDDA from 100 mM DAME using PpAlkB wild type, H292L/F253I/S313P and F253I/S313P mutants. The reaction was performed in potassium phosphate buffer (100 mM, pH 7.5) supplemented with 30 OD_{600}, 100 mM DAME, 1%(w/v) glucose at 30℃ for 12 hours. Gray box means 12-HDA and white box means DDDA.
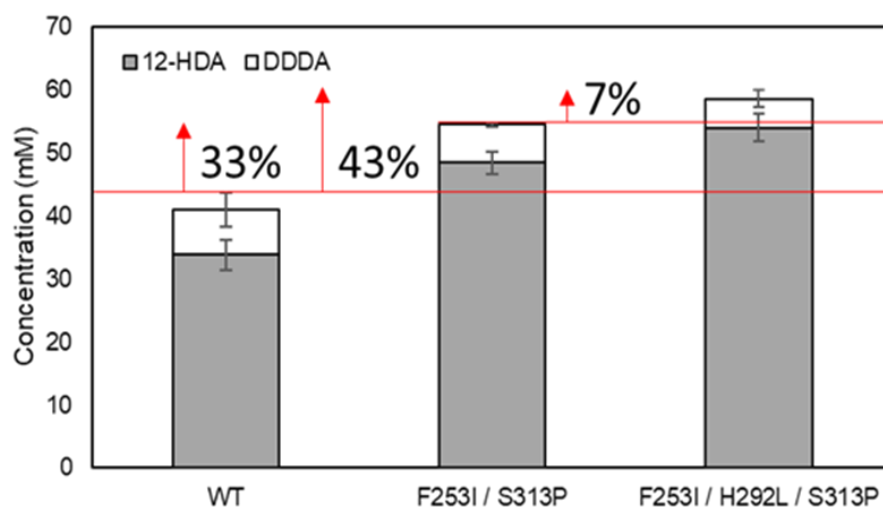
Figure 4. 16 Biphasic reaction for the production of 12-HDA and DDDA with DAME as organic phase and substrate using PpAlkB wild type, H292L/F253I/S313P and F253I/S313P mutants. The reaction was performed in potassium phosphate buffer (100 mM, pH 7.5) supplemented with 30 OD_{600}, 100 mM DAME, 1%(w/v) glucose at 30℃ for 12 hours. Gray box means 12-HDA and white box means DDDA.

4.4 Conclusion

In this study, *in vivo* screening system combining TtFadR and the antibiotic resistance gene was constructed and PpAlkB mutants with increased activity toward DAME were evaluated. F253I/S313P mutant showed 58% improved activity than that of the WT. Single mutant evaluation showed H292L and S313P with 35% and 21% increased activity than that of the WT, respectively. However, introduction of H292L into F253I/S313P mutant did not improve the activity toward DAME. This research is expected to contribute to the study of alkane monooxygenase.

Chapter 5. Overall conclusion and further suggestion

5.1 Overall conclusion: Biosynthesis of 12-hydroxy lauric acid and biopolymer monomers in *Escherichia coli* using alkane monooxygenase

AlkB, a well known non-heme alkane monooxygenase, has been studied in many groups since its first discovery from *Pseudomonas oleovorans* (Eggink et al. 1987). AlkB, which receives electrons from AlkG and AlkT, and transfers a hydroxyl group to the terminal position of medium chain alkane, has the advantage of a regio-selective hydroxylation reaction. To biosynthesize bioplastics, efficient production of ω-hydroxy fatty acid (ω-HFA) is the key (Zhang et al. 2020). Therefore, it is important to implement AlkBGT to biosynthesize monomers of the biopolymer as an alternative to the chemical synthesis method, which regio-selective reactions are very difficult.

In this study, production of 12-hydroxy dodecanoic acid (12-HDA) was achieved with the AlkBGT system in *E. coli* through i) the identification of novel monooxygenase, ii) development of chimeric transporter, and iii) optimization of protein expression in *E. coli*. 76.6 mM (44.8 mM of 12-HDA and 31.8 mM of dodecanedioic acid (DDDA)) was produced from dodecanoic acid methyl ester

(DAME) in *E. coli*. Next, based on successful 12-HDA production in *E. coli*, we constructed multi-enzymatic cascade reaction with three cell modules [Hydroxylation module (Cell-H^m), Amination module (Cell-A^m), and Reduction module (Cell-R^m)] to biosynthesize various biopolymer monomers from DAME. The multi-enzymatic cascade reactions with product specific combination of these cell modules generated 46.3 mM 12-amino dodecanoic acid, 27 mM 1,12-dodecanediol, and 21.5 mM 1,12-diaminododecane from 100 mM dodecanoic acid methyl ester. Additionally, various carbon chain length products (C8, C10, C12) were synthesized via the enzyme cascade reaction. Finally, to find PpAlkB mutant with enhanced activity toward DAME, we designed in vivo screening system with TtFadR and antibiotic resistance gene. This screening method is based on lauroyl-CoA sensitive promoter activation, where antibiotic resistance gene was expressed and the cell growth rate was accelerated with increased dodecanoic acid concentrations. PpAlkB with F253I/S313P mutation showed 58% enhanced activity toward DAME than that of WT. In addition, through single mutant evaluations, it was confirmed that the H292L mutant had 35% better activity than that of WT. However, the

mutant that introduced H292L into F253I/S313P had similar activity toward DAME compared to F253I/S313P. 12.95 mM (11 mM of 12-HDA and 1.96 mM of DDDA) of products was produced from 100 mM DAME by PpAlkB with F253I/H292L/S313P mutation which shows 64% improved than WT.

5.2 Further suggestion: Saturation mutagenesis of PpAlkB

From the results in Chapter 4, F253I/H292L/S313P mutant showed enhanced activity toward DAME than that of the WT. Since the library of PpAlkB was generated by error-prone PCR, we could not test all the possible mutants of PpAlkB. Single mutant evaluation confirmed that the H292L and S313P mutations were the key mutations that improved the activity. Therefore, there is a possibility that the activity will be further improved when the corresponding residues are mutated to other amino acids.

Site-saturation mutagenesis is a method in which a single amino acid is replaced with other 19 possible substitutions (Siloto and Weselake 2012). Provided with high throughput screening method, site-saturation mutagenesis is advantageous in terms of work load and time over site-directed mutagenesis to 19 other amino acids. Since one single mutant and one double mutant were found in Chapter 4, saturation mutagenesis on these residues is highly suggested.

Iterative saturation mutagenesis is developed by Reetz and Carballeira to allow quick searching of beneficial mutants by

applying site－saturation mutagenesis on top of a beneficial mutant as a starting point (Reetz and Carballeira 2007). Although it is a prominent method for protein engineering, there are some drawbacks of this method. One of the greatest drawbacks is that the method does not compare all the possible combinations of variants. Exploring all possible sequence space is always the desired outcome that the scientists want. However, applying site－saturation mutagenesis on more than four sites increases the required number of transformants (i.e. 95% coverage of 4 NNK sites requires 3 x 10^7) significantly (Reetz, Kahakeaw, and Lohmer 2008).

Since only three residues were identified in this study, site－saturation mutagenesis on all three residues using NNK codon is suggested to explore as many combinations of variants as possible. The screening method developed in this study is suitable for screening 10^5 transformants, which is the required number of 3 NNK site－saturation with 95% coverage (Reetz, Kahakeaw, and Lohmer 2008).

Darwin assebly, which is known as fast, efficient, multi－site bespoke mutagenesis method, was selected for the construct of saturation mutagenesis libraries (Cozens and Pinheiro 2018).

Plasmid with target gene and nicking endonuclease site is nicked by a nicking endonuclease and the cut strand degraded by exonuclease III to generate ssDNA. Boundary and inner (mutagenic) oligonucleotides are annealed to the ssDNA plasmid. After annealing, primers are extended and ligated in an isothermal assembly reaction. The assembled strand can be isolated by streptavidin purification and cloning to the target vector (Figure 5.1)
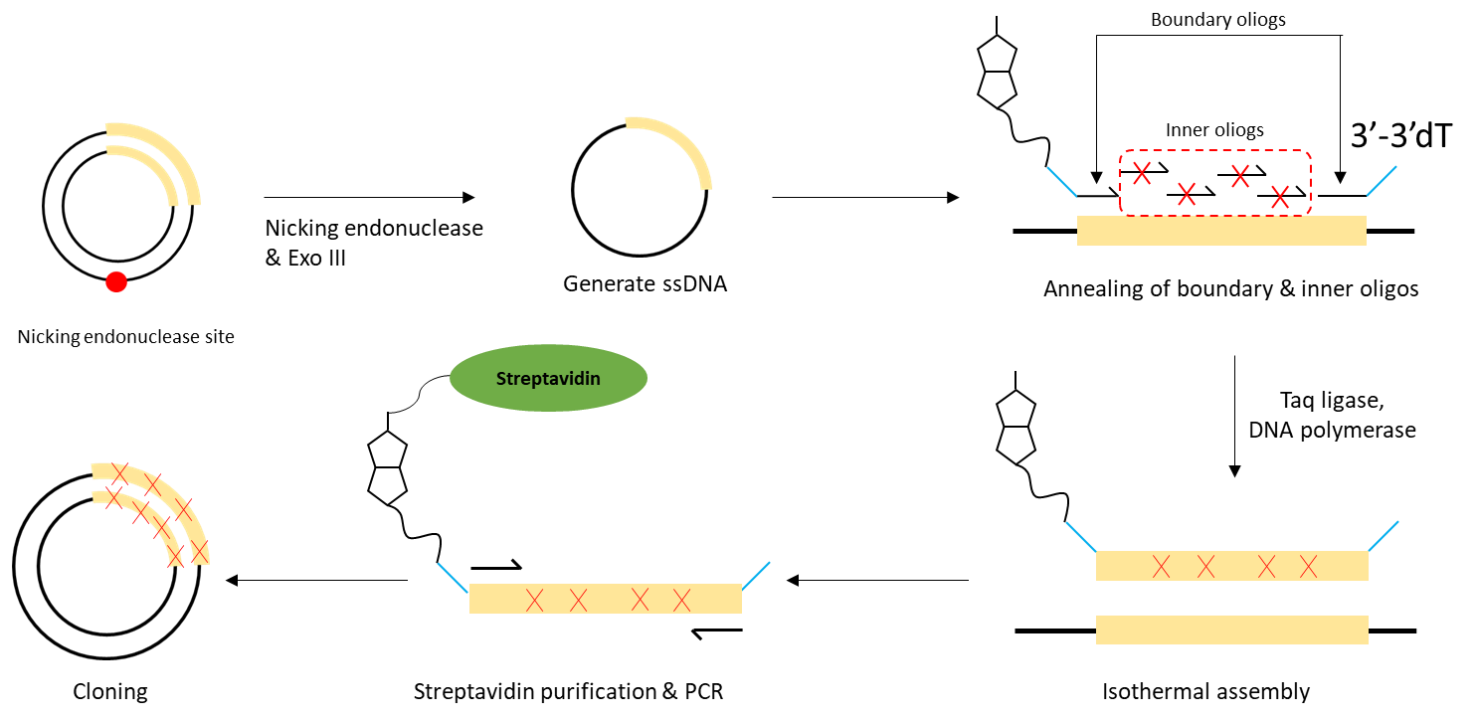
Figure 5. 1 Principles of Darwin Assembly

6. References

Agari, Yoshihiro, Kazuko Agari, Keiko Sakamoto, Seiki Kuramitsu, and Akeo Shinkai. 2011. "TetR-family transcriptional repressor Thermus thermophilus FadR controls fatty acid degradation." *Microbiology* 157 (6):1589-1601.

Ahsan, Md Murshidul, Sihyong Sung, Hyunwoo Jeon, Mahesh D. Patil, Taeowan Chung, and Hyungdon Yun. 2017. "Biosynthesis of Medium- to Long-Chain α,ω-Diols from Free Fatty Acids Using CYP153A Monooxygenase, Carboxylic Acid Reductase, and E. coli Endogenous Aldehyde Reductases." *Catalysts* 8 (1):4.

Ahsan, Md, Mahesh Patil, Hyunwoo Jeon, Sihyong Sung, Taeowan Chung, and Hyungdon Yun. 2018. "Biosynthesis of Nylon 12 Monomer, ω-Aminododecanoic Acid Using Artificial Self-Sufficient P450, AlkJ and ω-TA." *Catalysts* 8 (9):400.

Akhtar, M. K., N. J. Turner, and P. R. Jones. 2013. "Carboxylic acid reductase is a versatile enzyme for the conversion of fatty acids into fuels and chemical commodities." *Proc Natl Acad Sci U S A* 110 (1):87-92. doi: 10.1073/pnas.1216516110.

Alonso, Hernan, Oded Kleifeld, Adva Yeheskel, Poh C Ong, Yu C Liu, Jeanette E Stok, James J De Voss, and Anna Roujeinikova. 2014. "Structural and mechanistic insight into alkane hydroxylation by Pseudomonas putida AlkB." *Biochemical Journal* 460 (2):283-293.

Alonso, Hernan, and Anna Roujeinikova. 2012. "Characterization and two-dimensional crystallization of membrane component AlkB of the medium-chain alkane hydroxylase system from Pseudomonas putida GPo1." *Applied and environmental microbiology* 78 (22):7946-7953.

Bae, Jin H., Beom Gi Park, Eunok Jung, Pyung-Gang Lee, and Byung-Gee Kim. 2014. "fadD deletion and fadL overexpression in Escherichia coli increase hydroxy long-chain fatty acid productivity." *Applied Microbiology and Biotechnology* 98 (21):8917-8925. doi: 10.1007/s00253-014-5974-2.

Beilen, Jan B. van, and Enrico G. Funhoff. 2005. "Expanding the alkane oxygenase toolbox: new enzymes and applications." *Current Opinion in Biotechnology* 16 (3):308-314. doi:

https://doi.org/10.1016/j.copbio.2005.04.005.

Bernhardt, Rita, and Vlada B. Urlacher. 2014. "Cytochromes P450 as promising catalysts for biotechnological application: chances and limitations." *Applied Microbiology and Biotechnology* 98 (14):6185-6203. doi: 10.1007/s00253-014-5767-7.

Bertrand, Erin, Ryo Sakai, Elena Rozhkova-Novosad, Luke Moe, Brian G Fox, John T Groves, and Rachel N Austin. 2005. "Reaction mechanisms of non-heme diiron hydroxylases characterized in whole cells." *Journal of inorganic biochemistry* 99 (10):1998-2006.

Burch, R., and M. J. Hayes. 1995. "C-H bond activation in hydrocarbon oxidation on solid catalysts." *Journal of Molecular Catalysis A: Chemical* 100 (1):13-33. doi: https://doi.org/10.1016/1381-1169(95)00133-6.

Call, Toby P, M Kalim Akhtar, Frank Baganz, and Chris Grant. 2016. "Modulating the import of medium-chain alkanes in *E. coli* through tuned expression of FadL." *Journal of biological engineering* 10 (1):5.

Canavaci, Adriana M. C., Juan M. Bustamante, Angel M. Padilla, Cecilia M. Perez Brandan, Laura J. Simpson, Dan Xu, Courtney L. Boehlke, and Rick L. Tarleton. 2010. "In Vitro and In Vivo High-Throughput Assays for the Testing of Anti-Trypanosoma cruzi Compounds." *PLOS Neglected Tropical Diseases* 4 (7):e740. doi: 10.1371/journal.pntd.0000740.

Cao, Peigang, André Y. Tremblay, Marc A. Dubé, and Katie Morse. 2007. "Effect of Membrane Pore Size on the Performance of a Membrane Reactor for Biodiesel Production." *Industrial & Engineering Chemistry Research* 46 (1):52-58. doi: 10.1021/ie060555o.

Cao, Yujin, Tao Cheng, Guang Zhao, Wei Niu, Jiantao Guo, Mo Xian, and Huizhou Liu. 2016. "Metabolic engineering of Escherichia coli for the production of hydroxy fatty acids from glucose." *BMC biotechnology* 16 (1):26.

Chae, Tong Un, Jung Ho Ahn, Yoo-Sung Ko, Je Woong Kim, Jong An Lee, Eon Hui Lee, and Sang Yup Lee. 2020. "Metabolic engineering for the production of dicarboxylic acids and diamines." *Metabolic Engineering* 58:2-16. doi:

https://doi.org/10.1016/j.ymben.2019.03.005.

Chizzolini, Fabio, Michele Forlin, Dario Cecchi, and Sheref S Mansy. 2013. "Gene Position More Strongly Influences Cell-Free Protein Expression from Operons than T7 Transcriptional Promoter Strength." *ACS synthetic biology* 3 (6):363-371.

Choi, Kwon-Young, Hyung-Yeon Park, and Byung-Gee Kim. 2010. "Characterization of bi-functional CYP154 from Nocardia farcinica IFM10152 in the O-dealkylation and ortho-hydroxylation of formononetin." *Enzyme and Microbial Technology* 47 (7):327-334.

Clomburg, James M, Matthew D Blankschien, Jacob E Vick, Alexander Chou, Seohyoung Kim, and Ramon Gonzalez. 2015. "Integrated engineering of β-oxidation reversal and ω-oxidation pathways for the synthesis of medium chain ω-functionalized carboxylic acids." *Metabolic engineering* 28:202-212.

Coleman, Jack, Masatoshi Inukai, and Masayori Inouye. 1985. "Dual Functions of the Signal Peptide in Protein Transfer Across the Membrane." *Cell* 43 (1):351-360. doi: https://doi.org/10.1016/0092-8674(85)90040-6.

Collier, D. N. 1994. "Escherichia coli signal peptides direct inefficient secretion of an outer membrane protein (OmpA) and periplasmic proteins (maltose-binding protein, ribose-binding protein, and alkaline phosphatase) in Bacillus subtilis." *Journal of bacteriology* 176 (10):3013-3020.

Cozens, Christopher, and Vitor B Pinheiro. 2018. "Darwin Assembly: fast, efficient, multi-site bespoke mutagenesis." Nucleic Acids Research 46 (8):e51-e51.

de Sousa, BG, JIN Oliveira, EL Albuquerque, UL Fulco, VE Amaro, and CAG Blaha. 2017. "Molecular modelling and quantum biochemistry computations of a naturally occurring bioremediation enzyme: Alkane hydroxylase from Pseudomonas putida P1." *Journal of Molecular Graphics and Modelling* 77:232-239.

Denks, Kärt, Andreas Vogt, Ilie Sachelaru, Narcis-Adrian Petriman, Renuka Kudva, and Hans-Georg Koch. 2014. "The Sec translocon mediated protein transport in prokaryotes and eukaryotes." *Molecular Membrane Biology* 31 (2-3):58-84. doi: 10.3109/09687688.2014.907455.

Durairaj, Pradeepraj, Sailesh Malla, Saravanan Prabhu Nadarajan, Pyung-Gang Lee, Eunok Jung, Hyun Ho Park, Byung-Gee Kim, and Hyungdon Yun. 2015. "Fungal cytochrome P450 monooxygenases of *Fusarium oxysporum* for the synthesis of ω-hydroxy fatty acids in engineered *Saccharomyces cerevisiae*." *Microbial cell factories* 14 (1):45.

Eggink, Gerrit, Roland G Lageveen, Bert Altenburg, and Bernard Witholt. 1987. "Controlled and functional expression of the Pseudomonas oleovorans alkane utilizing system in Pseudomonas putida and Escherichia coli." *Journal of Biological Chemistry* 262 (36):17712-17718.

England, Thomas E., and Olke C. Uhlenbeck. 1978. "Enzymatic Oligoribonucleotide Synthesis with T4 RNA Ligase." *Biochemistry* 17 (11):2069-2076. doi: 10.1021/bi00604a008.

Fedorchuk, Tatiana P., Anna N. Khusnutdinova, Elena Evdokimova, Robert Flick, Rosa Di Leo, Peter Stogios, Alexei Savchenko, and Alexander F. Yakunin. 2020. "One-Pot Biocatalytic Transformation of Adipic Acid to 6-Aminocaproic Acid and 1,6-Hexamethylenediamine Using Carboxylic Acid Reductases and Transaminases." *Journal of the American Chemical Society* 142 (2):1038-1048. doi: 10.1021/jacs.9b11761.

France, Scott P., Lorna J. Hepworth, Nicholas J. Turner, and Sabine L. Flitsch. 2017. "Constructing Biocatalytic Cascades: In Vitro and in Vivo Approaches to de Novo Multi-Enzyme Pathways." *ACS Catalysis* 7 (1):710-724. doi: 10.1021/acscatal.6b02979.

Fujii, Tadashi, Tatsuya Narikawa, Futoshi Sumisa, Akira Arisawa, Koji Takeda, and Junichi Kato. 2006. "Production of α,ω-Alkanediols Using Escherichia coli Expressing a Cytochrome P450 from Acinetobacter sp. OC4." *Bioscience, Biotechnology, and Biochemistry* 70 (6):1379-1385. doi: 10.1271/bbb.50656.

Fujita, Yasutaro, Hiroshi Matsuoka, and Kazutake Hirooka. 2007. "Regulation of fatty acid metabolism in bacteria." *Molecular microbiology* 66 (4):829-839.

Ge, Jiawei, Xiaohong Yang, Hongwei Yu, and Lidan Ye. 2020. "High-yield whole cell biosynthesis of Nylon 12 monomer

with self-sufficient supply of multiple cofactors." *Metabolic Engineering* 62:172-185. doi: https://doi.org/10.1016/j.ymben.2020.09.006.

Gozzo, Franco. 2001. "Radical and non-radical chemistry of the Fenton-like systems in the presence of organic substrates." *Journal of Molecular Catalysis A: Chemical* 171 (1-2):1-22.

Grant, Chris, Dawid Deszcz, Yu-Chia Wei, Rubéns Julio Martínez-Torres, Phattaraporn Morris, Thomas Folliard, Rakesh Sreenivasan, John Ward, Paul Dalby, John M. Woodley, and Frank Baganz. 2014. "Identification and use of an alkane transporter plug-in for applications in biocatalysis and whole-cell biosensing of alkanes." *Scientific Reports* 4:5844. doi: 10.1038/srep05844
https://www.nature.com/articles/srep05844#supplementary-information.

Haak, Dale, Ken Gable, Troy Beeler, and Teresa Dunn. 1997. "Hydroxylation of *Saccharomyces cerevisiae* Ceramides Requires Sur2p and Scs7p." *Journal of Biological Chemistry* 272 (47):29704-29710. doi: 10.1074/jbc.272.47.29704.

Han, Sang-Woo, Youngho Jang, and Jong-Shik Shin. 2019. "In Vitro and In Vivo One-Pot Deracemization of Chiral Amines by Reaction Pathway Control of Enantiocomplementary ω-Transaminases." *ACS Catalysis* 9 (8):6945-6954. doi: 10.1021/acscatal.9b01546.

He, Qiaofei, George N. Bennett, Ka-Yiu San, and Hui Wu. 2019. "Biosynthesis of Medium-Chain ω-Hydroxy Fatty Acids by AlkBGT of Pseudomonas putida GPo1 With Native FadL in Engineered Escherichia coli." *Frontiers in Bioengineering and Biotechnology* 7 (273). doi: 10.3389/fbioe.2019.00273.

Horga, Luminita Gabriela, Samantha Halliwell, Tania Selas Castiñeiras, Chris Wyre, Cristina F. R. O. Matos, Daniela S. Yovcheva, Ross Kent, Rosa Morra, Steven G. Williams, Daniel C. Smith, and Neil Dixon. 2018. "Tuning recombinant protein expression to match secretion capacity." *Microbial Cell Factories* 17 (1):199. doi: 10.1186/s12934-018-1047-z.

Huf, Sabine, Sven Krügener, Thomas Hirth, Steffen Rupp, and Susanne Zibek. 2011. "Biotechnological synthesis of long-chain dicarboxylic acids as building blocks for polymers." *European Journal of Lipid Science and Technology* 113

(5):548-561.

Hwang, Sung Hee, Karen Wagner, Jian Xu, Jun Yang, Xichun Li, Zhengyu Cao, Christophe Morisseau, Kin Sing Stephen Lee, and Bruce D. Hammock. 2017. "Chemical synthesis and biological evaluation of ω-hydroxy polyunsaturated fatty acids." *Bioorganic & Medicinal Chemistry Letters* 27 (3):620-625. doi: https://doi.org/10.1016/j.bmcl.2016.12.002.

Jang, Hyun-Young, Kaushik Singha, Hwan-Hee Kim, Yong-Uk Kwon, and Jin-Byung Park. 2016. "Chemo-enzymatic synthesis of 11-hydroxyundecanoic acid and 1,11-undecanedioic acid from ricinoleic acid." *Green Chemistry* 18 (4):1089-1095. doi: 10.1039/C5GC01017A.

Ji-Won Song, Joo-Hyun Seo, Doek-Kun Oh ORCID logoc, Uwe T. Bornscheuer d and Jin-Byung Park ORCID logo*ae. 2020. "Design and engineering of whole-cell biocatalytic cascades for the valorization of fatty acids." *Catal. Sci. Technol.* 10:46-64.

Jiang, Y., and K. Loos. 2016a. "Enzymatic Synthesis of Biobased Polyesters and Polyamides." *Polymers (Basel)* 8 (7). doi: 10.3390/polym8070243.

Jiang, Yi, and Katja Loos. 2016b. "Enzymatic Synthesis of Biobased Polyesters and Polyamides." *Polymers* 8 (7):243.

Joo, Sung-Yeon, Hee-Wang Yoo, Sharad Sarak, Byung-Gee Kim, and Hyungdon Yun. 2019. "Enzymatic Synthesis of ω-Hydroxydodecanoic Acid By Employing a Cytochrome P450 from Limnobacter sp. 105 MED." *Catalysts* 9 (1):54.

Joo, Young-Chul, Eun-Sun Seo, Yeong-Su Kim, Kyoung-Rok Kim, Jin-Byung Park, and Deok-Kun Oh. 2012. "Production of 10-hydroxystearic acid from oleic acid by whole cells of recombinant Escherichia coli containing oleate hydratase from Stenotrophomonas maltophilia." *Journal of Biotechnology* 158 (1):17-23. doi: https://doi.org/10.1016/j.jbiotec.2012.01.002.

Julsing, Mattijs K, Manfred Schrewe, Sjef Cornelissen, Inna Hermann, Andreas Schmid, and Bruno Bühler. 2012. "Outer Membrane Protein AlkL Boosts Biocatalytic Oxyfunctionalization of Hydrophobic Substrates in *Escherichia coli*." *Applied and environmental microbiology*

78 (16):5724-5733.

Jung, Da-Hye, Wonji Choi, Kwon-Young Choi, Eunok Jung, Hyungdon Yun, Romas J. Kazlauskas, and Byung-Gee Kim. 2013. "Bioconversion of *p*-coumaric acid to *p*-hydroxystyrene using phenolic acid decarboxylase from *B. amyloliquefaciens* in biphasic reaction system." *Applied Microbiology and Biotechnology* 97 (4):1501-1511. doi: 10.1007/s00253-012-4358-8.

Jung, Eunok, Beom Gi Park, Md. Murshidul Ahsan, Joonwon Kim, Hyungdon Yun, Kwon-Young Choi, and Byung-Gee Kim. 2016. "Production of *ω*-hydroxy palmitic acid using CYP153A35 and comparison of cytochrome P450 electron transfer system in vivo." *Applied Microbiology and Biotechnology* 100 (24):10375-10384. doi: 10.1007/s00253-016-7675-5.

Jung, Eunok, Beom Gi Park, Hee-Wang Yoo, Joonwon Kim, Kwon-Young Choi, and Byung-Gee Kim. 2018. "Semi-rational engineering of CYP153A35 to enhance *ω*-hydroxylation activity toward palmitic acid." *Applied Microbiology and Biotechnology* 102 (1):269-277. doi: 10.1007/s00253-017-8584-y.

Kadisch, Marvin, Mattijs K Julsing, Manfred Schrewe, Nico Jehmlich, Benjamin Scheer, Martin von Bergen, Andreas Schmid, and Bruno Bühler. 2017. "Maximization of Cell Viability Rather Than Biocatalyst Activity Improves Whole-Cell *ω*-Oxyfunctionalization Performance." *Biotechnology and bioengineering* 114 (4):874-884.

Kadisch, Marvin, Andreas Schmid, and Bruno Bühler. 2017. "Hydrolase BioH knockout in E. coli enables efficient fatty acid methyl ester bioprocessing." *Journal of industrial microbiology & biotechnology* 44 (3):339-351.

Kadisch, Marvin, Christian Willrodt, Michael Hillen, Bruno Bühler, and Andreas Schmid. 2017. "Maximizing the stability of metabolic engineering-derived whole-cell biocatalysts." *Biotechnology Journal*.

Kang, Yun, Mike S. Son, and Tung T. Hoang. 2007. "One step engineering of T7-expression strains for protein production: increasing the host-range of the T7-expression system." *Protein expression and purification* 55 (2):325-333. doi:

10.1016/j.pep.2007.06.014.

Kaur, Jashandeep, Arbind Kumar, and Jagdeep Kaur. 2018. "Strategies for optimization of heterologous protein expression in *E. coli*: Roadblocks and reinforcements." *International Journal of Biological Macromolecules* 106:803–822. doi: https://doi.org/10.1016/j.ijbiomac.2017.08.080.

Kawaguchi, Hideo, Chiaki Ogino, and Akihiko Kondo. 2017. "Microbial conversion of biomass into bio-based polymers." *Bioresource Technology* 245:1664–1673. doi: https://doi.org/10.1016/j.biortech.2017.06.135.

Kelly, Jason R., Adam J. Rubin, Joseph H. Davis, Caroline M. Ajo-Franklin, John Cumbers, Michael J. Czar, Kim de Mora, Aaron L. Glieberman, Dileep D. Monie, and Drew Endy. 2009. "Measuring the activity of BioBrick promoters using an in vivo reference standard." *Journal of Biological Engineering* 3 (1):4. doi: 10.1186/1754-1611-3-4.

Kim, Geon-Hee, Hyunwoo Jeon, Taresh P. Khobragade, Mahesh D. Patil, Sihyong Sung, Sanghan Yoon, Yumi Won, In Suk Choi, and Hyungdon Yun. 2019. "Enzymatic synthesis of sitagliptin intermediate using a novel ω-transaminase." *Enzyme and Microbial Technology* 120:52–60. doi: https://doi.org/10.1016/j.enzmictec.2018.10.003.

Kim, Joonwon, Hee-Wang Yoo, Minsuk Kim, Eun-Jung Kim, Changmin Sung, Pyung-Gang Lee, Beom Gi Park, and Byung-Gee Kim. 2018. "Rewiring FadR regulon for the selective production of ω-hydroxy palmitic acid from glucose in *Escherichia coli*." *Metabolic Engineering* 47:414–422. doi: https://doi.org/10.1016/j.ymben.2018.04.021.

Kim, Tae-Hun, Su-Hwan Kang, Jeong-Eun Han, Eun-Ji Seo, Eun-Yeong Jeon, Go-Eun Choi, Jin-Byung Park, and Deok-Kun Oh. 2020. "Multilayer Engineering of Enzyme Cascade Catalysis for One-Pot Preparation of Nylon Monomers from Renewable Fatty Acids." *ACS Catalysis* 10 (9):4871–4878. doi: 10.1021/acscatal.9b05426.

Klatte, Stephanie, and Volker F. Wendisch. 2014. "Redox self-sufficient whole cell biotransformation for amination of alcohols." *Bioorganic & Medicinal Chemistry* 22 (20):5578–5585. doi: https://doi.org/10.1016/j.bmc.2014.05.012.

Ko, Yoo-Sung, Je Woong Kim, Jong An Lee, Taehee Han, Gi Bae

Kim, Jeong Eum Park, and Sang Yup Lee. 2020. "Tools and strategies of systems metabolic engineering for the development of microbial cell factories for chemical production." *Chemical Society Reviews* 49 (14):4615－4636. doi: 10.1039/D0CS00155D.

Koch, Daniel J, Mike M Chen, Jan B van Beilen, and Frances H Arnold. 2009. "In vivo evolution of butane oxidation by terminal alkane hydroxylases AlkB and CYP153A6." *Applied and environmental microbiology* 75 (2):337－344.

Kok, M, Roelof Oldenhuis, MP van der Linden, CH Meulenberg, Jaap Kingma, and Bernard Witholt. 1989. "The Pseudomonas oleovorans alkBAC operon encodes two structurally related rubredoxins and an aldehyde dehydrogenase." *Journal of Biological Chemistry* 264 (10):5442－5451.

Kok, M, Roelof Oldenhuis, MP Van Der Linden, Philip Raatjes, Jaap Kingma, Philip H van Lelyveld, and Bernard Witholt. 1989. "The Pseudomonas oleovorans alkane hydroxylase gene. Sequence and expression." *Journal of Biological Chemistry* 264 (10):5435－5441.

Kumar, Sudhir, Glen Stecher, and Koichiro Tamura. 2016. "MEGA7: Molecular Evolutionary Genetics Analysis Version 7.0 for Bigger Datasets." *Molecular Biology and Evolution* 33 (7):1870－1874. doi: 10.1093/molbev/msw054.

Kunjapur, Aditya M., Yekaterina Tarasova, and Kristala L. J. Prather. 2014. "Synthesis and Accumulation of Aromatic Aldehydes in an Engineered Strain of Escherichia coli." *Journal of the American Chemical Society* 136 (33):11644－11654. doi: 10.1021/ja506664a.

Ladkau, Nadine, Miriam Assmann, Manfred Schrewe, Mattijs K Julsing, Andreas Schmid, and Bruno Bühler. 2016. "Efficient production of the Nylon 12 monomer ω－aminododecanoic acid methyl ester from renewable dodecanoic acid methyl ester with engineered *Escherichia coli*." *Metabolic engineering* 36:1－9.

Lee, Heeseok, Changpyo Han, Hyeok－Won Lee, Gyuyeon Park, Wooyoung Jeon, Jungoh Ahn, and Hongweon Lee. 2018. "Development of a promising microbial platform for the production of dicarboxylic acids from biorenewable resources." *Biotechnology for Biofuels* 11 (1):310. doi:

10.1186/s13068-018-1310-x.

Lee, Michael E., Anil Aswani, Audrey S. Han, Claire J. Tomlin, and John E. Dueber. 2013. "Expression-level optimization of a multi-enzyme pathway in the absence of a high-throughput assay." *Nucleic acids research* 41 (22):10668-10678. doi: 10.1093/nar/gkt809.

Lee, Minwoo, Hyejin Um, and Michael W. Van Dyke. 2017. "Identification and characterization of preferred DNA-binding sites for the Thermus thermophilus transcriptional regulator FadR." *PloS one* 12 (9):e0184796-e0184796. doi: 10.1371/journal.pone.0184796.

Lee, Pyung-Gang, Joonwon Kim, Eun-Jung Kim, Sang-Hyuk Lee, Kwon-Young Choi, Romas J. Kazlauskas, and Byung-Gee Kim. 2017. "Biosynthesis of (-)-5-Hydroxy-equol and 5-Hydroxy-dehydroequol from Soy Isoflavone, Genistein Using Microbial Whole Cell Bioconversion." *ACS Chemical Biology* 12 (11):2883-2890. doi: 10.1021/acschembio.7b00624.

Leung, Dennis YC, Xuan Wu, and MKH Leung. 2010. "A review on biodiesel production using catalyzed transesterification." *Applied energy* 87 (4):1083-1095.

Leveson-Gower, Reuben B., Clemens Mayer, and Gerard Roelfes. 2019. "The importance of catalytic promiscuity for enzyme design and evolution." *Nature Reviews Chemistry* 3 (12):687-705. doi: 10.1038/s41570-019-0143-x.

Lin, Baixue, and Yong Tao. 2017. "Whole-cell biocatalysts by design." *Microbial Cell Factories* 16 (1):106. doi: 10.1186/s12934-017-0724-7.

Liu, Chen, Fei Liu, Jiali Cai, Wenchun Xie, Timothy E. Long, S. Richard Turner, Alan Lyons, and Richard A. Gross. 2011. "Polymers from Fatty Acids: Poly(ω-hydroxyl tetradecanoic acid) Synthesis and Physico-Mechanical Studies." *Biomacromolecules* 12 (9):3291-3298. doi: 10.1021/bm2007554.

Lu, Wenhua, Jon E Ness, Wenchun Xie, Xiaoyan Zhang, Jeremy Minshull, and Richard A Gross. 2010. "Biosynthesis of Monomers for Plastics from Renewable Oils." *Journal of the American Chemical Society* 132 (43):15451-15455.

Lundemo, MT, S Notonier, G Striedner, B Hauer, and JM Woodley.

2016. "Process limitations of a whole-cell P450 catalyzed reaction using a CYP153A-CPR fusion construct expressed in Escherichia coli." *Applied microbiology and biotechnology* 100 (3):1197-1208.

Malca, Sumire Honda, Daniel Scheps, Lisa Kühnel, Elena Venegas-Venegas, Alexander Seifert, Bettina M Nestl, and Bernhard Hauer. 2012. "Bacterial CYP153A monooxygenases for the synthesis of omega-hydroxylated fatty acids." *Chemical Communications* 48 (42):5115-5117.

McKeen, Laurence W. 2012. "8 - Polyamides (Nylons)." In *Film Properties of Plastics and Elastomers (Third Edition)*, edited by Laurence W. McKeen. Boston: William Andrew Publishing.

Metzger, J. O., and U. Bornscheuer. 2006. "Lipids as renewable resources: current state of chemical and biotechnological conversion and diversification." *Applied Microbiology and Biotechnology* 71 (1):13-22. doi: 10.1007/s00253-006-0335-4.

Mountanea, Olga G., Dimitris Limnios, Maroula G. Kokotou, Asimina Bourboula, and George Kokotos. 2019. "Asymmetric Synthesis of Saturated Hydroxy Fatty Acids and Fatty Acid Esters of Hydroxy Fatty Acids." *European Journal of Organic Chemistry* 2019 (10):2010-2019. doi: 10.1002/ejoc.201801881.

Mutlu, Hatice, and Michael A. R. Meier. 2010. "Castor oil as a renewable resource for the chemical industry." *European Journal of Lipid Science and Technology* 112 (1):10-30. doi: https://doi.org/10.1002/ejlt.200900138.

Naing, Swe-Htet, Saba Parvez, Marilla Pender-Cudlip, John T Groves, and Rachel N Austin. 2013. "Substrate specificity and reaction mechanism of purified alkane hydroxylase from the hydrocarbonoclastic bacterium Alcanivorax borkumensis (AbAlkB)." *Journal of inorganic biochemistry* 121:46-52.

Newton, Matilda S., Vickery L. Arcus, Monica L. Gerth, and Wayne M. Patrick. 2018. "Enzyme evolution: innovation is easy, optimization is complicated." *Current Opinion in Structural Biology* 48:110-116. doi: https://doi.org/10.1016/j.sbi.2017.11.007.

Nie, Yong, Chang-Qiao Chi, Hui Fang, Jie-Liang Liang, She-Lian Lu, Guo-Li Lai, Yue-Qin Tang, and Xiao-Lei Wu. 2014.

"Diverse alkane hydroxylase genes in microorganisms and environments." *Scientific reports* 4.

Nov, Yuval. 2012. "When Second Best Is Good Enough: Another Probabilistic Look at Saturation Mutagenesis." *Applied and Environmental Microbiology* 78 (1):258-262. doi: 10.1128/aem.06265-11.

Nuland, Youri M, Fons A Vogel, Gerrit Eggink, and Ruud A Weusthuis. 2017. "Expansion of the ω-oxidation system AlkBGTL of Pseudomonas putida GPo1 with AlkJ and AlkH results in exclusive mono-esterified dicarboxylic acid production in E. coli." *Microbial Biotechnology* 10 (3):594-603.

O'Reilly, Elaine, Valentin Köhler, Sabine L Flitsch, and Nicholas J Turner. 2011. "Cytochromes P450 as useful biocatalysts: addressing the limitations." *Chemical Communications* 47 (9):2490-2501.

Pandey, Bishnu Prasad, Nahum Lee, Kwon-Young Choi, Ji-Nu Kim, Eun-Jung Kim, and Byung-Gee Kim. 2014. "Identification of the specific electron transfer proteins, ferredoxin, and ferredoxin reductase, for CYP105D7 in Streptomyces avermitilis MA4680." *Applied Microbiology and Biotechnology* 98 (11):5009-5017. doi: 10.1007/s00253-014-5525-x.

Park, Eul-Soo, and Jong-Shik Shin. 2013. "ω-Transaminase from Ochrobactrum anthropi is devoid of substrate and product inhibitions." *Applied and environmental microbiology* 79 (13):4141-4144. doi: 10.1128/AEM.03811-12.

Patil, Mahesh D, Gideon Grogan, Andreas Bommarius, and Hyungdon Yun. 2018. "Recent Advances in ω-Transaminase-Mediated Biocatalysis for the Enantioselective Synthesis of Chiral Amines." *Catalysts* 8 (7):254.

Patil, Mahesh D., Manoj J. Dev, Ashok S. Shinde, Kiran D. Bhilare, Gopal Patel, Yusuf Chisti, and Uttam Chand Banerjee. 2017. "Surfactant-mediated permeabilization of *Pseudomonas putida KT2440* and use of the immobilized permeabilized cells in biotransformation." *Process Biochemistry* 63:113-121. doi: https://doi.org/10.1016/j.procbio.2017.08.002.

Patil, Mahesh D., Gideon Grogan, and Hyungdon Yun. 2018.

"Biocatalyzed C-C Bond Formation for the Production of Alkaloids." *ChemCatChem* 10 (21):4783-4804. doi: doi:10.1002/cctc.201801130.

Patil, Mahesh D., Vijay P. Rathod, Umesh R. Bihade, and Uttam Chand Banerjee. 2019. "Purification and characterization of arginine deiminase from *Pseudomonas putida*: Structural insights of the differential affinities of L-arginine analogues." *Journal of Bioscience and Bioengineering* 127 (2):129-137. doi: https://doi.org/10.1016/j.jbiosc.2018.07.021.

Perera, Frederica. 2017. "Pollution from Fossil-Fuel Combustion is the Leading Environmental Threat to Global Pediatric Health and Equity: Solutions Exist." *International journal of environmental research and public health* 15 (1):16. doi: 10.3390/ijerph15010016.

Pérez-Pérez, José Manuel, Héctor Candela, and José Luis Micol. 2009. "Understanding synergy in genetic interactions." *Trends in Genetics* 25 (8):368-376. doi: https://doi.org/10.1016/j.tig.2009.06.004.

Picataggio, Stephen, Tracy Rohrer, Kristine Deanda, Dawn Lanning, Robert Reynolds, Jonathan Mielenz, and L. Dudley Eirich. 1992. "Metabolic Engineering of Candida Tropicalis for the Production of Long-Chain Dicarboxylic Acids." *Bio/Technology* 10 (8):894-898. doi: 10.1038/nbt0892-894.

Quaglia, Daniela, Maximilian C. C. J. C. Ebert, Paul F. Mugford, and Joelle N. Pelletier. 2017. "Enzyme engineering: A synthetic biology approach for more effective library generation and automated high-throughput screening." *PLOS ONE* 12 (2):e0171741. doi: 10.1371/journal.pone.0171741.

Quan, Jiayuan, and Jingdong Tian. 2011. "Circular polymerase extension cloning for high-throughput cloning of complex and combinatorial DNA libraries." *Nature Protocols* 6:242. doi: 10.1038/nprot.2010.181

Reetz, Manfred T., and José Daniel Carballeira. 2007. "Iterative saturation mutagenesis (ISM) for rapid directed evolution of functional enzymes." *Nature Protocols* 2 (4):891-903. doi: 10.1038/nprot.2007.72.

Reetz, Manfred T., Daniel Kahakeaw, and Renate Lohmer. 2008. "Addressing the Numbers Problem in Directed Evolution." *ChemBioChem* 9 (11):1797-1804. doi:

https://doi.org/10.1002/cbic.200800298.

Reetz, Manfred T., Shreenath Prasad, José D. Carballeira, Yosephine Gumulya, and Marco Bocola. 2010. "Iterative Saturation Mutagenesis Accelerates Laboratory Evolution of Enzyme Stereoselectivity: Rigorous Comparison with Traditional Methods." *Journal of the American Chemical Society* 132 (26):9144–9152. doi: 10.1021/ja1030479.

Ricca, Emanuele, Birgit Brucher, and Joerg H. Schrittwieser. 2011. "Multi-Enzymatic Cascade Reactions: Overview and Perspectives." *Advanced Synthesis & Catalysis* 353 (13):2239–2262. doi: https://doi.org/10.1002/adsc.201100256.

Rojo, Fernando. 2005. "Specificity at the End of the Tunnel: Understanding Substrate Length Discrimination by the AlkB Alkane Hydroxylase." *Journal of Bacteriology* 187 (1):19–22. doi: 10.1128/jb.187.1.19–22.2005.

Rudroff, Florian, Marko D. Mihovilovic, Harald Gröger, Radka Snajdrova, Hans Iding, and Uwe T. Bornscheuer. 2018. "Opportunities and challenges for combining chemo- and biocatalysis." *Nature Catalysis* 1 (1):12–22. doi: 10.1038/s41929–017–0010–4.

Sakagami, Yuhki, Kenji Horiguchi, Yusuke Narita, Wariya Sirithep, Kohei Morita, and Yu Nagase. 2013. "Syntheses of a novel diol monomer and polyurethane elastomers containing phospholipid moieties." *Polymer Journal* 45 (11):1159–1166. doi: 10.1038/pj.2013.48.

Sarak, S., S. Sung, H. Jeon, M. D. Patil, T. P. Khobragade, A. D. Pagar, P. E. Dawson, and H. Yun. 2021. "An Integrated Cofactor/Co-Product Recycling Cascade for the Biosynthesis of Nylon Monomers from Cycloalkylamines." *Angew Chem Int Ed Engl* 60 (7):3481–3486. doi: 10.1002/anie.202012658.

Schaffer, Steffen, and Thomas Haas. 2014. "Biocatalytic and Fermentative Production of α,ω-Bifunctional Polymer Precursors." *Organic Process Research & Development* 18 (6):752–766. doi: 10.1021/op5000418.

Scheps, Daniel, Sumire Honda Malca, Sven M Richter, Karoline Marisch, Bettina M Nestl, and Bernhard Hauer. 2013. "Synthesis of ω-hydroxy dodecanoic acid based on an

engineered CYP153A fusion construct." *Microbial biotechnology* 6 (6):694－707.

Schoffelen, Sanne, and Jan C. M. van Hest. 2012. "Multi－enzyme systems: bringing enzymes together in vitro." *Soft Matter* 8 (6):1736－1746. doi: 10.1039/C1SM06452E.

Schrewe, Manfred, Mattijs K. Julsing, Kerstin Lange, Eik Czarnotta, Andreas Schmid, and Bruno Bühler. 2014. "Reaction and catalyst engineering to exploit kinetically controlled whole－cell multistep biocatalysis for terminal FAME oxyfunctionalization." *Biotechnology and Bioengineering* 111 (9):1820－1830. doi: 10.1002/bit.25248.

Schrewe, Manfred, Anders O Magnusson, Christian Willrodt, Bruno Bühler, and Andreas Schmid. 2011. "Kinetic Analysis of Terminal and Unactivated C－H Bond Oxyfunctionalization in Fatty Acid Methyl Esters by Monooxygenase-Based Whole-Cell Biocatalysis." *Advanced Synthesis & Catalysis* 353 (18):3485－3495.

Seo, Eun－Ji, Chae Won Kang, Ji－Min Woo, Sungho Jang, Young Joo Yeon, Gyoo Yeol Jung, and Jin－Byung Park. 2019. "Multi－level engineering of Baeyer－Villiger monooxygenase－based Escherichia coli biocatalysts for the production of C9 chemicals from oleic acid." *Metabolic Engineering* 54:137－144. doi: https://doi.org/10.1016/j.ymben.2019.03.012.

Seo, Eun－Ji, Young Joo Yeon, Joo－Hyun Seo, Jung－Hoo Lee, Jhoanne P. Boñgol, Yuri Oh, Jong Moon Park, Sang－Min Lim, Choul－Gyun Lee, and Jin－Byung Park. 2018. "Enzyme/whole－cell biotransformation of plant oils, yeast derived oils, and microalgae fatty acid methyl esters into n－nonanoic acid, 9－hydroxynonanoic acid, and 1,9－nonanedioic acid." *Bioresource Technology* 251:288－294. doi: https://doi.org/10.1016/j.biortech.2017.12.036.

Shanklin, John, and Edward Whittle. 2003. "Evidence linking the Pseudomonas oleovorans alkane ω－hydroxylase, an integral membrane diiron enzyme, and the fatty acid desaturase family." *FEBS Letters* 545 (2－3):188－192. doi: 10.1016/s0014－5793(03)00529－5.

Sherkhanov, Saken, Tyler P. Korman, Steven G. Clarke, and James U. Bowie. 2016. "Production of FAME biodiesel in *E. coli* by direct methylation with an insect enzyme." *Scientific*

Reports 6:24239. doi: 10.1038/srep24239.

Sikkema, J, J A de Bont, and B Poolman. 1994. "Interactions of Cyclic Hydrocarbons with Biological Membran." *Journal of Biological Chemistry* 269 (11):8022-8028.

Siloto, Rodrigo M. P., and Randall J. Weselake. 2012. "Site saturation mutagenesis: Methods and applications in protein engineering." *Biocatalysis and Agricultural Biotechnology* 1 (3):181-189. doi: https://doi.org/10.1016/j.bcab.2012.03.010.

Singh, Pranveer, Likhesh Sharma, S. Rajendra Kulothungan, Bharat V. Adkar, Ravindra Singh Prajapati, P. Shaik Syed Ali, Beena Krishnan, and Raghavan Varadarajan. 2013. "Effect of Signal Peptide on Stability and Folding of Escherichia coli Thioredoxin." *PLOS ONE* 8 (5):e63442. doi: 10.1371/journal.pone.0063442.

Song, J. H., R. J. Murphy, R. Narayan, and G. B. H. Davies. 2009. "Biodegradable and compostable alternatives to conventional plastics." *Philosophical transactions of the Royal Society of London. Series B, Biological sciences* 364 (1526):2127-2139. doi: 10.1098/rstb.2008.0289.

Steen, Eric J, Yisheng Kang, Gregory Bokinsky, Zhihao Hu, Andreas Schirmer, Amy McClure, Stephen B Del Cardayre, and Jay D Keasling. 2010. "Microbial production of fatty-acid-derived fuels and chemicals from plant biomass." *Nature* 463 (7280):559.

Stemmer, Willem P. C., Andreas Crameri, Kim D. Ha, Thomas M. Brennan, and Herbert L. Heyneker. 1995. "Single-step assembly of a gene and entire plasmid from large numbers of oligodeoxyribonucleotides." *Gene* 164 (1):49-53. doi: https://doi.org/10.1016/0378-1119(95)00511-4.

Stephan and Mohar, B. 2006. "Simple Preparation of Highly Pure Monomeric ω-Hydroxycarboxylic Acids." *Stephan, M. M. S., & Mohar, B. (2006). Simple Preparation of Highly Pure Monomeric ω-Hydroxycarboxylic Acids. Organic Process Research & Development, 10(3), 481-483. doi:10.1021/op0502046*

Sun, Yuhan, Weiqiao Zeng, Abdelkrim Benabbas, Xin Ye, Ilia Denisov, Stephen G Sligar, Jing Du, John H Dawson, and Paul M Champion. 2013. "Investigations of heme ligation and

ligand switching in cytochromes p450 and p420." *Biochemistry* 52 (34):5941−5951.

Sung, Changmin, Eunok Jung, Kwon−Young Choi, Jin−hyung Bae, Minsuk Kim, Joonwon Kim, Eun−Jung Kim, Pyoung Il Kim, and Byung−Gee Kim. 2015. "The production of ω−hydroxy palmitic acid using fatty acid metabolism and cofactor optimization in Escherichia coli." *Applied microbiology and biotechnology* 99 (16):6667−6676.

Sung, Sihyong, Hyunwoo Jeon, Sharad Sarak, Md Murshidul Ahsan, Mahesh D Patil, Wolfgang Kroutil, Byung−Gee Kim, and Hyungdon Yun. 2018. "Parallel anti−sense two−step cascade for alcohol amination leading to ω−amino fatty acids and α, ω−diamines." *Green Chemistry* 20 (20):4591−4595.

Szklarczyk, Damian, John H Morris, Helen Cook, Michael Kuhn, Stefan Wyder, Milan Simonovic, Alberto Santos, Nadezhda T Doncheva, Alexander Roth, Peer Bork, Lars J. Jensen, and Christian von Mering. 2016. "The STRING database in 2017: quality−controlled protein–protein association networks, made broadly accessible." *Nucleic Acids Research* 45 (D1):D362−D368. doi: 10.1093/nar/gkw937.

Van Beilen, Jan B, D Penninga, and Bernard Witholt. 1992. "Topology of the membrane−bound alkane hydroxylase of Pseudomonas oleovorans." *Journal of Biological Chemistry* 267 (13):9194−9201.

Van Beilen, Jan B, Theo HM Smits, Franz F Roos, Tobias Brunner, Stefanie B Balada, Martina Röthlisberger, and Bernard Witholt. 2005. "Identification of an amino acid position that determines the substrate range of integral membrane alkane hydroxylases." *Journal of bacteriology* 187 (1):85−91.

van Beilen, Jan B., Wouter A. Duetz, Andreas Schmid, and Bernard Witholt. 2003. "Practical issues in the application of oxygenases." *Trends in Biotechnology* 21 (4):170−177. doi: https://doi.org/10.1016/S0167−7799(03)00032−5.

van Beilen, Jan B., Jaap Kingma, and Bernard Witholt. 1994. "Substrate specificity of the alkane hydroxylase system of Pseudomonas oleovorans GPo1." *Enzyme and Microbial Technology* 16 (10):904−911. doi: https://doi.org/10.1016/0141−0229(94)90066−3.

Van Bogaert, Inge NA, Marjan Demey, Dirk Develter, Wim Soetaert,

and Erick J Vandamme. 2009. "Importance of the cytochrome P450 monooxygenase CYP52 family for the sophorolipid-producing yeast Candida bombicola." *FEMS yeast research* 9 (1):87-94.

van Eunen, Karen, and Barbara M. Bakker. 2014. "The importance and challenges of in vivo-like enzyme kinetics." *Perspectives in Science* 1 (1):126-130. doi: https://doi.org/10.1016/j.pisc.2014.02.011.

van Nuland, Youri M, Gerrit Eggink, and Ruud A Weusthuis. 2016. "Application of AlkBGT and AlkL from Pseudomonas putida GPo1 for selective alkyl ester ω-oxyfunctionalization in Escherichia coli." *Applied and environmental microbiology* 82 (13):3801-3807.

Venkitasubramanian, Padmesh, Lacy Daniels, and John P. N. Rosazza. 2007. "Reduction of Carboxylic Acids by Nocardia Aldehyde Oxidoreductase Requires a Phosphopantetheinylated Enzyme*." *Journal of Biological Chemistry* 282 (1):478-485. doi: https://doi.org/10.1074/jbc.M607980200.

Voorhees, Rebecca M., and Ramanujan S. Hegde. 2016. "Structure of the Sec61 channel opened by a signal sequence." *Science (New York, N.Y.)* 351 (6268):88-91. doi: 10.1126/science.aad4992.

Wachtmeister, Jochen, and Dörte Rother. 2016. "Recent advances in whole cell biocatalysis techniques bridging from investigative to industrial scale." *Current Opinion in Biotechnology* 42:169-177. doi: https://doi.org/10.1016/j.copbio.2016.05.005.

Wadumesthrige, Kapila, Steven O. Salley, and K. Y. Simon Ng. 2009. "Effects of partial hydrogenation, epoxidation, and hydroxylation on the fuel properties of fatty acid methyl esters." *Fuel Processing Technology* 90 (10):1292-1299. doi: https://doi.org/10.1016/j.fuproc.2009.06.013.

Wang, Fei, Jing Zhao, Qian Li, Jun Yang, Renjie Li, Jian Min, Xiaojuan Yu, Gao-Wei Zheng, Hui-Lei Yu, Chao Zhai, Carlos G. Acevedo-Rocha, Lixin Ma, and Aitao Li. 2020. "One-pot biocatalytic route from cycloalkanes to α,ω-dicarboxylic acids by designed Escherichia coli consortia." *Nature Communications* 11 (1):5035. doi: 10.1038/s41467-020-

18833-7.

Wilding, Matthew, Ellen F. A. Walsh, Susan J. Dorrian, and Colin
    Scott. 2015. "Identification of novel transaminases from a
    12-aminododecanoic   acid-metabolizing   Pseudomonas
    strain." *Microbial Biotechnology* 8 (4):665-672. doi:
    https://doi.org/10.1111/1751-7915.12278.

Witholt, Bernard, Marie-José de Smet, Jaap Kingma, Jan B. van
    Beilen, Menno Kok, Roland G. Lageveen, and Gerrit Eggink.
    1990.   "Bioconversions   of   aliphatic   compounds
    byPseudomonas   oleovorans   in   multiphase   bioreactors:
    background   and   economic   potential."   *Trends   in
    Biotechnology* 8:46-52. doi: https://doi.org/10.1016/0167-
    7799(90)90133-I.

Xiao, Yi, Christopher H. Bowen, Di Liu, and Fuzhong Zhang. 2016.
    "Exploiting nongenetic cell-to-cell variation for enhanced
    biosynthesis." *Nature Chemical Biology* 12:339. doi:
    10.1038/nchembio.2046
https://www.nature.com/articles/nchembio.2046#supplementary-
    information.

Yamane, K, K Kawasaki, K Sone, T Hara, and T Prakoso. 2007.
    "Oxidation stability of biodiesel and its effects on diesel
    combustion   and   emission   characteristics."   *International
    Journal   of   Engine   Research*   8   (3):307-319.   doi:
    10.1243/14680874jer00207.

Yokota, Tadafumi, and Akio Watanabe. 1993. Process for producing
    ω-hydroxy fatty acids. Google Patents.

Yoo, Hee-Wang, Joonwon Kim, Mahesh D. Patil, Beom Gi Park,
    Sung-yeon Joo, Hyungdon Yun, and Byung-Gee Kim. 2019.
    "Production of 12-hydroxy dodecanoic acid methyl ester
    using a signal peptide sequence-optimized transporter AlkL
    and a novel monooxygenase." *Bioresource Technology*
    291:121812.   doi:
    https://doi.org/10.1016/j.biortech.2019.121812.

Yu, Ai-Qun, Nina Kurniasih Pratomo Juwono, Susanna Su Jan
    Leong, and Matthew Wook Chang. 2014. Production of Fatty
    Acid-derived valuable chemicals in synthetic microbes.
    Frontiers   in   bioengineering   and   biotechnology   2:   78.
    Accessed 2014. doi:10.3389/fbioe.2014.00078.

Zhang, Wuyuan, Jeong-Hoo Lee, Sabry H. H. Younes, Fabio Tonin,

Peter-Leon Hagedoorn, Harald Pichler, Yoonjin Baeg, Jin-Byung Park, Robert Kourist, and Frank Hollmann. 2020. "Photobiocatalytic synthesis of chiral secondary fatty alcohols from renewable unsaturated fatty acids." *Nature Communications* 11 (1):2258. doi: 10.1038/s41467-020-16099-7.

Zorn, Katja, Isabel Oroz-Guinea, Henrike Brundiek, and Uwe T. Bornscheuer. 2016. "Engineering and application of enzymes for lipid modification, an update." *Progress in Lipid Research* 63:153-164. doi: https://doi.org/10.1016/j.plipres.2016.06.001.

Appendix

AI. Enzymatic Synthesis of ω-hydroxydodecanoic acid employing a Cytochrome P450 from *Limnobacter* sp. 105 MED

AI. 1 Abstract

ω-Hydroxylated fatty acids are valuable and versatile building blocks for the production of various adhesives, lubricants, cosmetic intermediates, etc. Biosynthesis of ω-hydroxydodecanoic acid from vegetable oils is one of the important green pathways to their chemical-based synthesis. In the present study, the novel monooxygenase CYP153AL.m from Limnobacter sp. 105 MED was used for the whole-cell biotransformations. We constructed three component system comprising CYP153AL.m, putidaredoxin and putidaredoxin reductase from Pseudomonas putida. This in vivo study demonstrated that CYP153AL.m is a powerful catalyst for the biosynthesis of ω-hydroxydodecanoic acid. Under optimized conditions, the application of solid state powdered substrate rather than substrate dissolved in DMSO gave significant enhancement in overall reaction titer of the process. Employing this efficient system, 2 g/L of 12-hydroxydodecanoic acid (12-OHDDA) was produced from 4 g/L of its corresponding fatty acid, i.e. dodecanoic acid. Furthermore, the system was extended to produce 3.28 g/L of 12-OHDDA using 4 g/L of substrate by introducing native redox

partners. These results demonstrate the feasibility of CYP153AL.m-catalyzed biotransformations for the industrial production of 12-OHDDA and other valuable building blocks.

AI. 2 Introduction

ω – Hydroxylated fatty acids (ω-OHFAs) obtained from medium- and long-chain length fatty acids are versatile building blocks used as precursors for bioplastics (Soliday and Kolattukudy 1977) and high-end polymers in the chemical industry (Liu et al. 2011, Ebata, Toshima, and Matsumura 2008). In addition, oxygenated fatty acids could be used in the cosmetics industry to produce perfumes and for pharmaceutical applications as anticancer agents and polyketide antibiotics (Abe and Sugiyama 2005, Bordeaux et al. 2011). To synthesize ω-OHFAs, various chemical routes such as cross-metathesis of unsaturated fatty acid esters, followed by the hydroformylation and hydrogenation of the carbonyl group (Metzger and Bornscheuer 2006) or by the reduction of α, ω –dicarboxylic acids, have been reported. However, the chemical-based processes for the oxidation of the unreactive carbon atom require very harsh conditions, multiple steps, dependence on nonrenewable feedstocks and poor selectivity (Labinger 2004).

For these reasons, biological approaches have been in the focus of attention. Wenhua Lu and co-workers have reported

biotransformation of 200 g/L methyl tetradecanoate, which resulted into 174 g/L and 6 g/L of its corresponding OHFAs and α, ω－dicarboxylic acids (ω－DCAs), respectively using an engineered Candida tropicalis (Lu et al. 2010). Although remarkable progress has been made, these production platforms have not been exploited to a larger extent yet. Factors affecting the applicability of these processes for the large－scale production are low productivity, instability of biocatalyst and the requirement of economically feasible production facilities (Scheps et al. 2013).

To overcome these limitations, alternative bacterial－based processes have been investigated. In these processes the main key enzyme is CYP153As. The CYP153s are bacterial class I P450 enzymes that operate as three－component systems, containing a heme－dependent monooxygenase core (CYP) and two additional redox partners and/or domains, namely an iron－sulfur electron carrier (ferredoxin, Fdx) and a FAD－containing reductase (ferredoxin reductase, FdR), which transfer electrons from NAD(P)H to the monooxygenase active site (Funhoff et al. 2007). This subfamily has an excellent activity towards the ω－

hydroxylation of alkanes, primary alcohols and fatty acids (Scheps et al. 2011).

Recently, Bernhard Hauer and co-workers have demonstrated the construction of a chimeric protein, where the heme domain of CYP153AM.aq. was fused to the reductase domain of CYP102A1 isolated from Bacillus megaterium (B. megaterium) (CPRBM3), the most catalytically active P450 reported to date (Narhi and Fulco 1987). Additionally, they introduced the G307A mutant based on the GGNDT motif in the I-helix, conserved in CYP153A subfamily, which showed 2 to 20 fold more activity toward medium chain fatty acids (Malca et al. 2012).

The CYP153A.M. aq.-CPRBM3 fusion construct has been used for in vivo hydroxylation to produce ω-OHDDA. This reaction resulted into 1.2 g/L of ω–hydroxydodecanoic acid (ω-OHDDA) with high regioselectivity (> 95% ω-regioselectivity) for the terminal position by using 10 g/L of its corresponding free fatty acid as a substrate (Scheps et al. 2013). However, feasible productivity and yield at an industrial scale are not reached yet. In the current study, an enzyme mining approach revealed that three-component systems containing an excellent CYP153A is a powerful

catalyst. During this study, the application of solid state powdered

substrate rather than substrate dissolved in DMSO and introducing

the native redox partner were shown to be an effective strategy

(Figure I.1).
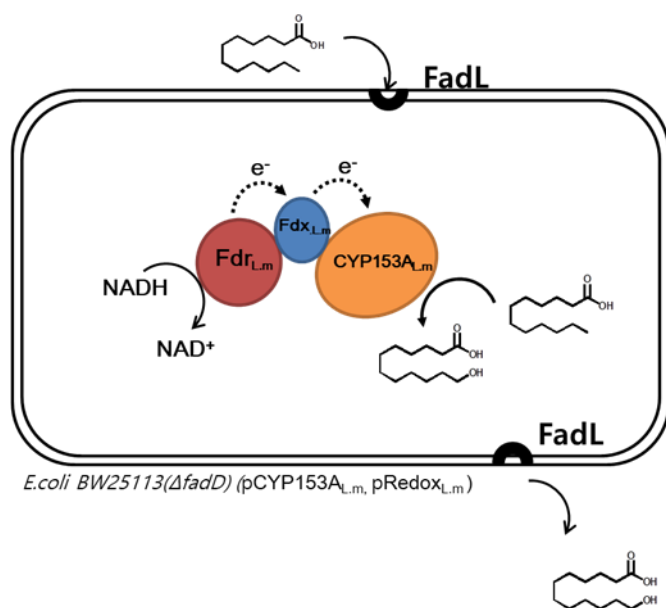
Figure I. 1 Synthesis of $\omega-$
hydroxydodecanoic acid from dodecanoic acid
using CYP153A three-component system

AI.3 Material and Method

AI.3.1 Chemicals and media

All chemicals, such as dodecanoic acid, ω−OHDDA, dimethyl sulfoxide (DMSO), isopropyl−thio−β−D−galactopyranoside (IPTG), 5−aminolevulinic acid (5−ALA), N, O−Bis (trimethylsilyl)−trifluoroacetamide (BSTFA, were purchased from Sigma−Aldrich (St. Louis, MO, USA). Chloroform was obtained from Junsei (Tokyo, Japan). Bacteriological agar, Luria Bertani (LB) broth, and terrific broth (TB) media were purchased from BD Difco (Franklin Lakes, NJ, USA). All chemicals used in this study were of analytical grade.

AI.3.2 Plasmid construction

For efficient substrate uptake, IPTG−inducible pCDF_duet1 vector having outer membrane long chain fatty acid (LCFA) transporter, *fadL* was used. The genes encoding various CYPs were codon−optimized and synthesized from Bionics (Seoul, Korea) and then each gene was inserted into the IPTG−inducible pCDF_duet1 vectors using *Nde*I and *Xho*I as a restriction site. For redox partners, CamA (ferredoxin reductase) and CamB (ferredoxin)

from *Pseudomonas putida* and LimA and LimB from *limnobacter* sp. MED 105 were cloned into pET_duet1 vector using BamHI & SacI and NdeI & EcorV respectively.

AI.3.3 Protein expression and purification

E. coli BW25113 (DE3) Δ*fadD* strain [10] was utilized for the biotransformation studies, wherein fatty acid degrading $\beta-$ oxidation pathway was blocked. Plasmid DNA were transformed into host strains using standard heat shock method. For the expression and purification of enzymes, fresh colonies from agar plates of transformants were cultured in 2 mL of LB medium containing appropriate antibiotics at 37 ˚C overnight.

The seed-cultured cells were inoculated into 50 mL Terrific- Broth (TB) in 250 mL baffle flask and cultured at 37 ˚C until the cell concentration reached an optical density at 600 nm (OD_{600}) of 0.6-0.8 for IPTG induction. The induction was performed by adding 0.01 mM IPTG, 0.25 mM 5-ALA as heme precursor, and 0.5 mM $FeSO_4$ at 30 ˚C for 16 h. MaqCYP153A, CYP153ALim, CamA/CamB, and LimA/LimB expression were carried out in 1 L of Terrific-Broth (TB) in a 3 L flask and induction was performed by

adding 0.01 mM of IPTG, 0.25 mM 5-ALA as heme precursor, and 0.5 mM $FeSO_4$ or only 0.01 mM for the redox-partners at 30 ° C for 16 h. For the purification of enzymes, cells were harvested by centrifugation at 4° C 4400 g in 15 min, washed and re-suspended in the 20 mL potassium phosphate buffer (100 mM, pH 7.5), and disrupted by sonication.

The soluble fraction of each lysate was collected after centrifugation at 16,000 rpm for 30 min and the enzymes were purified using a His-Trap-^{TM} HP column (GE Healthcare Bio-Sciences AB, Uppsala, Sweden). The Ni-NTA-bound enzymes were washed twice with 50 mM sodium phosphate buffer (pH 8.0) containing 300 mM NaCl and 20 mM imidazole. Next, the enzymes were eluted out with the same buffer containing 250 mM imidazole. Finally, the purified protein was concentrated by ultra-filtration, followed by removing the imidazole and sodium chloride *via* sequential dialysis. Purified proteins were subjected to SDS-PAGE analysis.

AI.3.4 CO-binding assay

UV absorption spectrum of CO-bound recombinant CYP proteins

after sodium dithionite reduction were measured by Multi-scan UV-Vis spectrometry (Thermo fisher scientific, USA) by scanning wavelengths ranging from 400 to 500 nm with every 5 nm interval. The concentration of P450 was measured using an extinction coefficient of 91.9 mM^{-1} cm^{-1} at 450 nm.

AI.3.5 In-vitro oxidation assay of CYP153As

The coupling efficiency of each CYPs with redox partner was evaluated using C12:0 saturated fatty acids as a substrate. The biotransformation's were performed using a final volume of 0.5 mL of 100 mM potassium phosphate buffer (pH 7.5), containing 2 μM CYP153A, ferredoxin reductase and ferredoxin *i.e* P450, CamA and CamB (1:5:10 ratio) or P450, LimA and LimB (1:5:10 ratio) at 25 °C (Pandey et al. 2014). Fatty acids were added at a final concentration of 0.5 mM (25 mM stock in DMSO). The reaction was started by the addition of the 0.2 mM NADH. Furthermore, the consumption of NADH was monitored by measuring absorbance at 340 nm (e340 = 6.22 mM^{-1} cm^{-1}). After completion the reaction was stopped by adding HCl and samples were analyzed by GC/FID analysis.

AI.3.6 Resting cell reaction

 Cells were harvested by centrifugation and washed with 100 mM potassium phosphate buffer (pH 7.5), followed by resuspension in the same buffer. The cell buffer resuspension was taken into 100 mL shake flask, with the cell density adjusted to OD_{30} in final 10 ml volume. The resting cell reaction was initiated by adding 20 mM dodecanoic acid (1 M stock in DMSO or powder form). The reactants were incubated at 30 ° C and 200 rpm, and 0.5 mL sample aliquots were collected every 2 or 6 hours. The sample preparation for product analysis was done as follows: 500 μL of the whole cell culture was acidified with 6 M HCl to pH 2 and extracted with chloroform by vigorous vortexing for 1 min. The organic phases were then collected and derivatized by using trimethylsilyl (TMS) and incubation at 50 ° C for 20 min, with an excess of BSTFA.

AI.3.7 Product identification and quantification

 Quantitative analysis was performed by gas chromatography, HP

6890 Series (Agilent Technologies, Santa Clara, CA, USA) with flame ionization detector (GC/FID). 1 μL of the sample was injected by split less mode (a split less time of 0.8 min) and analyzed using a nonpolar capillary column (5% phenyl methyl siloxane capillary 30 m×320 μm i.d. 0.25 μm film thickness, HP-5 ms).

 The oven temperature started at 50 ° C for 1 min, and then increased by 15 ° C/min to 250 ° C, holding at this temperature for 10 min. The temperature of the inlet was kept at 250 ° C, and the temperature of the detector was 280 ° C. The flow rate of the carrier gas was 1.0 mL/min, while flow rates of hydrogen, air, and helium in the FID were 45, 400, and 20 mL/min, respectively. Each peak was identified by comparison of the GC chromatogram with that of an authentic sample. Errors in the analysis were corrected by using heptadecanoic acid as an internal standard.

AI.4 Results and discussion

AI.4.1 *Construction of a CYP153A three-component system*

Bioinformatic tools have been routinely used for searching new enzymes and analysis of the similarity among already available enzymes (Zhang and Wei 2015, Darabi, Seddigh, and Abarshahr 2017, Fischer et al. 2007) Previously, A CYP153A from Marinobacter aquaeolei (CYP153AM.aq.) was reported for its high activity and selectivity toward ω-hydroxylation of C12-FA (63% conversion, 95% ω-regioselectivity) (Malca et al. 2012). For the identification of more suitable CYP153As, Basic Local Alignment Search Tool (BLAST) search was performed using CYP153AM.aq as a query sequence and 100 candidates showing resemblance to the query sequence were selected. Among them, seven CYP153As were randomly selected from various groups based on a phylogenetic tree (Figure I.2). The genes encoding CYP153As were cloned into pCDF_duet vector and expressed in E. coli BW25113 ΔfadD (DE3). As CYP153As from Oceanococcus atlanticus, Alcanivorax jadensis T9 and Nocardioides luteus (CYP53AO.a, CYP153AA.j and CYP153AN.l, respectively) were

expressed as inclusion bodies, they were neglected for the further studies. SDS－PAGE analysis and CO－binding assays confirmed the production of the other three CYP153As in soluble and active forms (Figure I.3 and Figure I.4).

To compare the performance of the active P450s, whole－cell (0.11 gCDW/mL) reactions were carried out at 30 °C and 200 rpm using cells with the active P450s, co－expressing CamA (putidaredoxin reductase) and CamB (putidaredoxin) from Pseudomonas putida in potassium phosphate buffer (100 mM, pH 7.5) in the presence of 1% (w/v) glucose. The Cells with CYP153AA.d from Alcanivorax dieselolei produced the lowest ω－OHDDA (0.38 g/L) in 24 h, while those of CYP153AS.f from Solimonas flava and CYP153AM.aq gave 0.72 g/L and 1.13 g/L from 4 g/L of dodecanoic acid (Figure I.5).

The performance of CYP153AM.aq expressing cells was similar to that of CYP153A.M. aq.－CPRBM3 fusion construct (Scheps et al. 2013). Also, those with CYP153AL.m showed the best ω－OHDDA production (1.5 g/L) from 4 g/L of dodecanoic acid (Figure I.5). Interestingly, the yields achieved herein are the highest via batch reaction so far to best of our knowledge. Further,

we attempted to make a more detailed comparison and found the concentration of the active P450s by CO—binding assay (Figure I.6). After normalization by the amount of active P450s, CYP153AL.m was shown to be more active than the other P450s (Figure I.7). Therefore, through the enzyme mining approach, the CYP153AL.m containing three component system was identified as an efficient catalyst for the bioconversion of dodecanoic acid to ω—OHDDA.

WP 079691829.1 cytochrome P450 Psychrobacter sp. DAB AL43B
WP 089554452.1 cytochrome P450 Psychrobacter sp. DAB AL32B
ORE86852.1 cytochrome P450 alkane hydroxylase Oceanococcus atlanticus
WP 026094007.1 cytochrome P450 Acinetobacter venetianus
WP 056888913.1 cytochrome P450 Nocardioides sp. Soil777
EKU55808.1 unspecific monooxygenase domain protein Acinetobacter baumannii WC-348
cytochrome P450 Moraxellaceae'
plasmid
OUS27221.1 cytochrome Gammaproteobacteria bacterium 45 16 T64
SEA50895.1 Cytochrome P450 Mycobacterium sp. 283mftsu
WP 082981516.1 cytochrome P450 Mycobacterium mucogenicum
WP 061010197.1 cytochrome P450 Mycobacterium mucogenicum
1-443 cytochrome P450 Alcanivorax sp. 97CO-5'
cytochrome P450 Alcanivorax sp. NBRC 101098 662234294
cytochrome P450 alkane hydroxylase Alcanivorax diesolei B5 407253242
KGD60654.1 cytochrome P450 alkane hydroxylase Alcanivorax jadensis T9
cytochrome P450 supertamily Alcanivorax sp. DG881 196155058
WP 008737108.1 cytochrome P450 Alcanivorax pacificus
WP 083559283.1 cytochrome P450 Oceanococcus atlanticus
WP 067723479.1 cytochrome P450 Acinetobacter sp. SFC
WP 044388071.1 cytochrome P450 Marinobacter excellens
WP 061333171.1 cytochrome P450 Marinobacter excellens
cytochrome P450 Marinobacter santoriniensis 496225176
WP 046552251.1 cytochrome P450 Marinobacter hydrocarbonoclasticus
WP 023007705.1 cytochrome P450 Marinobacter sp. EVN1
WP 052378730.1 cytochrome P450 Polycyclovorans algicola
P450 monooxygenase Alcanivorax borkumensis SK2 46102349
alcanivorax borkumensis 46102349
cytochrome P450 Limnobacter sp. MED105 495322395
cytochrome P450 Marinobacter sp. EN3 552558827
MULTISPECIES cytochrome P450 Marinobacter 552169052
MULTISPECIES cytochrome P450 Marinobacter 500108137
marinobacter aguaeolei VT8 120323386
cytochrome P450 Marinobacter sp. C1S70 552524414
cytochrome P450 Marinobacter sp. LQ44 954179751
cytochrome P450 Marinobacter sp. DSM 26291 1223606669
cytochrome P450 Marinobacter 753944309'
cytochrome P450 Marinobacter 495445616'
cytochrome P450 Alcanivorax 499906764'
cytochrome P450 alkane hydroxylase Alcanivorax borkumensis 57336817
cytochrome P450 alkane hydroxylase Alcanivorax borkumensis 57336815
cytochrome P450 Alcanivorax sp. NBRC 101098 822532359
cytochrome P450 Oceanococcus atlanticus 1180042306
cytochrome P450 gamma proteobacterium HdN1 303026854
WP 026913393.1 cytochrome P450 Perlucidibaca piscinae
cytochrome P450 Alcanivorax 652556050'
cytochrome P450 Alcanivorax sp. CP2C 1056084787
1-467 cytochrome Thalassospira sp. Nap 22'
cytochrome P450 Alcanivorax sp. N3-7A 1215197718
cytochrome P450 Alcanivorax sp. NBRC 102024 1012707324
cytochrome P450 Alcanivorax sp. P2S70 551584898
cytochrome P450 Alcanivorax 748668388'
cytochrome P450 Alcanivorax 302608298'
cytochrome P450 Alcanivorax 496215991'
mycobacterium parascrofulaceum'
linalool 8-monooxygenase-like Brassica napus'
WP 081405418.1 cytochrome P450 Acinetobacter sp. 1245249
alkane hydroxylase cytochrome P450 Marinobacter goseongensis 536463895
marinobacter goseongensis 536463895
Cytochrome P450 alkane hydroxylase Marinobacter hydrocarbonoclasticus ATCC 49840 302608298
marinobacter hydrocarbonoclasticus 381340255
polarmonas sp. js666 bpro 5301
cytochrome P450 Alcanivorax jadensis 737265016
WP 039926945.1 cytochrome P450 Alcanivorax sp. DG881
WP 007079146.1 cytochrome P450 Aeromicrobium marinum
mycobacterium marinum mmar 3154
WP 005214790.1 CYP153 Acinetobacter sp. ANC 3862
BAE78452.1 CYP153 Acinetobacter sp. OC4
WP 010924803.1 cytochrome P450 Acinetobacter sp. EB104
WP 035270174.1 cytochrome P450 Acinetobacter sp. Ver3
cytochrome P450 Acinetobacter'
ERU36701.1 unspecific monooxygenase domain protein Acinetobacter sp. WC-141
EKK05338.1 unspecific monooxygenase domain protein Acinetobacter baumannii OIFC0162
acinetobacter baumannii 408503579
EKU50546.1 unspecific monooxygenase domain protein Acinetobacter sp. WC-323
ASP29103.1 cytochrome P450 Bacterioplanes sanyensis
WP 051225852.1 cytochrome P450 Solimonas flava
WP 051101823.1 cytochrome P450 Solimonas varicoloris
gordonia amicalis 441450514
OUR88502.1 cytochrome Gammaproteobacteria bacterium 42 54 T18
OUR90030.1 cytochrome Gammaproteobacteria bacterium 42 54 T18
cytochrome P450 Spongiibacteraceae'
WP 068756286.1 cytochrome P450 Oleiphilus sp. HI0125
WP 068473608.1 cytochrome P450 Oleiphilus sp. HI0067
WP 022983596.1 cytochrome P450 Alcanivorax sp. P2S70
hypothetical protein T9A 02486 Alcanivorax jadensis T9 686987662
EDX90518.1 Cytochrome P450 superfamily Alcanivorax sp. DG881
SDW13231.1 hypothetical protein SAMN04487960 101387 Marinobacter mobilis
WP 012139345.1 cytochrome P450 Marinobacter lipolyticus
marinobacter lipolyticus 499159750
WP 014579434.1 cytochrome P450 Marinobacter adhaerens
WP 062787108.1 cytochrome P450 Marinobacter sp. YWL01
WP 075839400.1 cytochrome P450 Rhodococcus sp. CUA-806
WP 064441942.1 cytochrome P450 Hoyosella altamirensis
WP 013807609.1 cytochrome P450 Hoyosella subflava
cytochrome P450 Gordonia'
WP 006901781.1 cytochrome P450 Gordonia paraffinivorans
WP 005201060.1 cytochrome P450 Gordonia rubripertincta
WP 006864915.1 cytochrome P450 Gordonia namibiensis
WP 068858456.1 cytochrome P450 Perlucidibaca aquatica
cytochrome P450 Perlucidibaca piscinae 551336998
WP 023547320.1 cytochrome P450 actinobacterium LLX17
WP 043586587.1 cytochrome P450 Nocardioides luteus
WP 005560910.1 cytochrome P450 Rhodococcus wratislaviensis
cytochrome P450 Rhodococcus 639145283'
cytochrome P450 Rhodococcus 490040014'

Figure I. 2 Phylogenetic tree used in this study

Figure I. 3 . A SDS-PAGE analysis of protein expression of CYP153As. *E. coli* BW25113 (Δ*fadD*, DE3) was used, Protein expression was carried out using 0.01 mM IPTG, 0.5 mM 5-ALA and trace mineral mixtures (2.5 mL/L) at 30 °C temp. CamB (12.75 kDa), CamA (47 kDa), FadL(48.8kDa), CYP153As (52.28 kDa)

Figure I. 4 A CO-binding analysis of CYP153A expressing
strains used in this study

Figure I. 5 ω−Hydroxylation of 20 mM DDA by CYP153A and
Cam AB containing cells, Reaction conditions: Volume, 10 mL in
100 mL flask; Temp, 30°C; Cell type, BW25113 (Δ *fadD*, DE3)
having CYP153AM.aq, CYP153AL.m, CYP153AS.f and
CYP153AA.d respectively, with CamA/B; Cell OD_{600}, 30;
Phosphate buffer, 100 mM; pH, 7.5; glucose 1% (w/v). with 20
mM DDA (DMSO 1%)
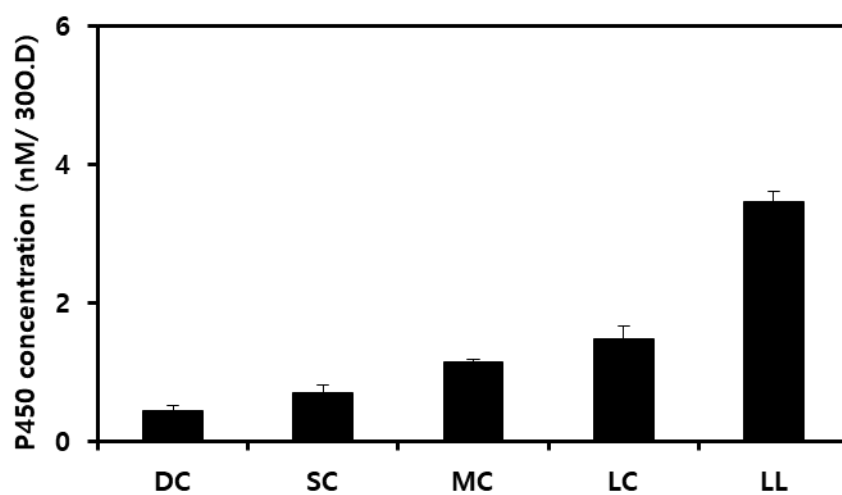
Figure I. 6 An active P450 concentration used in this study. The concentration of P450 was measured using an extinction coefficient of 91.9 mM^{-1} cm^{-1} at 450 nm.
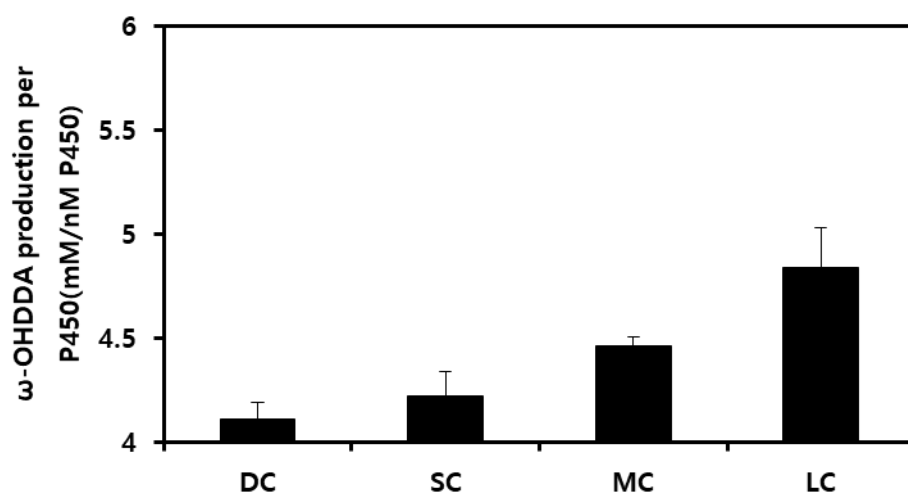
Figure I. 7 ω－OHDDA production normalized by amount of active P450s. The final titer was normalized by the amount of active P450s in Figure I.4

AI.4.2 *Use of solid state powdered substrate in bioconversion*

In many cases, substrates for reactions catalyzed by P450 have limited water solubility. For example, medium chain fatty acids (C10−C16) are water soluble from ~7 mg/L to 61 mg/L. Moreover, to increase the industrial feasibility of the process, two−liquid phase systems have been described (Tian 2005, von Bühler, Le− Huu, and Urlacher 2013). Also, the addition of co−solvents or cyclodextrins has been reported (Donova et al. 2007, Kühnel et al. 2007). However, the excessive use of DMSO as a co−solvent could damage the catalyst as well as host cell (Rammler and Zaffaroni 1967). Moreover, Lundemo and co−workers demonstrated that a DMSO free strategy in whole−cell P450 catalyzed reactions were advantageous (Lundemo et al. 2016).

Based on these previous reports, cells were subjected to resting cell reaction in the absence of DMSO. The CYP153AL.m expressing strain was shown to give the highest yields in the conversion of dodecanoic acid (4 g/L) to ω−OHDDA (2 g/L), whereas, CYP153AM.aq, CYP153AS.f and CYP153AA.d gave 0.9 g/L, 0.63 g/L and 0.3 g/L respectively (Figure I.8). There is no

significant difference in the amount of product obtained using solid s

tate powdered substrate or substrate dissolved in DMSO. The use

of substrate in the solid state appeared to have a negligible effect on

CYP153AM.aq, CYP153A.d and CYP153AS.f, showing a slightly

declined amount of conversion. Nevertheless, only CYP153A.Lm−

catalyzed reaction titer was shown to be improved using powdered

substrate. Any efficient biocatalytic conversion requisites the

effective uptake of the substrate followed by its conversion to the

desired product (Rimal et al. 2015, Lin and Tao 2017). The better

uptake of a powdered substrate in absence of DMSO could be the

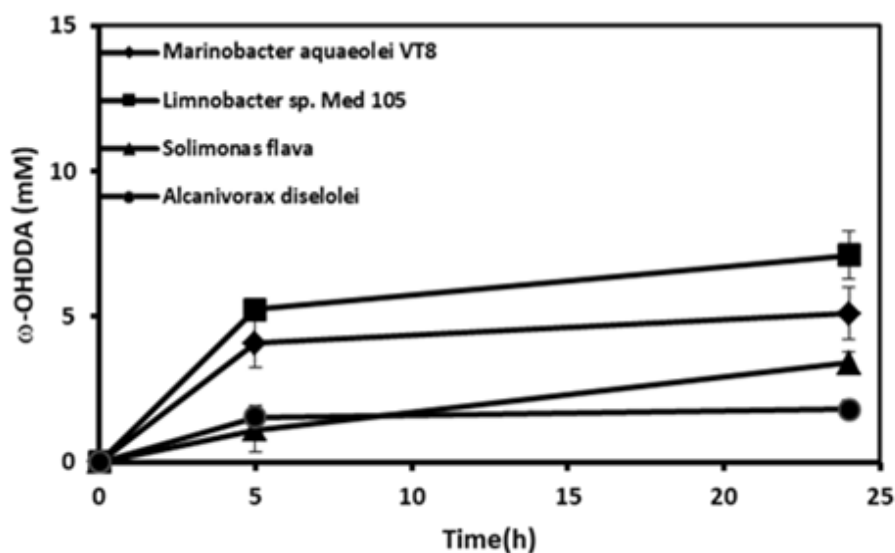plausible reason for the better titer achieved by the cells

expressing CYP153A.Lm.
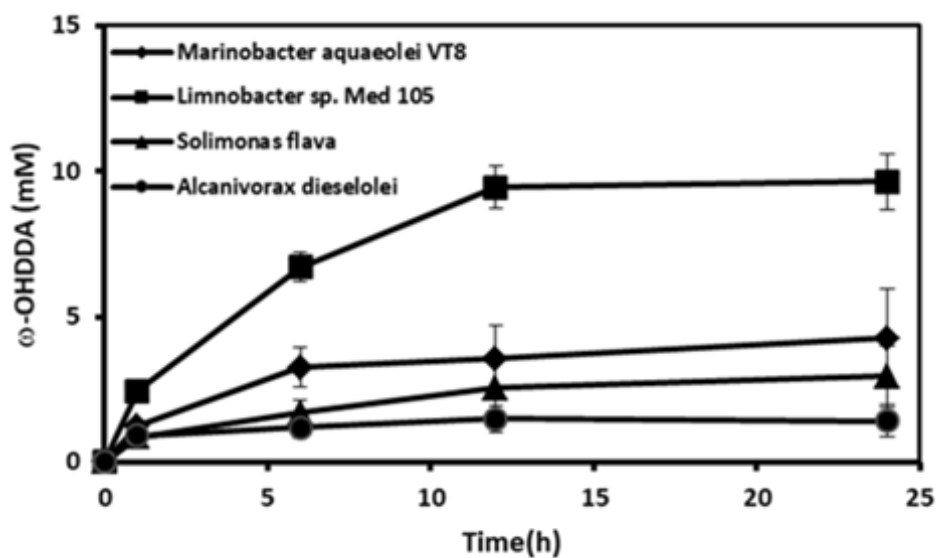
Figure I. 8 ω−Hydroxylation of 20 mM DDA by CYP153A and Cam AB containing cells, Reaction conditions: Volume, 10 mL in 100 mL flask; Temp, 30° C; Cell type, BW25113 ($\Delta fadD$, DE3) having CYP153AM.aq, CYP153AL.m, CYP153AS.f and CYP153AA.d respectively, with CamA/B; Cell OD_{600}, 30; Phosphate buffer, 100 mM; pH, 7.5; glucose 1% (w/v) with 20 mM of solid−state powdered substrate.

AI.4.3 Effect of homogeneous redox partners

Generally, it has been accepted that the optimal redox partners for a P450 enzyme should be homogeneous ones (Wachtmeister and Rother 2016, Pandey et al. 2014). Therefore, we tried to introduce native redox partners of *Limnobacter* sp. *105 MED*. Using the functional protein association network database STRING v10.5 (Szklarczyk et al. 2016), a network comprising CYP153AL.m was obtained, and we found that there are two Fdxs and one FdR from *Limnobacter* sp. 105 MED (Figure I.9). The FdR (LimA) and a Fdx (LimB) with high value score were codon-optimized and synthesized into pETduet_vector and they were expressed and purified together with CYP153AL.m, CYP153AM.aq and CamA/B (Figure I.10).

To evaluate the native redox partner chains, *in vitro* biotransformation was carried out with final volume of 0.5 mL of 100 mM potassium phosphate buffer (pH 7.5), containing 2 μM CYP153A, ferredoxin reductase and ferredoxin (1: 10: 5 ratio) and dodecanoic acid was added at a final concentration of 0.5 mM (25 mM stock in DMSO). The reaction was started by the addition of

0.2 mM NADH and the coupling efficiencies were obtained by determining the ratio of the initial product forming rate and the NADH consumption rate as previously described (Jung et al. 2016).

Although the coupling efficiencies of CYPs are similar regardless of redox partners, the CYP153AL.m CYP153AL.m has a higher initial product forming rate (8.91±0.89 μM/min) than CYP153AM.aq (7.41±0.70 μM/min), and a higher NADH consumption than CYP153AM.aq (17.04 ±0.32 μM/min and 13.83± 1.16 μM/min, respectively). Moreover, the native redox partners of CYP153A.L.m improved the performance with the highest initial product forming rate (9.81±1.60 μM/min) and the highest NADH consumption (20.26±0.57 μM/min) (Table I.1).

After confirming the performance of the native redox partner chain, the proteins of the redox partner chain were further investigated *in vivo.* Whole-cell (0.11 g_{CDW} /mL) reactions were carried out at 30 ˚C and 200 rpm using cells with CYP153A.L.m, co-expressing LimA and LimB in potassium phosphate buffer (100 mM, pH 7.5) in the presence of 1% (w/v) glucose. Ideally, the *in vivo* endogenous three-component system produced 3.28 g/L of 12-OHDDA from 4 g/L dodecanoic acid (Figure I.11). Therefore,

our data is the example that the application of naturally occurring redox partners could enhance the reactivity *in vivo* and *in vitro.*
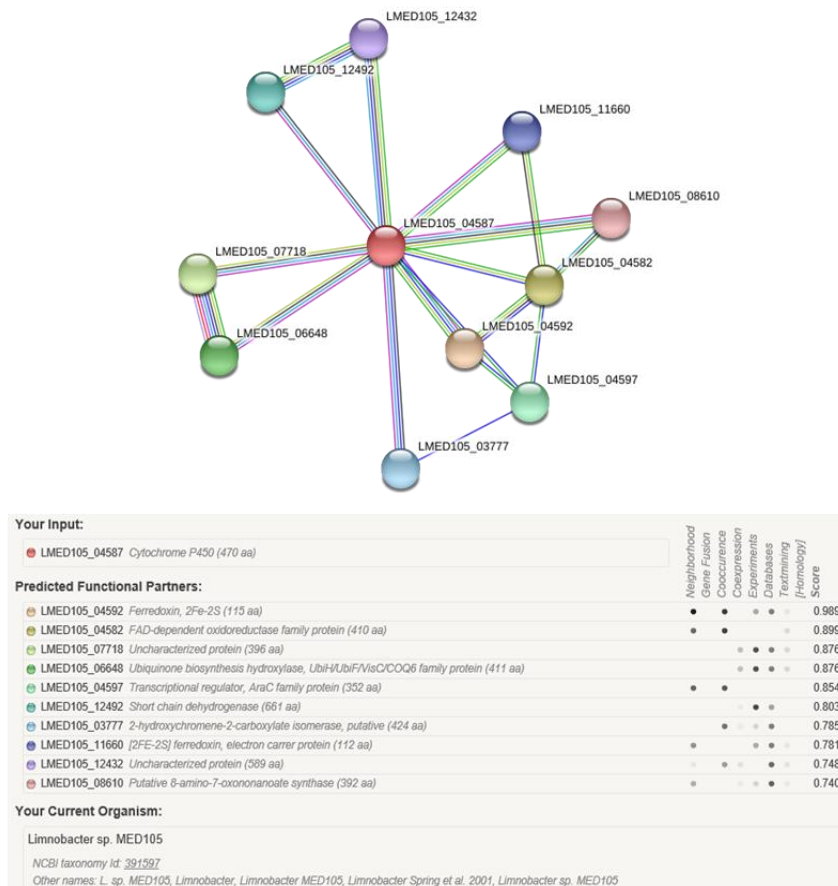
Figure I. 9 Protein-protein network of CYP153AL.m (LMED105_04587). There are two 2Fe-2S ferredoxin in the network (LMED105_04592, LMED105_11660) having score 0.989 and 0.781 respectively. LMED105_04592(LimB) was used in this study as it has higher score than LMED105_11660 also LMED10504582(LimA) was used as its corresponding reductase.
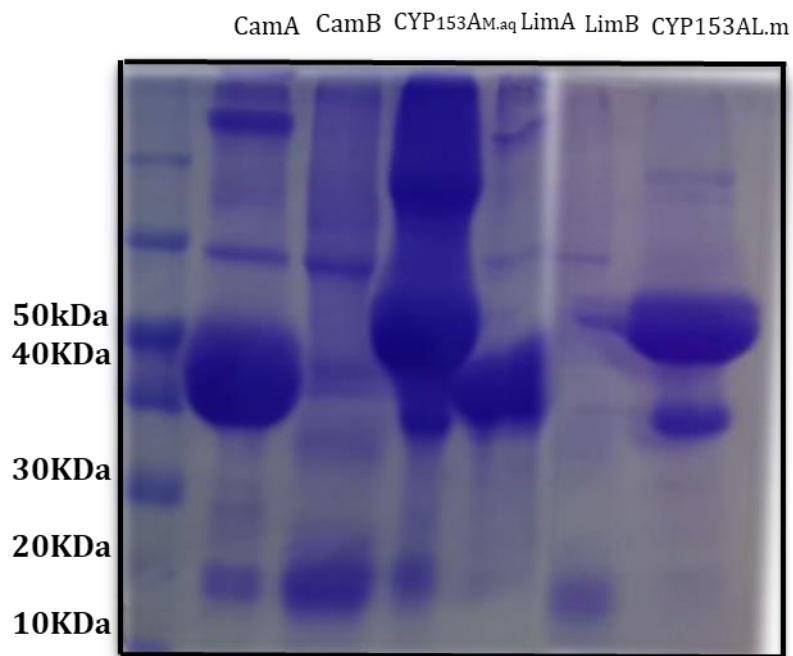
Figure I. 10 SDS−PAGE gel picture of purified protein of CamB (12.75 kDa), CamA (47 kDa), CYP153AM.aq (52.28 kDa) ,LimB (11.87 kDa), LimA (45.61 kDa), and CYP153AL.m (52.28 kDa).

Table I.1. In vitro evaluation of native redox partners of CYP153AL.m.

Entry	CYP153AM.aq CamA + CamB	CYP153AL.m CamA + CamB	CYP153AL.m LimA+ LimB
Coupling efficiency (%)	53.6±5.5	52.3±3.6	48.4±5.4
Initial product forming rate (μM/min)	7.41±0.70	8.91±0.89	9.81±1.60
NADH consumption rate (μM/min)	13.83±1.16	17.04±0.32	20.26±0.57
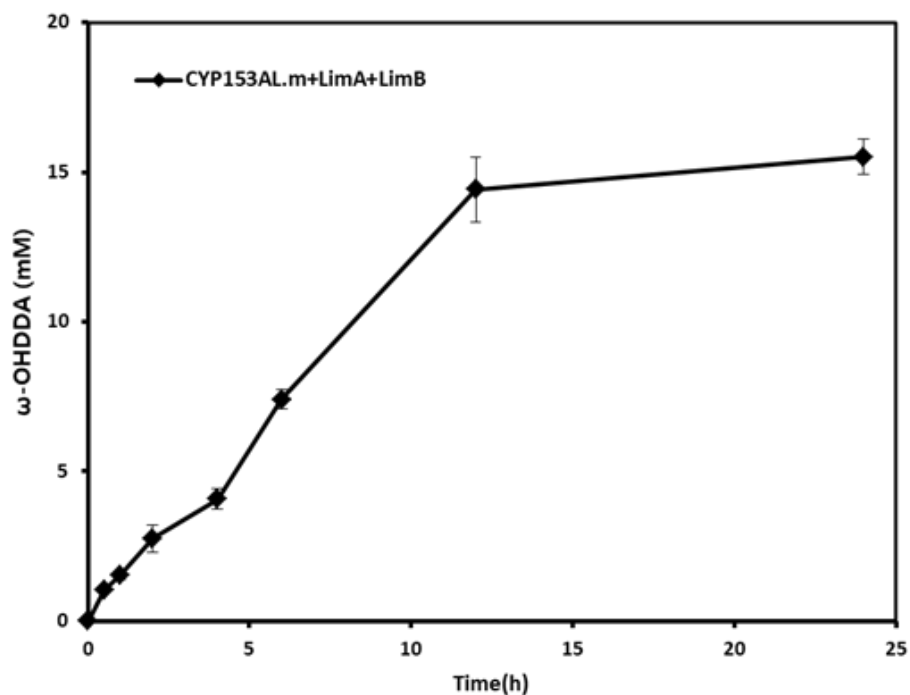
Figure I. 11 ω-Hydroxylation of 20 mM dodecanoic acid by CYP153AL.m and LimAB containing cells. Reaction conditions: Substrate concentration, 20 mM; Volume, 10 mL in 100 mL flask; Temp, 30˚C; Cell type, BW25113 (*ΔfadD*, DE3) expressing CYP153AL.m and Lim A/B; Cell OD_{600}, 30; Phosphate buffer, 100 mM; pH, 7.5; glucose 1% (w/v).

AI.4.4 *Limitations of the CYP153AL three component system*

Frequently, stability issues of CYPs are mentioned, which are caused by uncoupling of the NADH oxidation during product formation (Lundemo et al. 2016, Bernhardt and Urlacher 2014). To evaluate the stability of our system, a series of four rounds was carried out with whole cells expressing CYP153AL.m and Cam A/B. In each round, the cells were purified and reused in every 6 h for the next round as equilibrium is reached in a relatively short 6 hours (Figure I.8). In the second round, product obtained from the whole cells considerably decreased (53%) compared to the 1st round and further decreased to 35% in the 3rd round (Figure I.12). This data implies that our system suffered from instability, and thus a relatively short process time is desirable.

Additionally, the residual activity in the 3rd round didn't compensate the product conversion after 12 h (Figure I.8). We speculate that the phenomenon is caused by product inhibition which was previously mentioned by Lundemo and resting cell reaction was carried out in the additional presence of 5 mM and 10 mM ω−OHDDA (Lundemo et al. 2016). The product forming rate

has significantly decreased from 1.59 ± 0.09 mM/h to 0.44 ± 0.17 mM/h, as initial product concentration increased from 0 to 10mM (Figure I.13), indicating significant product inhibition. The results of these studies demonstrated that CYP153AL.m three component system suffered from severe product inhibition, which should necessarily be overcome to produce high concentrations of the products.
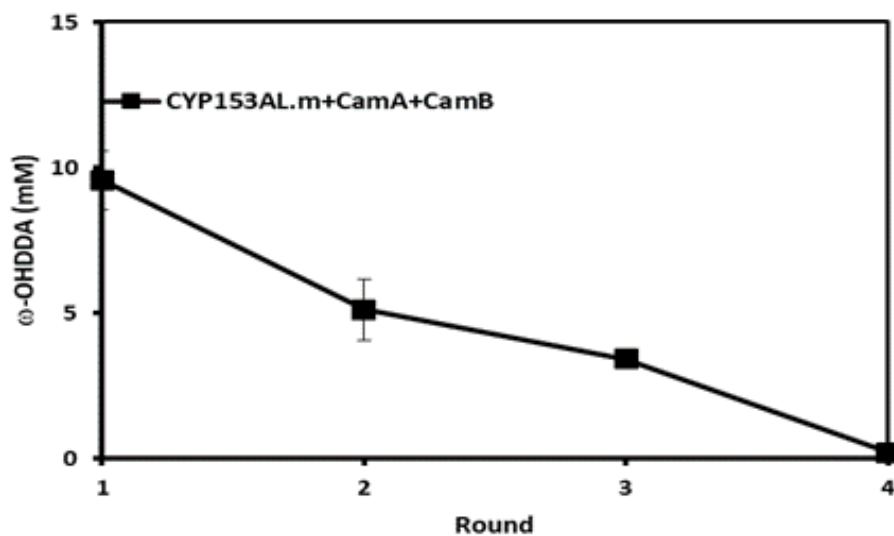
Figure I. 12 Residual stability of whole cells expressing CYP153AL.m. Reaction conditions: Substrate concentration, 20mM; Volume, 10 mL in 100 mL flask; Temp, 30° C; Cell type, BW25113 (*Δ fadD*, DE3) having CYP153AL.m and CamA/B; Cell OD_{600}, 30; Phosphate buffer, 100 mM; pH, 7.5; glucose 1% (w/v), The biocatalysts in the each round (every 6 h) were re-used to next round
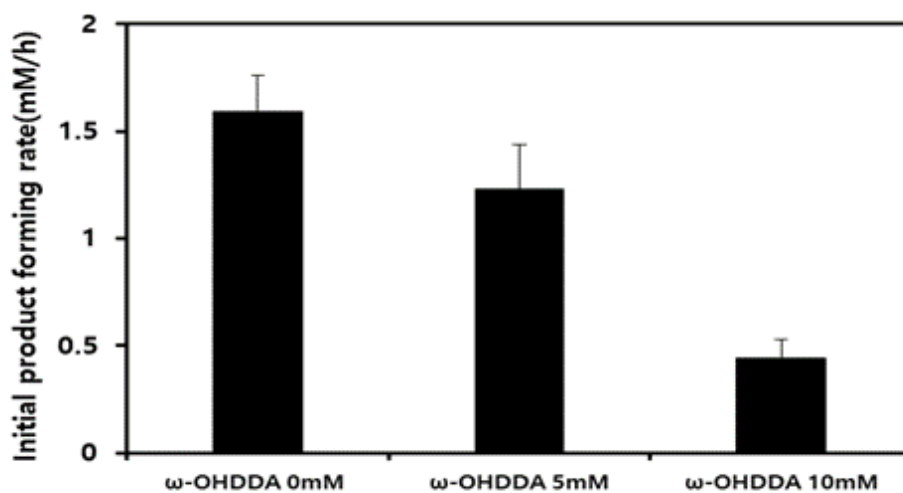
Figure I. 13 Product inhibited ω-hydroxylation of 20 mM
dodecanoic acid. Reaction condition is the same with **3** ω-
hydroxylation of 20 mM fatty acids by CYP153A and Cam AB
containing cells, Note that: 0, 5 and 10 mM of ω-OHDDA was
initially added.

Table I.2 Plasmids and strains used in this study

Plasmids	Description	Refference
pET24ma	P15A ori lacI T7 promoter, KmR	(Jung et al. 2016)
pETDuet-1	pBR322 ori lacI T7 promoter, AmpR	*Novagen*
pCDFDuet-1 CDF	CDF ori lacI T7 promoter, SmR	*Novagen*
pCamAB	pETDuet-1 encoding CamA/B	(Bae et al. 2014)
pRedox$_{L.m}$	pETDuet-1 encoding LimA/B	This study
pAM.aq	pCDFDuet-1 CDF encoding fadL and CYP153AM.aq	This study
pAA.d	pCDFDuet-1 CDF encoding fadL and CYP153AA.d	This study
pAS.f	pCDFDuet-1 CDF encoding fadL and CYP153AS.f	This study
pAL.m	pCDFDuet-1 CDF encoding fadL and CYP153AL.m	This study
pCYP153A$_{M.aq}$	pET28a encoding CYP153A$_{M.aq}$	(Jung et al. 2016)
pCamA	pET28a encoding CamA	(Choi, Park, and Kim 2010)
pCamB	pET28a encoding CamB	(Choi, Park, and Kim 2010)

pCYP153A_{L.m}	pET24ma encoding CYP153A_{L.m}	This study
pLimA	pet24ma encoding LimA	This study
pLimB	pet24ma encoding LimB	This study

Strains	Description	Refference
BW25113(DE3)	rrnB3 ΔlacZ4787 hsdR514 Δ(araBAD)567 Δ(rhaBAD)568 rph−1 λ(DE3)	(Jung et al. 2016)
DL	BW25113(DE3) ΔfadD	(Jung et al. 2016)
MC	DL carrying pAM.aq and pCamAB	This study
DC	DL carrying pAA.d and pCamAB	This study
SC	DL carrying pAS.f and pCamAB	This study
LC	DL carrying pCYP153AL.m and pCamAB	This study
LL	DL carrying pCYP153AL.m and pRedox_{L.m}	This study
DLM	DL carrying pCYP153 M.aq	This study
DLCA	DL carrying pCamA	This study
DLCB	DL carrying pCamB	This study
DLL	DL carrying pCYP153L.m	This study
DLLA	DL carrying pLimA	This study
DLLB	DL carrying pLimB	This study

AI.5 Conclusion

This study reports ω-hydroxy fatty acid production platform employing efficient CYP153A from *Limnobacter* sp. MED 105. Furthermore, the application of powder substrate and introducing the native redox partner was successfully reported in the study. However, product inhibition is a hurdle for the industrial feasibility of this biocatalytic process. In conclusion, with the help of the heterologous expression of novel non-native enzymes in *E. coli*, we successfully produced 3.28 g/L of ω-OHDDA from 4 g/L of dodecanoic acid.

AI.6 References

Agari, Yoshihiro, Kazuko Agari, Keiko Sakamoto, Seiki Kuramitsu, and Akeo Shinkai. 2011. "TetR-family transcriptional repressor Thermus thermophilus FadR controls fatty acid degradation." *Microbiology* 157 (6):1589-1601.

Ahsan, Md Murshidul, Sihyong Sung, Hyunwoo Jeon, Mahesh D. Patil, Taeowan Chung, and Hyungdon Yun. 2017. "Biosynthesis of Medium- to Long-Chain α,ω-Diols from Free Fatty Acids Using CYP153A Monooxygenase, Carboxylic Acid Reductase, and E. coli Endogenous Aldehyde Reductases." *Catalysts* 8 (1):4.

Ahsan, Md, Mahesh Patil, Hyunwoo Jeon, Sihyong Sung, Taeowan Chung, and Hyungdon Yun. 2018. "Biosynthesis of Nylon 12 Monomer, ω-Aminododecanoic Acid Using Artificial Self-Sufficient P450, AlkJ and ω-TA." *Catalysts* 8 (9):400.

Akhtar, M. K., N. J. Turner, and P. R. Jones. 2013. "Carboxylic acid reductase is a versatile enzyme for the conversion of fatty acids into fuels and chemical commodities." *Proc Natl Acad Sci U S A* 110 (1):87-92. doi: 10.1073/pnas.1216516110.

Alonso, Hernan, Oded Kleifeld, Adva Yeheskel, Poh C Ong, Yu C Liu, Jeanette E Stok, James J De Voss, and Anna Roujeinikova. 2014. "Structural and mechanistic insight into alkane hydroxylation by Pseudomonas putida AlkB." *Biochemical Journal* 460 (2):283-293.

Alonso, Hernan, and Anna Roujeinikova. 2012. "Characterization and two-dimensional crystallization of membrane component AlkB of the medium-chain alkane hydroxylase system from Pseudomonas putida GPo1." *Applied and environmental microbiology* 78 (22):7946-7953.

Bae, Jin H, Beom Gi Park, Eunok Jung, Pyung-Gang Lee, and Byung-Gee Kim. 2014. "*fadD* deletion and *fadL* overexpression in Escherichia coli increase hydroxy long-chain fatty acid productivity." *Applied microbiology and biotechnology* 98 (21):8917-8925.

Beilen, Jan B. van, and Enrico G. Funhoff. 2005. "Expanding the alkane oxygenase toolbox: new enzymes and applications." *Current Opinion in Biotechnology* 16 (3):308-314. doi: https://doi.org/10.1016/j.copbio.2005.04.005.

Bernhardt, Rita, and Vlada B. Urlacher. 2014. "Cytochromes P450

as promising catalysts for biotechnological application: chances and limitations." *Applied Microbiology and Biotechnology* 98 (14):6185-6203. doi: 10.1007/s00253-014-5767-7.

Bertrand, Erin, Ryo Sakai, Elena Rozhkova-Novosad, Luke Moe, Brian G Fox, John T Groves, and Rachel N Austin. 2005. "Reaction mechanisms of non-heme diiron hydroxylases characterized in whole cells." *Journal of inorganic biochemistry* 99 (10):1998-2006.

Burch, R., and M. J. Hayes. 1995. "C-H bond activation in hydrocarbon oxidation on solid catalysts." *Journal of Molecular Catalysis A: Chemical* 100 (1):13-33. doi: https://doi.org/10.1016/1381-1169(95)00133-6.

Call, Toby P, M Kalim Akhtar, Frank Baganz, and Chris Grant. 2016. "Modulating the import of medium-chain alkanes in *E. coli* through tuned expression of FadL." *Journal of biological engineering* 10 (1):5.

Canavaci, Adriana M. C., Juan M. Bustamante, Angel M. Padilla, Cecilia M. Perez Brandan, Laura J. Simpson, Dan Xu, Courtney L. Boehlke, and Rick L. Tarleton. 2010. "In Vitro and In Vivo High-Throughput Assays for the Testing of Anti-Trypanosoma cruzi Compounds." *PLOS Neglected Tropical Diseases* 4 (7):e740. doi: 10.1371/journal.pntd.0000740.

Cao, Peigang, André Y. Tremblay, Marc A. Dubé, and Katie Morse. 2007. "Effect of Membrane Pore Size on the Performance of a Membrane Reactor for Biodiesel Production." *Industrial & Engineering Chemistry Research* 46 (1):52-58. doi: 10.1021/ie060555o.

Cao, Yujin, Tao Cheng, Guang Zhao, Wei Niu, Jiantao Guo, Mo Xian, and Huizhou Liu. 2016. "Metabolic engineering of Escherichia coli for the production of hydroxy fatty acids from glucose." *BMC biotechnology* 16 (1):26.

Chae, Tong Un, Jung Ho Ahn, Yoo-Sung Ko, Je Woong Kim, Jong An Lee, Eon Hui Lee, and Sang Yup Lee. 2020. "Metabolic engineering for the production of dicarboxylic acids and diamines." *Metabolic Engineering* 58:2-16. doi: https://doi.org/10.1016/j.ymben.2019.03.005.

Chizzolini, Fabio, Michele Forlin, Dario Cecchi, and Sheref S Mansy.

2013. "Gene Position More Strongly Influences Cell-Free Protein Expression from Operons than T7 Transcriptional Promoter Strength." *ACS synthetic biology* 3 (6):363-371.

Choi, Kwon-Young, Hyung-Yeon Park, and Byung-Gee Kim. 2010. "Characterization of bi-functional CYP154 from Nocardia farcinica IFM10152 in the O-dealkylation and ortho-hydroxylation of formononetin." *Enzyme and Microbial Technology* 47 (7):327-334.

Clomburg, James M, Matthew D Blankschien, Jacob E Vick, Alexander Chou, Seohyoung Kim, and Ramon Gonzalez. 2015. "Integrated engineering of β-oxidation reversal and ω-oxidation pathways for the synthesis of medium chain ω-functionalized carboxylic acids." *Metabolic engineering* 28:202-212.

Coleman, Jack, Masatoshi Inukai, and Masayori Inouye. 1985. "Dual Functions of the Signal Peptide in Protein Transfer Across the Membrane." *Cell* 43 (1):351-360. doi: https://doi.org/10.1016/0092-8674(85)90040-6.

Collier, D. N. 1994. "Escherichia coli signal peptides direct inefficient secretion of an outer membrane protein (OmpA) and periplasmic proteins (maltose-binding protein, ribose-binding protein, and alkaline phosphatase) in Bacillus subtilis." *Journal of bacteriology* 176 (10):3013-3020.

Cozens, Christopher, and Vitor B Pinheiro. 2018. "Darwin Assembly: fast, efficient, multi-site bespoke mutagenesis." *Nucleic Acids Research* 46 (8):e51-e51. doi: 10.1093/nar/gky067.

de Sousa, BG, JIN Oliveira, EL Albuquerque, UL Fulco, VE Amaro, and CAG Blaha. 2017. "Molecular modelling and quantum biochemistry computations of a naturally occurring bioremediation enzyme: Alkane hydroxylase from Pseudomonas putida P1." *Journal of Molecular Graphics and Modelling* 77:232-239.

Denks, Kärt, Andreas Vogt, Ilie Sachelaru, Narcis-Adrian Petriman, Renuka Kudva, and Hans-Georg Koch. 2014. "The Sec translocon mediated protein transport in prokaryotes and eukaryotes." *Molecular Membrane Biology* 31 (2-3):58-84. doi: 10.3109/09687688.2014.907455.

Durairaj, Pradeepraj, Sailesh Malla, Saravanan Prabhu Nadarajan,

Pyung-Gang Lee, Eunok Jung, Hyun Ho Park, Byung-Gee Kim, and Hyungdon Yun. 2015. "Fungal cytochrome P450 monooxygenases of *Fusarium oxysporum* for the synthesis of ω-hydroxy fatty acids in engineered *Saccharomyces cerevisiae*." *Microbial cell factories* 14 (1):45.

Eggink, Gerrit, Roland G Lageveen, Bert Altenburg, and Bernard Witholt. 1987. "Controlled and functional expression of the Pseudomonas oleovorans alkane utilizing system in Pseudomonas putida and Escherichia coli." *Journal of Biological Chemistry* 262 (36):17712-17718.

England, Thomas E., and Olke C. Uhlenbeck. 1978. "Enzymatic Oligoribonucleotide Synthesis with T4 RNA Ligase." *Biochemistry* 17 (11):2069-2076. doi: 10.1021/bi00604a008.

Fedorchuk, Tatiana P., Anna N. Khusnutdinova, Elena Evdokimova, Robert Flick, Rosa Di Leo, Peter Stogios, Alexei Savchenko, and Alexander F. Yakunin. 2020. "One-Pot Biocatalytic Transformation of Adipic Acid to 6-Aminocaproic Acid and 1,6-Hexamethylenediamine Using Carboxylic Acid Reductases and Transaminases." *Journal of the American Chemical Society* 142 (2):1038-1048. doi: 10.1021/jacs.9b11761.

France, Scott P., Lorna J. Hepworth, Nicholas J. Turner, and Sabine L. Flitsch. 2017. "Constructing Biocatalytic Cascades: In Vitro and in Vivo Approaches to de Novo Multi-Enzyme Pathways." *ACS Catalysis* 7 (1):710-724. doi: 10.1021/acscatal.6b02979.

Fujii, Tadashi, Tatsuya Narikawa, Futoshi Sumisa, Akira Arisawa, Koji Takeda, and Junichi Kato. 2006. "Production of α,ω-Alkanediols Using Escherichia coli Expressing a Cytochrome P450 from Acinetobacter sp. OC4." *Bioscience, Biotechnology, and Biochemistry* 70 (6):1379-1385. doi: 10.1271/bbb.50656.

Fujita, Yasutaro, Hiroshi Matsuoka, and Kazutake Hirooka. 2007. "Regulation of fatty acid metabolism in bacteria." *Molecular microbiology* 66 (4):829-839.

Ge, Jiawei, Xiaohong Yang, Hongwei Yu, and Lidan Ye. 2020. "High-yield whole cell biosynthesis of Nylon 12 monomer with self-sufficient supply of multiple cofactors." *Metabolic*

Engineering 62:172−185. doi: https://doi.org/10.1016/j.ymben.2020.09.006.

Gozzo, Franco. 2001. "Radical and non−radical chemistry of the Fenton−like systems in the presence of organic substrates." *Journal of Molecular Catalysis A: Chemical* 171 (1−2):1−22.

Grant, Chris, Dawid Deszcz, Yu−Chia Wei, Rubéns Julio Martínez−Torres, Phattaraporn Morris, Thomas Folliard, Rakesh Sreenivasan, John Ward, Paul Dalby, John M. Woodley, and Frank Baganz. 2014. "Identification and use of an alkane transporter plug−in for applications in biocatalysis and whole−cell biosensing of alkanes." *Scientific Reports* 4:5844. doi: 10.1038/srep05844 https://www.nature.com/articles/srep05844#supplementary−information.

Haak, Dale, Ken Gable, Troy Beeler, and Teresa Dunn. 1997. "Hydroxylation of *Saccharomyces cerevisiae* Ceramides Requires Sur2p and Scs7p." *Journal of Biological Chemistry* 272 (47):29704−29710. doi: 10.1074/jbc.272.47.29704.

Han, Sang−Woo, Youngho Jang, and Jong−Shik Shin. 2019. "In Vitro and In Vivo One−Pot Deracemization of Chiral Amines by Reaction Pathway Control of Enantiocomplementary ω−Transaminases." *ACS Catalysis* 9 (8):6945−6954. doi: 10.1021/acscatal.9b01546.

He, Qiaofei, George N. Bennett, Ka−Yiu San, and Hui Wu. 2019. "Biosynthesis of Medium−Chain ω−Hydroxy Fatty Acids by AlkBGT of Pseudomonas putida GPo1 With Native FadL in Engineered Escherichia coli." *Frontiers in Bioengineering and Biotechnology* 7 (273). doi: 10.3389/fbioe.2019.00273.

Horga, Luminita Gabriela, Samantha Halliwell, Tania Selas Castiñeiras, Chris Wyre, Cristina F. R. O. Matos, Daniela S. Yovcheva, Ross Kent, Rosa Morra, Steven G. Williams, Daniel C. Smith, and Neil Dixon. 2018. "Tuning recombinant protein expression to match secretion capacity." *Microbial Cell Factories* 17 (1):199. doi: 10.1186/s12934−018−1047−z.

Huf, Sabine, Sven Krügener, Thomas Hirth, Steffen Rupp, and Susanne Zibek. 2011. "Biotechnological synthesis of long−chain dicarboxylic acids as building blocks for polymers." *European Journal of Lipid Science and Technology* 113 (5):548−561.

Hwang, Sung Hee, Karen Wagner, Jian Xu, Jun Yang, Xichun Li, Zhengyu Cao, Christophe Morisseau, Kin Sing Stephen Lee, and Bruce D. Hammock. 2017. "Chemical synthesis and biological evaluation of ω-hydroxy polyunsaturated fatty acids." *Bioorganic & Medicinal Chemistry Letters* 27 (3):620-625. doi: https://doi.org/10.1016/j.bmcl.2016.12.002.

Jang, Hyun-Young, Kaushik Singha, Hwan-Hee Kim, Yong-Uk Kwon, and Jin-Byung Park. 2016. "Chemo-enzymatic synthesis of 11-hydroxyundecanoic acid and 1,11-undecanedioic acid from ricinoleic acid." *Green Chemistry* 18 (4):1089-1095. doi: 10.1039/C5GC01017A.

Ji-Won Song, Joo-Hyun Seo, Doek-Kun Oh ORCID logoc, Uwe T. Bornscheuer d and Jin-Byung Park ORCID logo*ae. 2020. "Design and engineering of whole-cell biocatalytic cascades for the valorization of fatty acids." *Catal. Sci. Technol.* 10:46-64.

Jiang, Y., and K. Loos. 2016a. "Enzymatic Synthesis of Biobased Polyesters and Polyamides." *Polymers (Basel)* 8 (7). doi: 10.3390/polym8070243.

Jiang, Yi, and Katja Loos. 2016b. "Enzymatic Synthesis of Biobased Polyesters and Polyamides." *Polymers* 8 (7):243.

Joo, Sung-Yeon, Hee-Wang Yoo, Sharad Sarak, Byung-Gee Kim, and Hyungdon Yun. 2019. "Enzymatic Synthesis of ω-Hydroxydodecanoic Acid By Employing a Cytochrome P450 from Limnobacter sp. 105 MED." *Catalysts* 9 (1):54.

Joo, Young-Chul, Eun-Sun Seo, Yeong-Su Kim, Kyoung-Rok Kim, Jin-Byung Park, and Deok-Kun Oh. 2012. "Production of 10-hydroxystearic acid from oleic acid by whole cells of recombinant Escherichia coli containing oleate hydratase from Stenotrophomonas maltophilia." *Journal of Biotechnology* 158 (1):17-23. doi: https://doi.org/10.1016/j.jbiotec.2012.01.002.

Julsing, Mattijs K, Manfred Schrewe, Sjef Cornelissen, Inna Hermann, Andreas Schmid, and Bruno Bühler. 2012. "Outer Membrane Protein AlkL Boosts Biocatalytic Oxyfunctionalization of Hydrophobic Substrates in *Escherichia coli*." *Applied and environmental microbiology* 78 (16):5724-5733.

Jung, Da-Hye, Wonji Choi, Kwon-Young Choi, Eunok Jung, Hyungdon Yun, Romas J. Kazlauskas, and Byung-Gee Kim. 2013. "Bioconversion of *p*-coumaric acid to *p*-hydroxystyrene using phenolic acid decarboxylase from *B. amyloliquefaciens* in biphasic reaction system." *Applied Microbiology and Biotechnology* 97 (4):1501-1511. doi: 10.1007/s00253-012-4358-8.

Jung, Eunok, Beom Gi Park, Md. Murshidul Ahsan, Joonwon Kim, Hyungdon Yun, Kwon-Young Choi, and Byung-Gee Kim. 2016. "Production of ω-hydroxy palmitic acid using CYP153A35 and comparison of cytochrome P450 electron transfer system in vivo." *Applied Microbiology and Biotechnology* 100 (24):10375-10384. doi: 10.1007/s00253-016-7675-5.

Jung, Eunok, Beom Gi Park, Hee-Wang Yoo, Joonwon Kim, Kwon-Young Choi, and Byung-Gee Kim. 2018. "Semi-rational engineering of CYP153A35 to enhance ω-hydroxylation activity toward palmitic acid." *Applied Microbiology and Biotechnology* 102 (1):269-277. doi: 10.1007/s00253-017-8584-y.

Kadisch, Marvin, Mattijs K Julsing, Manfred Schrewe, Nico Jehmlich, Benjamin Scheer, Martin von Bergen, Andreas Schmid, and Bruno Bühler. 2017. "Maximization of Cell Viability Rather Than Biocatalyst Activity Improves Whole-Cell ω-Oxyfunctionalization Performance." *Biotechnology and bioengineering* 114 (4):874-884.

Kadisch, Marvin, Andreas Schmid, and Bruno Bühler. 2017. "Hydrolase BioH knockout in E. coli enables efficient fatty acid methyl ester bioprocessing." *Journal of industrial microbiology & biotechnology* 44 (3):339-351.

Kadisch, Marvin, Christian Willrodt, Michael Hillen, Bruno Bühler, and Andreas Schmid. 2017. "Maximizing the stability of metabolic engineering-derived whole-cell biocatalysts." *Biotechnology Journal*.

Kang, Yun, Mike S. Son, and Tung T. Hoang. 2007. "One step engineering of T7-expression strains for protein production: increasing the host-range of the T7-expression system." *Protein expression and purification* 55 (2):325-333. doi: 10.1016/j.pep.2007.06.014.

Kaur, Jashandeep, Arbind Kumar, and Jagdeep Kaur. 2018. "Strategies for optimization of heterologous protein expression in *E. coli*: Roadblocks and reinforcements." *International Journal of Biological Macromolecules* 106:803–822. doi: https://doi.org/10.1016/j.ijbiomac.2017.08.080.

Kawaguchi, Hideo, Chiaki Ogino, and Akihiko Kondo. 2017. "Microbial conversion of biomass into bio-based polymers." *Bioresource Technology* 245:1664–1673. doi: https://doi.org/10.1016/j.biortech.2017.06.135.

Kelly, Jason R., Adam J. Rubin, Joseph H. Davis, Caroline M. Ajo-Franklin, John Cumbers, Michael J. Czar, Kim de Mora, Aaron L. Glieberman, Dileep D. Monie, and Drew Endy. 2009. "Measuring the activity of BioBrick promoters using an in vivo reference standard." *Journal of Biological Engineering* 3 (1):4. doi: 10.1186/1754-1611-3-4.

Kim, Geon-Hee, Hyunwoo Jeon, Taresh P. Khobragade, Mahesh D. Patil, Sihyong Sung, Sanghan Yoon, Yumi Won, In Suk Choi, and Hyungdon Yun. 2019. "Enzymatic synthesis of sitagliptin intermediate using a novel ω-transaminase." *Enzyme and Microbial Technology* 120:52–60. doi: https://doi.org/10.1016/j.enzmictec.2018.10.003.

Kim, Joonwon, Hee-Wang Yoo, Minsuk Kim, Eun-Jung Kim, Changmin Sung, Pyung-Gang Lee, Beom Gi Park, and Byung-Gee Kim. 2018. "Rewiring FadR regulon for the selective production of ω-hydroxy palmitic acid from glucose in *Escherichia coli*." *Metabolic Engineering* 47:414–422. doi: https://doi.org/10.1016/j.ymben.2018.04.021.

Kim, Tae-Hun, Su-Hwan Kang, Jeong-Eun Han, Eun-Ji Seo, Eun-Yeong Jeon, Go-Eun Choi, Jin-Byung Park, and Deok-Kun Oh. 2020. "Multilayer Engineering of Enzyme Cascade Catalysis for One-Pot Preparation of Nylon Monomers from Renewable Fatty Acids." *ACS Catalysis* 10 (9):4871–4878. doi: 10.1021/acscatal.9b05426.

Klatte, Stephanie, and Volker F. Wendisch. 2014. "Redox self-sufficient whole cell biotransformation for amination of alcohols." *Bioorganic & Medicinal Chemistry* 22 (20):5578–5585. doi: https://doi.org/10.1016/j.bmc.2014.05.012.

Ko, Yoo-Sung, Je Woong Kim, Jong An Lee, Taehee Han, Gi Bae Kim, Jeong Eum Park, and Sang Yup Lee. 2020. "Tools and

strategies of systems metabolic engineering for the development of microbial cell factories for chemical production." *Chemical Society Reviews* 49 (14):4615−4636. doi: 10.1039/D0CS00155D.

Koch, Daniel J, Mike M Chen, Jan B van Beilen, and Frances H Arnold. 2009. "In vivo evolution of butane oxidation by terminal alkane hydroxylases AlkB and CYP153A6." *Applied and environmental microbiology* 75 (2):337−344.

Kok, M, Roelof Oldenhuis, MP van der Linden, CH Meulenberg, Jaap Kingma, and Bernard Witholt. 1989. "The Pseudomonas oleovorans alkBAC operon encodes two structurally related rubredoxins and an aldehyde dehydrogenase." *Journal of Biological Chemistry* 264 (10):5442−5451.

Kok, M, Roelof Oldenhuis, MP Van Der Linden, Philip Raatjes, Jaap Kingma, Philip H van Lelyveld, and Bernard Witholt. 1989. "The Pseudomonas oleovorans alkane hydroxylase gene. Sequence and expression." *Journal of Biological Chemistry* 264 (10):5435−5441.

Kumar, Sudhir, Glen Stecher, and Koichiro Tamura. 2016. "MEGA7: Molecular Evolutionary Genetics Analysis Version 7.0 for Bigger Datasets." *Molecular Biology and Evolution* 33 (7):1870−1874. doi: 10.1093/molbev/msw054.

Kunjapur, Aditya M., Yekaterina Tarasova, and Kristala L. J. Prather. 2014. "Synthesis and Accumulation of Aromatic Aldehydes in an Engineered Strain of Escherichia coli." *Journal of the American Chemical Society* 136 (33):11644−11654. doi: 10.1021/ja506664a.

Ladkau, Nadine, Miriam Assmann, Manfred Schrewe, Mattijs K Julsing, Andreas Schmid, and Bruno Bühler. 2016. "Efficient production of the Nylon 12 monomer ω−aminododecanoic acid methyl ester from renewable dodecanoic acid methyl ester with engineered *Escherichia coli*." *Metabolic engineering* 36:1−9.

Lee, Heeseok, Changpyo Han, Hyeok−Won Lee, Gyuyeon Park, Wooyoung Jeon, Jungoh Ahn, and Hongweon Lee. 2018. "Development of a promising microbial platform for the production of dicarboxylic acids from biorenewable resources." *Biotechnology for Biofuels* 11 (1):310. doi: 10.1186/s13068−018−1310−x.

Lee, Michael E., Anil Aswani, Audrey S. Han, Claire J. Tomlin, and John E. Dueber. 2013. "Expression-level optimization of a multi-enzyme pathway in the absence of a high-throughput assay." *Nucleic acids research* 41 (22):10668-10678. doi: 10.1093/nar/gkt809.

Lee, Minwoo, Hyejin Um, and Michael W. Van Dyke. 2017. "Identification and characterization of preferred DNA-binding sites for the Thermus thermophilus transcriptional regulator FadR." *PloS one* 12 (9):e0184796-e0184796. doi: 10.1371/journal.pone.0184796.

Lee, Pyung-Gang, Joonwon Kim, Eun-Jung Kim, Sang-Hyuk Lee, Kwon-Young Choi, Romas J. Kazlauskas, and Byung-Gee Kim. 2017. "Biosynthesis of (−)-5-Hydroxy-equol and 5-Hydroxy-dehydroequol from Soy Isoflavone, Genistein Using Microbial Whole Cell Bioconversion." *ACS Chemical Biology* 12 (11):2883-2890. doi: 10.1021/acschembio.7b00624.

Leung, Dennis YC, Xuan Wu, and MKH Leung. 2010. "A review on biodiesel production using catalyzed transesterification." *Applied energy* 87 (4):1083-1095.

Leveson-Gower, Reuben B., Clemens Mayer, and Gerard Roelfes. 2019. "The importance of catalytic promiscuity for enzyme design and evolution." *Nature Reviews Chemistry* 3 (12):687-705. doi: 10.1038/s41570-019-0143-x.

Lin, Baixue, and Yong Tao. 2017. "Whole-cell biocatalysts by design." *Microbial Cell Factories* 16 (1):106. doi: 10.1186/s12934-017-0724-7.

Liu, Chen, Fei Liu, Jiali Cai, Wenchun Xie, Timothy E. Long, S. Richard Turner, Alan Lyons, and Richard A. Gross. 2011. "Polymers from Fatty Acids: Poly(ω-hydroxyl tetradecanoic acid) Synthesis and Physico-Mechanical Studies." *Biomacromolecules* 12 (9):3291-3298. doi: 10.1021/bm2007554.

Lu, Wenhua, Jon E Ness, Wenchun Xie, Xiaoyan Zhang, Jeremy Minshull, and Richard A Gross. 2010. "Biosynthesis of Monomers for Plastics from Renewable Oils." *Journal of the American Chemical Society* 132 (43):15451-15455.

Lundemo, MT, S Notonier, G Striedner, B Hauer, and JM Woodley. 2016. "Process limitations of a whole-cell P450 catalyzed

reaction using a CYP153A-CPR fusion construct expressed in Escherichia coli." *Applied microbiology and biotechnology* 100 (3):1197-1208.

Malca, Sumire Honda, Daniel Scheps, Lisa Kühnel, Elena Venegas-Venegas, Alexander Seifert, Bettina M Nestl, and Bernhard Hauer. 2012. "Bacterial CYP153A monooxygenases for the synthesis of omega-hydroxylated fatty acids." *Chemical Communications* 48 (42):5115-5117.

McKeen, Laurence W. 2012. "8 - Polyamides (Nylons)." In *Film Properties of Plastics and Elastomers (Third Edition)*, edited by Laurence W. McKeen. Boston: William Andrew Publishing.

Metzger, J. O., and U. Bornscheuer. 2006. "Lipids as renewable resources: current state of chemical and biotechnological conversion and diversification." *Applied Microbiology and Biotechnology* 71 (1):13-22. doi: 10.1007/s00253-006-0335-4.

Mountanea, Olga G., Dimitris Limnios, Maroula G. Kokotou, Asimina Bourboula, and George Kokotos. 2019. "Asymmetric Synthesis of Saturated Hydroxy Fatty Acids and Fatty Acid Esters of Hydroxy Fatty Acids." *European Journal of Organic Chemistry* 2019 (10):2010-2019. doi: 10.1002/ejoc.201801881.

Mutlu, Hatice, and Michael A. R. Meier. 2010. "Castor oil as a renewable resource for the chemical industry." *European Journal of Lipid Science and Technology* 112 (1):10-30. doi: https://doi.org/10.1002/ejlt.200900138.

Naing, Swe-Htet, Saba Parvez, Marilla Pender-Cudlip, John T Groves, and Rachel N Austin. 2013. "Substrate specificity and reaction mechanism of purified alkane hydroxylase from the hydrocarbonoclastic bacterium Alcanivorax borkumensis (AbAlkB)." *Journal of inorganic biochemistry* 121:46-52.

Newton, Matilda S., Vickery L. Arcus, Monica L. Gerth, and Wayne M. Patrick. 2018. "Enzyme evolution: innovation is easy, optimization is complicated." *Current Opinion in Structural Biology* 48:110-116. doi: https://doi.org/10.1016/j.sbi.2017.11.007.

Nie, Yong, Chang-Qiao Chi, Hui Fang, Jie-Liang Liang, She-Lian Lu, Guo-Li Lai, Yue-Qin Tang, and Xiao-Lei Wu. 2014. "Diverse alkane hydroxylase genes in microorganisms and

environments." *Scientific reports* 4.

Nuland, Youri M, Fons A Vogel, Gerrit Eggink, and Ruud A Weusthuis. 2017. "Expansion of the ω-oxidation system AlkBGTL of Pseudomonas putida GPo1 with AlkJ and AlkH results in exclusive mono-esterified dicarboxylic acid production in E. coli." *Microbial Biotechnology* 10 (3):594‒603.

O'Reilly, Elaine, Valentin Köhler, Sabine L Flitsch, and Nicholas J Turner. 2011. "Cytochromes P450 as useful biocatalysts: addressing the limitations." *Chemical Communications* 47 (9):2490‒2501.

Pandey, Bishnu Prasad, Nahum Lee, Kwon‒Young Choi, Ji‒Nu Kim, Eun‒Jung Kim, and Byung‒Gee Kim. 2014. "Identification of the specific electron transfer proteins, ferredoxin, and ferredoxin reductase, for CYP105D7 in Streptomyces avermitilis MA4680." *Applied Microbiology and Biotechnology* 98 (11):5009‒5017. doi: 10.1007/s00253‒014‒5525‒x.

Park, Eul‒Soo, and Jong‒Shik Shin. 2013. "ω‒Transaminase from Ochrobactrum anthropi is devoid of substrate and product inhibitions." *Applied and environmental microbiology* 79 (13):4141‒4144. doi: 10.1128/AEM.03811‒12.

Patil, Mahesh D, Gideon Grogan, Andreas Bommarius, and Hyungdon Yun. 2018. "Recent Advances in ω‒Transaminase‒Mediated Biocatalysis for the Enantioselective Synthesis of Chiral Amines." *Catalysts* 8 (7):254.

Patil, Mahesh D., Manoj J. Dev, Ashok S. Shinde, Kiran D. Bhilare, Gopal Patel, Yusuf Chisti, and Uttam Chand Banerjee. 2017. "Surfactant‒mediated permeabilization of *Pseudomonas putida KT2440* and use of the immobilized permeabilized cells in biotransformation." *Process Biochemistry* 63:113‒121. doi: https://doi.org/10.1016/j.procbio.2017.08.002.

Patil, Mahesh D., Gideon Grogan, and Hyungdon Yun. 2018. "Biocatalyzed C‒C Bond Formation for the Production of Alkaloids." *ChemCatChem* 10 (21):4783‒4804. doi: doi:10.1002/cctc.201801130.

Patil, Mahesh D., Vijay P. Rathod, Umesh R. Bihade, and Uttam Chand Banerjee. 2019. "Purification and characterization of

arginine deiminase from *Pseudomonas putida*: Structural insights of the differential affinities of L−arginine analogues." *Journal of Bioscience and Bioengineering* 127 (2):129−137. doi: https://doi.org/10.1016/j.jbiosc.2018.07.021.

Perera, Frederica. 2017. "Pollution from Fossil−Fuel Combustion is the Leading Environmental Threat to Global Pediatric Health and Equity: Solutions Exist." *International journal of environmental research and public health* 15 (1):16. doi: 10.3390/ijerph15010016.

Pérez−Pérez, José Manuel, Héctor Candela, and José Luis Micol. 2009. "Understanding synergy in genetic interactions." *Trends in Genetics* 25 (8):368−376. doi: https://doi.org/10.1016/j.tig.2009.06.004.

Picataggio, Stephen, Tracy Rohrer, Kristine Deanda, Dawn Lanning, Robert Reynolds, Jonathan Mielenz, and L. Dudley Eirich. 1992. "Metabolic Engineering of Candida Tropicalis for the Production of Long−Chain Dicarboxylic Acids." *Bio/Technology* 10 (8):894−898. doi: 10.1038/nbt0892−894.

Quaglia, Daniela, Maximilian C. C. J. C. Ebert, Paul F. Mugford, and Joelle N. Pelletier. 2017. "Enzyme engineering: A synthetic biology approach for more effective library generation and automated high−throughput screening." *PLOS ONE* 12 (2):e0171741. doi: 10.1371/journal.pone.0171741.

Quan, Jiayuan, and Jingdong Tian. 2011. "Circular polymerase extension cloning for high−throughput cloning of complex and combinatorial DNA libraries." *Nature Protocols* 6:242. doi: 10.1038/nprot.2010.181
https://www.nature.com/articles/nprot.2010.181#supplementary−information.

Reetz, Manfred T., and José Daniel Carballeira. 2007. "Iterative saturation mutagenesis (ISM) for rapid directed evolution of functional enzymes." *Nature Protocols* 2 (4):891−903. doi: 10.1038/nprot.2007.72.

Reetz, Manfred T., Daniel Kahakeaw, and Renate Lohmer. 2008. "Addressing the Numbers Problem in Directed Evolution." *ChemBioChem* 9 (11):1797−1804. doi: https://doi.org/10.1002/cbic.200800298.

Ricca, Emanuele, Birgit Brucher, and Joerg H. Schrittwieser. 2011. "Multi−Enzymatic Cascade Reactions: Overview and

Perspectives." *Advanced Synthesis & Catalysis* 353 (13):2239−2262. doi: https://doi.org/10.1002/adsc.201100256.

Rojo, Fernando. 2005. "Specificity at the End of the Tunnel: Understanding Substrate Length Discrimination by the AlkB Alkane Hydroxylase." *Journal of Bacteriology* 187 (1):19−22. doi: 10.1128/jb.187.1.19−22.2005.

Rudroff, Florian, Marko D. Mihovilovic, Harald Gröger, Radka Snajdrova, Hans Iding, and Uwe T. Bornscheuer. 2018. "Opportunities and challenges for combining chemo− and biocatalysis." *Nature Catalysis* 1 (1):12−22. doi: 10.1038/s41929−017−0010−4.

Sakagami, Yuhki, Kenji Horiguchi, Yusuke Narita, Wariya Sirithep, Kohei Morita, and Yu Nagase. 2013. "Syntheses of a novel diol monomer and polyurethane elastomers containing phospholipid moieties." *Polymer Journal* 45 (11):1159−1166. doi: 10.1038/pj.2013.48.

Sarak, S., S. Sung, H. Jeon, M. D. Patil, T. P. Khobragade, A. D. Pagar, P. E. Dawson, and H. Yun. 2021. "An Integrated Cofactor/Co−Product Recycling Cascade for the Biosynthesis of Nylon Monomers from Cycloalkylamines." *Angew Chem Int Ed Engl* 60 (7):3481−3486. doi: 10.1002/anie.202012658.

Schaffer, Steffen, and Thomas Haas. 2014. "Biocatalytic and Fermentative Production of α,ω−Bifunctional Polymer Precursors." *Organic Process Research & Development* 18 (6):752−766. doi: 10.1021/op5000418.

Scheps, Daniel, Sumire Honda Malca, Sven M Richter, Karoline Marisch, Bettina M Nestl, and Bernhard Hauer. 2013. "Synthesis of ω-hydroxy dodecanoic acid based on an engineered CYP153A fusion construct." *Microbial biotechnology* 6 (6):694−707.

Schoffelen, Sanne, and Jan C. M. van Hest. 2012. "Multi−enzyme systems: bringing enzymes together in vitro." *Soft Matter* 8 (6):1736−1746. doi: 10.1039/C1SM06452E.

Schrewe, Manfred, Mattijs K. Julsing, Kerstin Lange, Eik Czarnotta, Andreas Schmid, and Bruno Bühler. 2014. "Reaction and catalyst engineering to exploit kinetically controlled whole−cell multistep biocatalysis for terminal FAME

oxyfunctionalization." *Biotechnology and Bioengineering* 111 (9):1820-1830. doi: 10.1002/bit.25248.

Schrewe, Manfred, Anders O Magnusson, Christian Willrodt, Bruno Bühler, and Andreas Schmid. 2011. "Kinetic Analysis of Terminal and Unactivated C-H Bond Oxyfunctionalization in Fatty Acid Methyl Esters by Monooxygenase-Based Whole-Cell Biocatalysis." *Advanced Synthesis & Catalysis* 353 (18):3485-3495.

Seo, Eun-Ji, Chae Won Kang, Ji-Min Woo, Sungho Jang, Young Joo Yeon, Gyoo Yeol Jung, and Jin-Byung Park. 2019. "Multi-level engineering of Baeyer-Villiger monooxygenase-based Escherichia coli biocatalysts for the production of C9 chemicals from oleic acid." *Metabolic Engineering* 54:137-144. doi: https://doi.org/10.1016/j.ymben.2019.03.012.

Seo, Eun-Ji, Young Joo Yeon, Joo-Hyun Seo, Jung-Hoo Lee, Jhoanne P. Boñgol, Yuri Oh, Jong Moon Park, Sang-Min Lim, Choul-Gyun Lee, and Jin-Byung Park. 2018. "Enzyme/whole-cell biotransformation of plant oils, yeast derived oils, and microalgae fatty acid methyl esters into n-nonanoic acid, 9-hydroxynonanoic acid, and 1,9-nonanedioic acid." *Bioresource Technology* 251:288-294. doi: https://doi.org/10.1016/j.biortech.2017.12.036.

Shanklin, John, and Edward Whittle. 2003. "Evidence linking the Pseudomonas oleovorans alkane ω-hydroxylase, an integral membrane diiron enzyme, and the fatty acid desaturase family." *FEBS Letters* 545 (2-3):188-192. doi: https://doi.org/10.1016/S0014-5793(03)00529-5.

Sherkhanov, Saken, Tyler P. Korman, Steven G. Clarke, and James U. Bowie. 2016. "Production of FAME biodiesel in *E. coli* by direct methylation with an insect enzyme." *Scientific Reports* 6:24239. doi: 10.1038/srep24239.

Sikkema, J, J A de Bont, and B Poolman. 1994. "Interactions of Cyclic Hydrocarbons with Biological Membran." *Journal of Biological Chemistry* 269 (11):8022-8028.

Siloto, Rodrigo M. P., and Randall J. Weselake. 2012. "Site saturation mutagenesis: Methods and applications in protein engineering." *Biocatalysis and Agricultural Biotechnology* 1 (3):181-189. doi: https://doi.org/10.1016/j.bcab.2012.03.010.

Singh, Pranveer, Likhesh Sharma, S. Rajendra Kulothungan, Bharat V. Adkar, Ravindra Singh Prajapati, P. Shaik Syed Ali, Beena Krishnan, and Raghavan Varadarajan. 2013. "Effect of Signal Peptide on Stability and Folding of Escherichia coli Thioredoxin." *PLOS ONE* 8 (5):e63442. doi: 10.1371/journal.pone.0063442.

Song, J. H., R. J. Murphy, R. Narayan, and G. B. H. Davies. 2009. "Biodegradable and compostable alternatives to conventional plastics." *Philosophical transactions of the Royal Society of London. Series B, Biological sciences* 364 (1526):2127-2139. doi: 10.1098/rstb.2008.0289.

Steen, Eric J, Yisheng Kang, Gregory Bokinsky, Zhihao Hu, Andreas Schirmer, Amy McClure, Stephen B Del Cardayre, and Jay D Keasling. 2010. "Microbial production of fatty-acid-derived fuels and chemicals from plant biomass." *Nature* 463 (7280):559.

Stemmer, Willem P. C., Andreas Crameri, Kim D. Ha, Thomas M. Brennan, and Herbert L. Heyneker. 1995. "Single-step assembly of a gene and entire plasmid from large numbers of oligodeoxyribonucleotides." *Gene* 164 (1):49-53. doi: https://doi.org/10.1016/0378-1119(95)00511-4.

Stephan and Mohar, B. 2006. "Simple Preparation of Highly Pure Monomeric ω-Hydroxycarboxylic Acids." *Stephan, M. M. S., & Mohar, B. (2006). Simple Preparation of Highly Pure Monomericω-Hydroxycarboxylic Acids. Organic Process Research & Development, 10(3), 481–483. doi:10.1021/op0502046*

Sun, Yuhan, Weiqiao Zeng, Abdelkrim Benabbas, Xin Ye, Ilia Denisov, Stephen G Sligar, Jing Du, John H Dawson, and Paul M Champion. 2013. "Investigations of heme ligation and ligand switching in cytochromes p450 and p420." *Biochemistry* 52 (34):5941-5951.

Sung, Changmin, Eunok Jung, Kwon-Young Choi, Jin-hyung Bae, Minsuk Kim, Joonwon Kim, Eun-Jung Kim, Pyoung Il Kim, and Byung-Gee Kim. 2015. "The production of ω-hydroxy palmitic acid using fatty acid metabolism and cofactor optimization in Escherichia coli." *Applied microbiology and biotechnology* 99 (16):6667-6676.

Sung, Sihyong, Hyunwoo Jeon, Sharad Sarak, Md Murshidul Ahsan,

Mahesh D Patil, Wolfgang Kroutil, Byung-Gee Kim, and Hyungdon Yun. 2018. "Parallel anti-sense two-step cascade for alcohol amination leading to ω-amino fatty acids and α, ω-diamines." *Green Chemistry* 20 (20):4591-4595.

Szklarczyk, Damian, John H Morris, Helen Cook, Michael Kuhn, Stefan Wyder, Milan Simonovic, Alberto Santos, Nadezhda T Doncheva, Alexander Roth, Peer Bork, Lars J. Jensen, and Christian von Mering. 2016. "The STRING database in 2017: quality-controlled protein–protein association networks, made broadly accessible." *Nucleic Acids Research* 45 (D1):D362-D368. doi: 10.1093/nar/gkw937.

Van Beilen, Jan B, D Penninga, and Bernard Witholt. 1992. "Topology of the membrane-bound alkane hydroxylase of Pseudomonas oleovorans." *Journal of Biological Chemistry* 267 (13):9194-9201.

Van Beilen, Jan B, Theo HM Smits, Franz F Roos, Tobias Brunner, Stefanie B Balada, Martina Röthlisberger, and Bernard Witholt. 2005. "Identification of an amino acid position that determines the substrate range of integral membrane alkane hydroxylases." *Journal of bacteriology* 187 (1):85-91.

van Beilen, Jan B., Wouter A. Duetz, Andreas Schmid, and Bernard Witholt. 2003. "Practical issues in the application of oxygenases." *Trends in Biotechnology* 21 (4):170-177. doi: https://doi.org/10.1016/S0167-7799(03)00032-5.

van Beilen, Jan B., Jaap Kingma, and Bernard Witholt. 1994. "Substrate specificity of the alkane hydroxylase system of Pseudomonas oleovorans GPo1." *Enzyme and Microbial Technology* 16 (10):904-911. doi: https://doi.org/10.1016/0141-0229(94)90066-3.

Van Bogaert, Inge NA, Marjan Demey, Dirk Develter, Wim Soetaert, and Erick J Vandamme. 2009. "Importance of the cytochrome P450 monooxygenase CYP52 family for the sophorolipid-producing yeast Candida bombicola." *FEMS yeast research* 9 (1):87-94.

van Eunen, Karen, and Barbara M. Bakker. 2014. "The importance and challenges of in vivo-like enzyme kinetics." *Perspectives in Science* 1 (1):126-130. doi: https://doi.org/10.1016/j.pisc.2014.02.011.

van Nuland, Youri M, Gerrit Eggink, and Ruud A Weusthuis. 2016.

"Application of AlkBGT and AlkL from Pseudomonas putida
GPo1 for selective alkyl ester ω-oxyfunctionalization in
Escherichia coli." *Applied and environmental microbiology*
82 (13):3801-3807.

Venkitasubramanian, Padmesh, Lacy Daniels, and John P. N.
Rosazza. 2007. "Reduction of Carboxylic Acids by Nocardia
Aldehyde Oxidoreductase Requires a
Phosphopantetheinylated Enzyme*." *Journal of Biological
Chemistry* 282 (1):478-485. doi:
https://doi.org/10.1074/jbc.M607980200.

Voorhees, Rebecca M., and Ramanujan S. Hegde. 2016. "Structure
of the Sec61 channel opened by a signal sequence." *Science
(New York, N.Y.)* 351 (6268):88-91. doi:
10.1126/science.aad4992.

Wachtmeister, Jochen, and Dörte Rother. 2016. "Recent advances in
whole cell biocatalysis techniques bridging from investigative
to industrial scale." *Current Opinion in Biotechnology*
42:169-177. doi:
https://doi.org/10.1016/j.copbio.2016.05.005.

Wadumesthrige, Kapila, Steven O. Salley, and K. Y. Simon Ng. 2009.
"Effects of partial hydrogenation, epoxidation, and
hydroxylation on the fuel properties of fatty acid methyl
esters." *Fuel Processing Technology* 90 (10):1292-1299.
doi: https://doi.org/10.1016/j.fuproc.2009.06.013.

Wang, Fei, Jing Zhao, Qian Li, Jun Yang, Renjie Li, Jian Min,
Xiaojuan Yu, Gao-Wei Zheng, Hui-Lei Yu, Chao Zhai, Carlos
G. Acevedo-Rocha, Lixin Ma, and Aitao Li. 2020. "One-pot
biocatalytic route from cycloalkanes to α,ω-dicarboxylic acids
by designed Escherichia coli consortia." *Nature
Communications* 11 (1):5035. doi: 10.1038/s41467-020-
18833-7.

Wilding, Matthew, Ellen F. A. Walsh, Susan J. Dorrian, and Colin
Scott. 2015. "Identification of novel transaminases from a
12-aminododecanoic acid-metabolizing Pseudomonas
strain." *Microbial Biotechnology* 8 (4):665-672. doi:
https://doi.org/10.1111/1751-7915.12278.

Witholt, Bernard, Marie-Jose´ de Smet, Jaap Kingma, Jan B. van
Beilen, Menno Kok, Roland G. Lageveen, and Gerrit Eggink.
1990. "Bioconversions of aliphatic compounds

byPseudomonas oleovorans in multiphase bioreactors: background and economic potential." *Trends in Biotechnology* 8:46-52. doi: https://doi.org/10.1016/0167-7799(90)90133-I.

Xiao, Yi, Christopher H. Bowen, Di Liu, and Fuzhong Zhang. 2016. "Exploiting nongenetic cell-to-cell variation for enhanced biosynthesis." *Nature Chemical Biology* 12:339. doi: 10.1038/nchembio.2046

https://www.nature.com/articles/nchembio.2046#supplementary-information.

Yamane, K, K Kawasaki, K Sone, T Hara, and T Prakoso. 2007. "Oxidation stability of biodiesel and its effects on diesel combustion and emission characteristics." *International Journal of Engine Research* 8 (3):307-319. doi: 10.1243/14680874jer00207.

Yokota, Tadafumi, and Akio Watanabe. 1993. Process for producing ω-hydroxy fatty acids. Google Patents.

Yoo, Hee-Wang, Joonwon Kim, Mahesh D. Patil, Beom Gi Park, Sung-yeon Joo, Hyungdon Yun, and Byung-Gee Kim. 2019. "Production of 12-hydroxy dodecanoic acid methyl ester using a signal peptide sequence-optimized transporter AlkL and a novel monooxygenase." *Bioresource Technology* 291:121812. doi: https://doi.org/10.1016/j.biortech.2019.121812.

Yu, Ai-Qun, Nina Kurniasih Pratomo Juwono, Susanna Su Jan Leong, and Matthew Wook Chang. 2014. Production of Fatty Acid-derived valuable chemicals in synthetic microbes. *Frontiers in bioengineering and biotechnology* 2: 78. Accessed 2014. doi:10.3389/fbioe.2014.00078.

Zhang, Wuyuan, Jeong-Hoo Lee, Sabry H. H. Younes, Fabio Tonin, Peter-Leon Hagedoorn, Harald Pichler, Yoonjin Baeg, Jin-Byung Park, Robert Kourist, and Frank Hollmann. 2020. "Photobiocatalytic synthesis of chiral secondary fatty alcohols from renewable unsaturated fatty acids." *Nature Communications* 11 (1):2258. doi: 10.1038/s41467-020-16099-7.

Zorn, Katja, Isabel Oroz-Guinea, Henrike Brundiek, and Uwe T. Bornscheuer. 2016. "Engineering and application of enzymes for lipid modification, an update." *Progress in Lipid*

Research 63:153−164. doi: https://doi.org/10.1016/j.plipres.2016.06.001.

국문초록

최근 석유 고갈 가능성 및 환경오염 문제가 대두되면서 식물 기름유도체로부터 폴리머의 단량체를 생산하는 방법의 중요성이 대두되고 있다. 특히 ω-수산화 지방산은 다양한 바이오폴리머 모노머의 전구체로 사용되는 물질이다. 그렇기 때문에 효소 반응을 사용한 친환경적인 방법으로 ω-수산화 지방산을 생산하는 연구가 전 세계적으로 활발히 연구진행되고 있다.

본 연구는, 대장균에서 12-수산화 라우르산을 메틸 라우르산으로부터 AlkBGT 시스템을 사용해서 생산하는 연구와 생산된 12-수산화 라우르산을 통하여 다양한 바이오폴리머 모노머(ω-아미노 지방산, α, ω-알칸다이올, α,ω-알칸다이아민)를 생산하는 연구를 진행하였다. 우리는 트랜스포터, 프로모터의 개량 및 새로운 알칸 모노옥시게나아제를 대장균에 도입하여 메틸 라우르산으로부터 이상계 반응을 통해 44.8 ± 7.5 mM of 12-수산화 지방산 및 31.8 ± 1.7 mM of 도데칸다이오산을 생산하였다. 또한 다중 효소 연속 반응을 수행하기 위한 3개의 대장균 모듈(수산화 모듈(Cell-H^m), 아미노화 모듈(Cell-A^m), 환원 모듈(Cell-R^m))을 구축하였다. 46.3 mM 12-아미노 라우르산, 27 mM 1,12 도데칸다이올, 21.5 mM 1,12-도데칸다이아민이 다중 효소 연속 반응을

통하여 100 mM의 메틸 라우르산으로부터 생산되었다. 퓨도모나스 펠라지아 유래의 알칸 모노옥시게나아제를 (PpAlkB)의 수산화 활성을 증가시키기 위하여 실수 유발 PCR을 통하여 PpAklB의 무작위 돌연변이 라이브러리를 구축하였으며, 활성이 높은 변이주를 고 처리량 분석방법을 통해 선별하였다. 대장균에서 항생제 내성 유전자의 발현을 PpAlkB에 의한 라우르산의 생산양과 결합되어 세포 성장에 의한 고 처리량 분석방법을 통해 생체 내 스크리닝을 진행 할 수 있다. 도데칸과 메틸 라우르산을 기질로 사용하여 2번의 스크리닝을 진행한 후 우리는 H292L/F253I/S313P의 돌연변이가 발생한 PpAlkB를 얻을 수 있었다. 12.95 mM (11 mM 12-수산화 라우르산, 1.96 mM 도데칸다이오산)이 100 mM 메틸 라우르산으로부터 PpAlkB 변이주를 포함한 대장균으로부터 생산되었으며, 이는 7.88 mM이 생산된 야생형 PpAlkB를 사용하였을 때보다 64% 증가된 수치이다.

결론적으로 본 연구는 대장균에서 메틸 라우르산을 기질로 사용하여 12-수산화 라우르산을 생산하였으며, 세 종류의 대장균 기반 세포 모듈을 만들어 다중 효소 연속 반응을 수행하여 다양한 바이오폴리머 모노머를 생산할 수 있었다. 또한 생체 내 스크리닝 시스템을 사용하여 메틸 라우르산의 수산화 활성이 높아진 PpAklB의 변이주를 찾을 수 있었다. 본 연구는 AlkB의 효소 공학 및 모듈화된 세포 반응을 통해 대장균에서 지방산 유도체의 생합성 연구 가능하게 했다는 점에서 의의가 있다

주요어 : 논-힘 알칸 모노옥시게나아제, AlkBGT, 12-수산화지방산, 생

체 내 스크리닝 시스템

학번 : 2015-21215